THERMOPLASTIC COATING OF CARBON FIBERS

Annual Report
1988-1989

by

D. D. Edie, G. C. Lickfield,
L. E. Allen and J. R. McCollum

CENTER FOR ADVANCED ENGINEERING FIBERS
CLEMSON UNIVERSITY
CLEMSON, S.C. 29634-0909

sponsored by

THE NATIONAL AERONAUTICS AND SPACE ADMINISTRATION
LANGLEY RESEARCH CENTER
HAMPTON, VA 23665

NASA Research Grant NAG-1-680

Robert M. Baucom
NASA Technical Officer

ABSTRACT

Carbon fiber composites are gaining widespread use because of their high specific strength and stiffness. The majority of carbon fiber composite materials produced today are made by embedding the fibers in a monomeric-liquid matrix, then curing the matrix to form a thermoset polymer around the fibers. This process is usually expensive because the composite part must often be laid-up by hand and the cure stage is time consuming. Thermoplastic polymers also may be used as composite matrices. This variety of polymer presents a number of advantages including easier handling, the elimination of the cure cycle, and better toughness in the final part. However, distributing a high viscosity thermoplastic matrix evenly among fibers proved difficult. One alternative is to impregnate the fibers with a finely divided thermoplastic powder. These pre-impregnated fibers, called a prepreg, may then be woven or braided into a preform and press-molded to form the final part.

In the present research, a continuous powder coating system was developed for coating carbon fiber with LaRC-TPI, a high-temperature thermoplastic polyimide invented by NASA Langley Research Center. The coating line developed used a pneumatic fiber spreader to separate the individual fibers. The polymer was applied within a recirculating powder coating chamber then melted using a combination of direct electrical resistance and convective heating to make it adhere to the fiber tow. The tension and speed of the line were controlled with a dancer arm and an electrically driven fiber wind-up and wind-off.

The effects of heating during the coating process on the flexibility of the prepreg produced were investigated. The uniformity with which the fiber tow could be coated with polymer also was examined. Composite specimens were fabricated from the prepreg and tested to determine optimum process conditions.

The study showed that a very uniform and flexible prepreg with up to 50% by volume polymer could be produced with this powder coating system. The coating line minimized powder loss and produced prepreg in lengths of up to 300 m. The fiber spreading was found to have a major effect on the coating uniformity and flexibility. Though tests results showed low composite tensile strengths, analysis of fracture surfaces under scanning electron microscope indicated that fiber/matrix adhesion was adequate.

TABLE OF CONTENTS

Table of Contents (Continued)

LIST OF TABLES

LIST OF FIGURES

List of Figures (Continued)

CHAPTER I

INTRODUCTION

In modern military and civilian aircraft applications the high specific strength and stiffness of composites often makes these materials preferable to steel, aluminum, and other alloys. The substitution of materials such as carbon fiber composites for conventional metals often leads to benefits such as decreased fuel consumption, higher maneuverability, and decreased stress on support members. However, the high price of these composite materials has limited their penetration into commercial aviation, automotive, and consumer markets. Since processing costs account for about two thirds of this price, the key to expanding the market for composite materials is developing improved, low cost processing methods.

Thermoset polymers are used, almost exclusively, in commercially available prepregs. Thermoset prepregs are carbon fiber bundles impregnated with low molecular weight, high viscosity resin. These prepregs are difficult to work with and require refrigeration before use and during shipping. Parts formed from this variety of prepreg often require hand lay-up and must be cured at high temperature and pressure.

A number of thermoplastic polymers, including polyarylene ethers, polyimides, and polysulfones are available today and exhibit superior physical and thermal properties when used as matrix materials in carbon fiber composites. These polymers potentially could be used to form prepregs which would not require refrigeration and which would be safer and easier to handle than comparable thermoset prepregs. The major obstacle to the use of these promising new polymers is the difficulty of uniformly distributing fibers in the thermoplastic matrix (1).

Several different impregnation methods have been tried for thermoplastics, including melt impregnation, solvent and slurry coating. Melt impregnation results in a stiff, "boardy" prepreg which is difficult to weave or braid into textile preforms. The use of solvent coating techniques is limited to only a few thermoplastics for which suitable solvents may be found. Most of these solvents have a low volatility, complicating solvent removal efforts. Slurry coating is a technique which employs a liquid and suspending agents to form a polymer slurry. The resulting prepreg must be dried before use. However, the suspending agents are difficult to completely remove and may be incorporated in the final part, compromising its strength. All three methods contribute to the formation of voids in the composite part. When a load is applied to such a composite, the voids result in stress concentrations which cause a premature failure of the part.

This thesis details the development of a novel process for prepreg formation using LaRC-TPI, a thermoplastic polyimide developed by Langley Research Center (2). This polymer is available from Mitsui Toatsu Chemical Company (MTC) and from Rogers Corporation in the form of a fine powder with a particle size ranging from 5 to 20 microns.

The prepreg formed by the Clemson process is highly flexible, does not require drying, and includes no impurities. The high flexibility of this prepreg should allow it to be processed on weaving, braiding , and even knitting equipment. It is hoped that the automated fabrication of textile preforms on this type of equipment will substantially reduce processing costs and, thus, expand the commercial market for composite materials.

CHAPTER II

LITERATURE REVIEW

Composites in Aircraft Structures

The use of composites in aircraft began in the early 1940s with the incorporation of paper reinforcement in a wing box beam (1). Further advances were required, however, before this technology could be considered for widespread use in aircraft structures. Glass fiber reinforcement of a thermoset polyester matrix followed soon after to give composite materials a higher specific strength than that attainable with metals. In the 1960's, boron fiber reinforcements were found to provide the missing high specific stiffness for composites. This combination of properties sparked great interest in composite materials which rapidly lead to the discovery of carbon/graphite, aramid, silicon carbide and other specialty fibers (3).

The difficulty of incorporating a high viscosity thermoplastic polymer into a continuous fiber reinforcement forced the use of thermoset resins in earlier composites, and these thermoset resins still are used in the bulk of high performance composites today (4). These resins come in four major varieties: epoxies, condensation polyimides, bismaleimides, and PMR (in situ Polymerization of Monomer Reactants) polyimides.

Epoxies

Today, epoxy resins, characterized by the presence of an epoxide or oxirane linkage, are the most widely used matrix material for carbon fiber reinforced composites. This is due, in part, to the fact that a wide assortment of epoxies are marketed, each with properties tailored to specific needs. Unlike many newer matrix

polymers, epoxies have excellent fiber adhesion, low cure shrinkage, and acceptable solvent resistance.

Most epoxies composites are formed using one of two methods. The first technique utilizes a prepreg which consists of a fiber tow, collimated tape, or woven mat impregnated with a low viscosity monomeric solution. This tacky and flexible material may then be stacked in layers, filament wound, or braided into the form of the desired part. The part is then cured under pressure and at elevated temperature for a curing time ranging from 2 to 10 hours. The second process called resin transfer molding uses woven mats or monolayer sheets of dry fibers which are put into near final form before the epoxy resin is applied. This is usually simpler than working with prepregs but often the resin is poorly distributed in the final part. Then, like the prepreg lay-up, the coated part is cured. Though both techniques are expensive, the technology is well established and reliable (1,3,5).

Condensation Polyimides

Thermoset polyimide matrix systems were developed by aerospace companies and the government to meet the higher temperature requirements of current military aircraft. While epoxies may be used at temperatures as high as 200°C, the aromatic-heterocyclic structure of polyimides allows their use up to 370°C. Though condensation polyimides themselves are not widely used, they serve as a baseline for comparison of other more useful imide systems. A typical polyimide structure and reaction scheme are shown in Figure 1.

Presently, polyimide composites are fabricated by first coating a fiber tow with a solution of polyamic acid in a high boiling solvent such as N-methylpyrrolidone. A condensation reaction converts the polyamic acid, covering the tow, to a polyimide. This prepreg then can be wound or laid-up like epoxy prepreg. Finally, the part must be consolidated in a very slow and carefully designed cure cycle to permit the

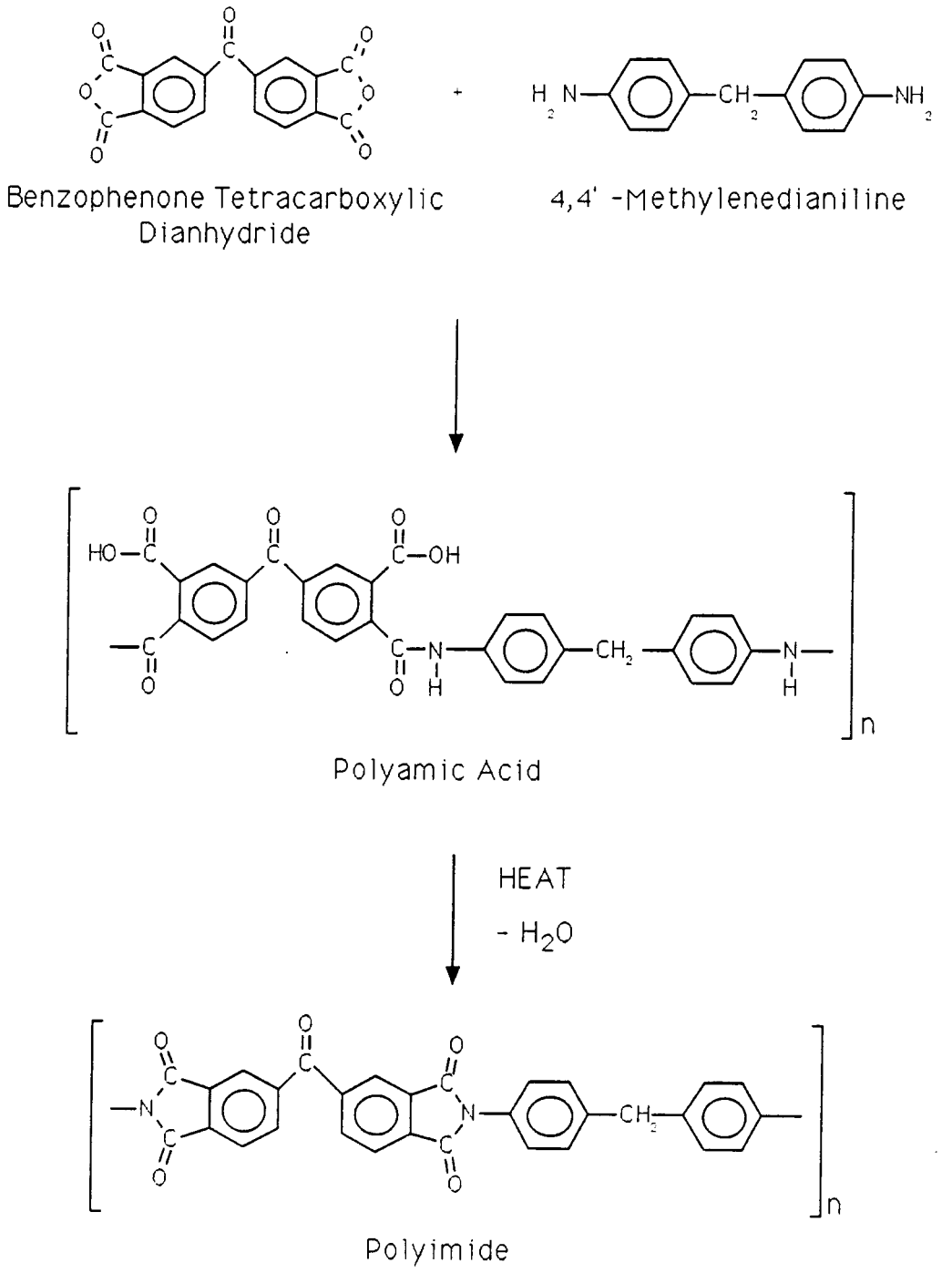

Figure 1. Chemical Reaction Scheme of Condensation Polyimides

condensation volatiles and solvent to escape. Because off-gassing becomes increasingly difficult as the polymerization proceeds, parts formed using this variety of composite matrix often contain a large number of voids (1,3).

PMR Polyimides

PMR polyimides were developed at NASA's Lewis Research center to alleviate the processing problems encountered with polyimide matrices. PMR resins currently are the leading high temperature composite matrix system (6). The monomers for this resin are designed to be soluble in low boiling solvents, such as methanol, which can be removed more readily during cure. The final cross-link step proceeds via a free-radical addition reaction and, thus, releases no volatiles. Figure 2 shows the components of PMR-15, the most widely used resin of this variety (3).

PMR-15 has been available to industry in a variety of solvent coated prepregs since the middle seventies, and a number of parts such as high tip speed fan blades, engine cowls and even the shuttle orbiter aft body flap have been produced and are scheduled for use. These parts, unlike those made from condensation polyimides, can be made nearly void-free using a less lengthy cure cycle (7).

BMI Polyimides

The properties of BMI's (bismaleimides) are intermediate between those of epoxies and polyimides (1). This class of resin, first introduced in the late sixties by the French, is currently the most studied of all thermoset polyimides (3).

BMI resins are composed of a mixture of either aromatic or aliphatic diamines reacted to form monomers with maleic anhydride. This low viscosity solution often contains additional diamines, permitting it to be prepreged. The major advantage of BMI systems is that they retain the drape and tack of an epoxy system, yet undergo

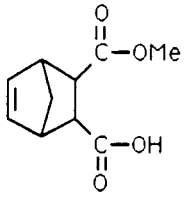

Monomethyl ester of
5-norbornene-2,2-
dicarboxylic acid

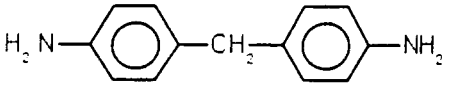

Methylene dianiline

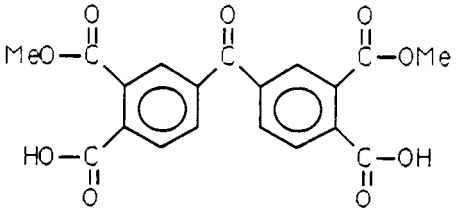

Dimethyl ester of 3,3',4,4' -
benzophenonetetracarboxylic acid

Figure 2. Chemical Structures of the Monomer Components of PMR-15 Resin

a free radical cure which does not evolve volatiles. Figure 3 illustrates the reactions which occur in the processing of BMI s (3).

The biggest disadvantage of the thermoset matrix materials is the unavoidably slow processing steps which, probably, ensure that they will remain expensive. Another significant problem is that their low toughness and poor damage tolerance limits their fatigue life. Table 1 compares the neat resin fracture energy, G_{Ic}, of a toughened epoxy, a BMI, and PMR-15. The glass transition temperatures, Tg, are listed for reference.

Table 1. Fracture Energy of Thermoset Matrix Polymers

Variety	Name	Manufacturer	Tg (°C)	G_{Ic} (J/m^2)	Reference
Epoxy	XU276/HT979	Ciba Geigy	195	210	8
BMI	Matrimid	Ciba Geigy	285	245	8
PMR	PMR-15	Hysol	352	85	5

Thermoplastic Composite Matrix Resins

Current interest in high temperature or high performance thermoplastics is due, in part, to developmental work on the Air Force's Advanced Tactical Fighter or ATF. As much as 50% (by weight) of the ATF is expected to be composite materials. Stringent requirements for matrix toughness and fatigue strength at high temperature have eliminated most thermoset matrix polymers from consideration. Only matrix materials with good hot/wet performance and fracture toughness at 177°C (350°F) are being considered for this project (3, 4). Virtually every major specialty chemical

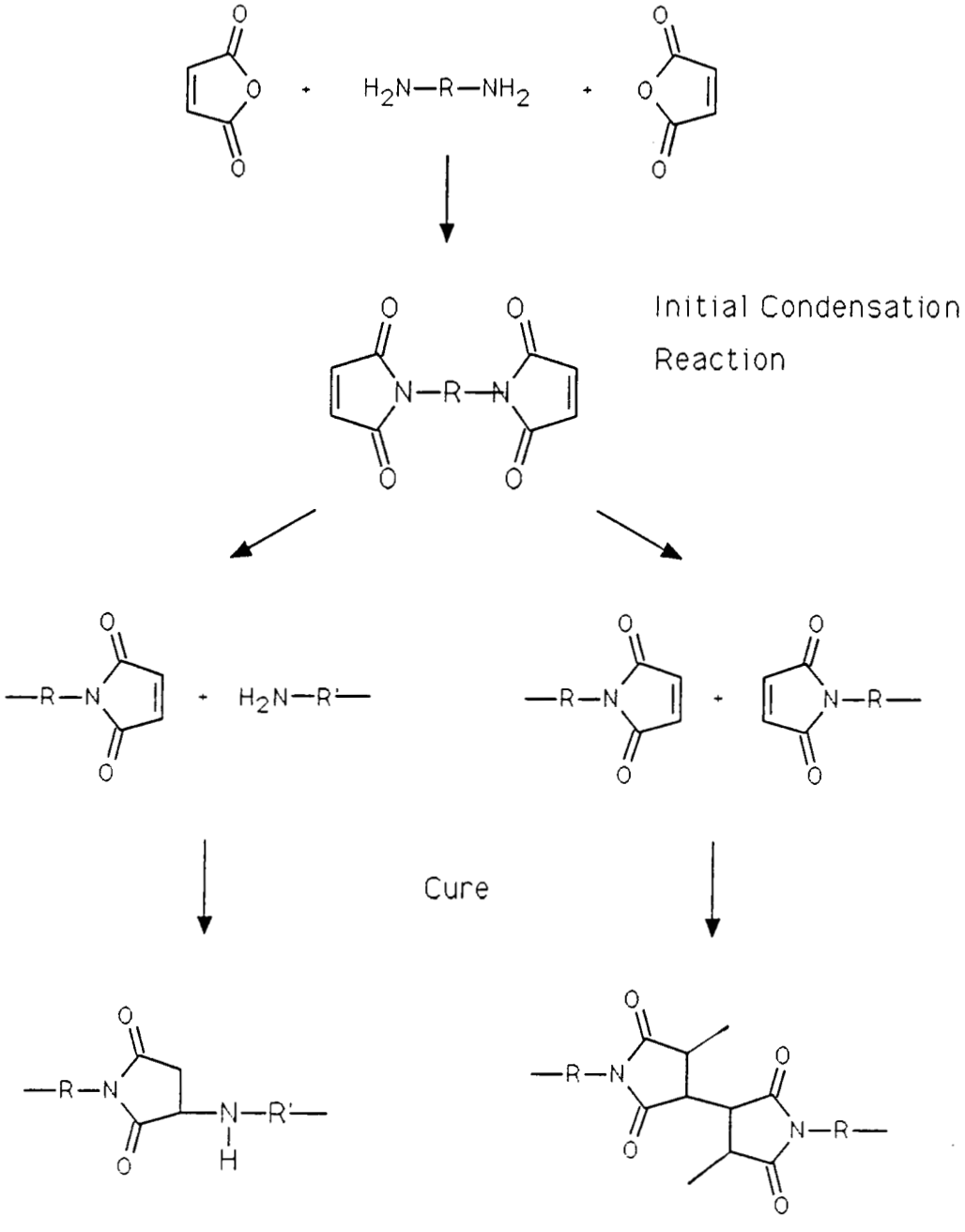

Figure 3. Chemical Reactions in the Processing of Bismaleimides (BMI s)

company in the United States and abroad has produced candidate resins for the ATF project, leading to numerous improved thermoplastic matrix polymers. However, each polymer has its own strengths and weaknesses which must be weighed before a selection can be made. The wide variety of performance requirements including specific solvent resistance, low temperature and pressure processability, high compression strength after impact, and low flammability make it unlikely that a single polymer will achieve preeminence (9,10,11).

The six major varieties of high performance thermoplastic matrix materials are: polyarylene ethers or sulfides, polysulfones, polyesters, amide or amideimide polymers, and polyimides (9). Even though each category of material includes an assortment of very different polymers, some properties are characteristic of an entire category. A few typical polymers from each category will be discussed to illustrate the properties which may be expected. However, since it was used in the present research, LaRC-TPI is described fully in a subsequent section. Figure 4 gives chemical structures of a number of these new thermoplastic matrix materials. Table 2 gives a comparison of neat resin properties.

Polyarylene Ethers

The category of polyarylene ethers or sulfides includes several resins that, because of their well demonstrated reliability, already are widely used. Polyetheretherketone, PEEK, developed by Imperial Chemical Industries, ICI, has been shown to have good toughness and excellent processability. This combination of properties makes PEEK, currently, the leading thermoplastic matrix material. PEEK is marketed in three grades: 150P, 380P, and 450P. These grades differ in molecular weight and, therefore, exhibit different mechanical properties (12). The 150P grade has the lowest molecular weight and the best processability, while 450P has the highest molecular weight and toughness. PEEK is available in pellet form, as

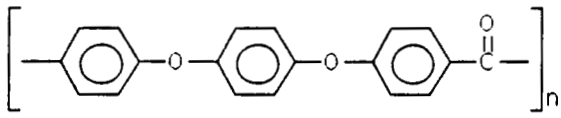

PEEK (ICI) Polyarylene Ether

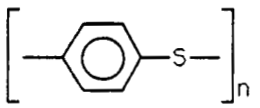

RYTON (Phillips) Polyphenylene Sulfide

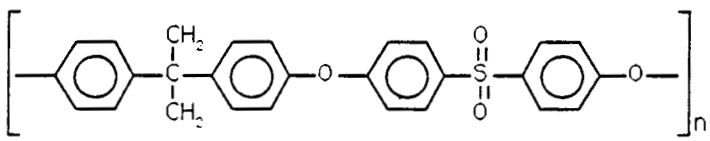

UDEL (Amoco) Polysulfone

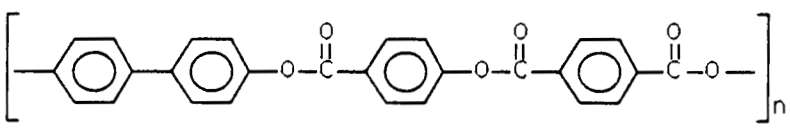

XYDAR (Dart Ind.) Polyester

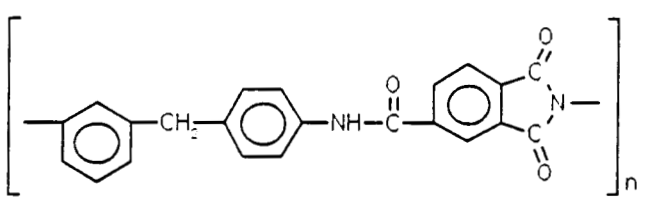

TORLON (Amoco) Polyamideimide

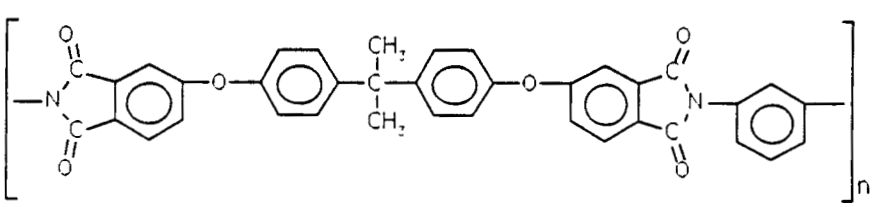

ULTEM (G.E.) Polyetherimide

Figure 4. Chemical Structures of Some Thermoplastic Matrix Polymers

a melt impregnated carbon fiber tape called APC-2 and as a commingled yarn (13, 14, 15). PEEK is an attractive composite matrix material because it exhibits good neat resin strength and modulus and high impact strength. Also, since it is relatively easy to process, PEEK is used as a matrix resin in short fiber reinforced composites (16,17). Even though the glass transition temperature of PEEK, 143°C, limits its use in high temperature environments, it displays very low creep up to a temperature of 250°C (18). Also, PEEK has lower solvent resistance than most polyimides (19).

Table 2. Neat Resin Properties of Some Thermoplastic Matrix Polymers

Polymer	Tg	Tensile Strength	Tensile Modulus	Notched Izod Impact Str.	G_{Ic}	Reference
	°C	MPa	GPa	N-m/m	J/m^2	
LaRC-TPI	264	119	4	21	*	9, 30
PEEK	170	103	3.8	85	4030	9, 20
Ryton	90	83	4.3	21	*	9, 22
Torlon	275	63	4.6	144	3400	9
Ultem	217	105	3.0	53	3330	9
Radel	220	72	2.1	641	3500	9
Xydar	350	138	16.5	128	1210	9

*Neat resin fracture energy was not found.

ICI has recently introduced a polyarylene ketone, HTX, which has a Tg of 204°C (12). This polymer is marketed in the form of a melt impregnated prepreg known as APC/HTX. Although this resin has slightly lower physical properties than PEEK, it is a candidate for use in the ATF project. The chemical structure of HTX is not yet

available, and more information on its physical properties will be required to evaluate its potential as a matrix polymer. One problem which has emerged with HTX is a tendency for the polymer to microcrack due to stresses resulting from density differences between crystalline and amorphous regions.

Other polyarylenethers include DuPont's recently introduced polyether-ketoneketone, PEKK. Even though the Tg of PEKK is comparable to that of PEEK, its viscosity is lower. However, typically the crystallinity of PEKK is 26% compared to 30% or more for PEEK (20). This may indicate that PEKK, which was designed to compete directly with PEEK, will have lower solvent resistance.

Polyphenylene sulfide, known as PPS or Ryton, is produced by Phillips Petroleum. Since its thermoplastic characteristics are similar to PEEK, it also is used for injection molding (21). Even though the glass transition temperature of PPS is only 90°C, it retains most of its creep resistance well above this temperature. Polyphenylene sulfide has a low compressive strength, much lower than average damage tolerance, but very high room temperature flexural modulus (9,19). PPS has been used as the subject of crystallization studies to provide insight on more complicated resin systems (23). Phillips markets continuous length PPS-carbon fiber laminates which can be post-formed (22). Also, PPS may be purchased from BASF in the form of a commingled carbon fiber tow (15).

An upgraded version of PPS, known as PAS-2, is now being tested by Phillips. This polymer has a glass transition temperature of 215°C and improved compressive strength (9). Not surprisingly, PAS-2 is considerably more difficult to process than PPS.

Polysulfones

Typically, polysulfones have good fracture toughness but often lack the solvent resistance of polyimides (19). However, polysulfones do have lower processing

temperatures than the less tractable polyimides (9). Amoco markets UDEL P1700 and introduced in the mid 1970 s an upgraded polysulfone, RADEL A400, containing biphenyl moieties. RADEL has higher toughness than UDEL and better chemical resistance, but still it is not able to withstand exposure to the hydraulic fluid and paint stripper which often contacts aeronautical parts. Attempts are being made to improve the chemical stability of polysulfones by incorporating crystalline block copolymers and the using of reactive end-groups to promote crosslinking. These techniques have shown limited success in the ongoing research at NASA's Langley Research Center and elsewhere (24).

Polyesters

Xydar SRT-300 from Dartco is the only liquid crystalline polyester which, with its exceptionally high glass transition temperature of 350°C, may be characterized as a high performance thermoplastic (9). This polymer can be injection molded at about 370°C and can be used as ovenware (10). As a matrix material it provides the excellent tensile properties, which would be expected for a system with ordered molecules (9).

Amideimide Polymers

The most notable amide or amideimide polymers are DuPont's J-polymer and Amoco's Torlon. J-polymer is perhaps the only high performance thermoplastic without a strong aromatic character, and this may explain its low glass transition temperature of 145°C and low density of from 1.04 to 1.15 g/cm^3 (25). Torlon, a polyamideimide, has a high glass transition temperature of 275°C, and is the primary matrix material used in a prototype ATF wing built by Boeing. Typically, Torlon is prepreged using N-methyl pyrrolidone as a solvent. The high viscosity of molten Torlon limits its use in neat resin form (26). Recently, a new variant of Torlon, called

Torlon-AIX638, has been introduced but, in general, there appears to be only limited research focused on this variety of thermoplastic.

Polyimides

On the other hand, considerable research is being directed toward improving polyimide composite matrix systems. Current thermoplastic polyimides share some of the favorable characteristics of their predecessors, the thermoset polyimides, which were known for their thermo-oxidative stability and solvent resistance. Notable polyimides are General Electric's Ultem, DuPont's Avamid K-III, and High Tech Services' polyimidesulfone, $PISO_2$. All of these polyimides, with the exception of Ultem, have a glass transition temperature of 250°C or higher (9, 27). In the past, the high thermal resistance and good physical properties of these materials have been offset by their high melt viscosities. However, newer resins, such as Mitsui Toatsu's LaRC-TPI, have demonstrated a transient molecular state which appears to improve melt flow. LaRC-TPI will be discussed in depth in the following section.

Since most polyimides have adequate physical properties and good solvent resistance, the majority of research has been aimed at tailoring the structure of the polymer to improve its processability (28, 29).

LaRC-TPI

LaRC-TPI (Langley Research Center-Thermoplastic Polyimide) is a linear thermoplastic polyimide which was developed in 1980 by NASA's Langley Research Center. The polymer was initially used as an adhesive material for bonding metals, films and composites.

The invention of LaRC-TPI followed an effort at Langley during the late 1970's directed toward developing a polymer adhesive to join polyimide film strips for the proposed heliogyro solar sail. The solar sail was to rendezvous with Halley's Comet

in 1986 (30). The high temperature adhesive which resulted from this work was dubbed LaRC-2. Figure 5 shows the structures of LaRC-2 and LaRC-TPI. LaRC-2, like LaRC-TPI, incorporates amine groups meta to the carbonyl in the dibenzophenone monomer. This meta bonding was found to greatly improve the adhesive strength and thermoplasticity of the polyimide (31). The carbonyl groups located between the aromatic rings provide flexibility to the repeat unit structure.

LaRC-2 had excellent adhesive properties; however, to decrease void formation in larger film joints an adhesive was needed which did not evolve volatiles. This adhesive was LaRC-TPI. LaRC-TPI did not create voids in adhesive joints because its low viscocity permitted the surfaces being bonded to be covered with the fully imidized thermoplastic, whereas, LaRC-2 was processed as a solution of the partially reacted polyamic acid. LaRC-TPI is prepared by the reaction scheme shown in Figure 6 (31). It is available as a dried, imidized molding powder from Rogers Corporation and as a dried powder or as 29 to 30% polyamic acid solution (LaRC-TPI precursor) in diglyme from MTC (32).

LaRC-TPI has a wide variety of applications. It is used as adhesive for metals including titanium, aluminum, copper, brass and stainless steel, as well as for composite materials (33, 34). Also, because it can withstand temperatures as high as that of molten solder, LaRC-TPI is used in film-laminated electronic circuits.

The analysis of powder samples of LaRC-TPI, produced by MTC using a proprietary process, yielded an important discovery. This powdered material, when heated to 300°C, exhibited a melt exotherm which indicated the presence of crystallinity. More importantly, upon melting, the initial viscosity of the polymer was much lower than that of any previously tested polyimide material (35). This created interest in using LaRC-TPI as a thermoplastic matrix for composites. Because of this, a study was conducted to determine the crystalline nature and to further improve the flow characteristics of the LaRC-TPI molding material produced by MTC. An

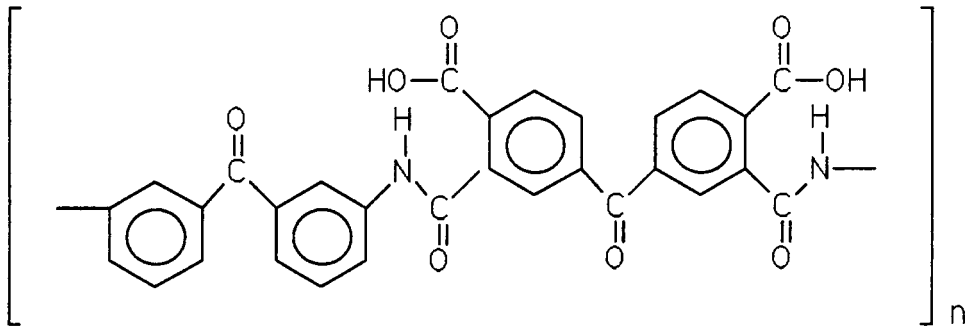

LaRC-2

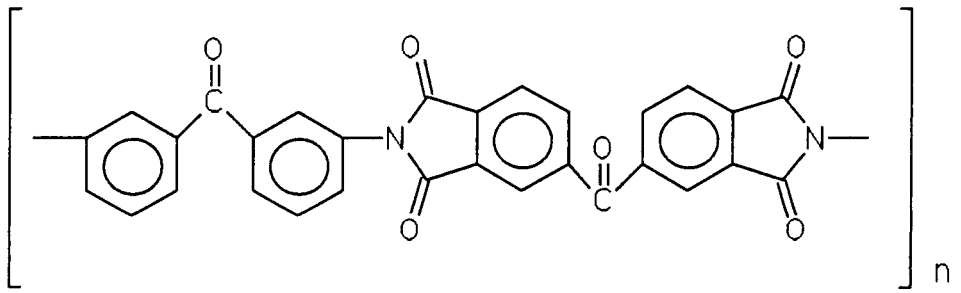

LaRC-TPI

Figure 5. Chemical Structures of LaRC-2 and LaRC-TPI

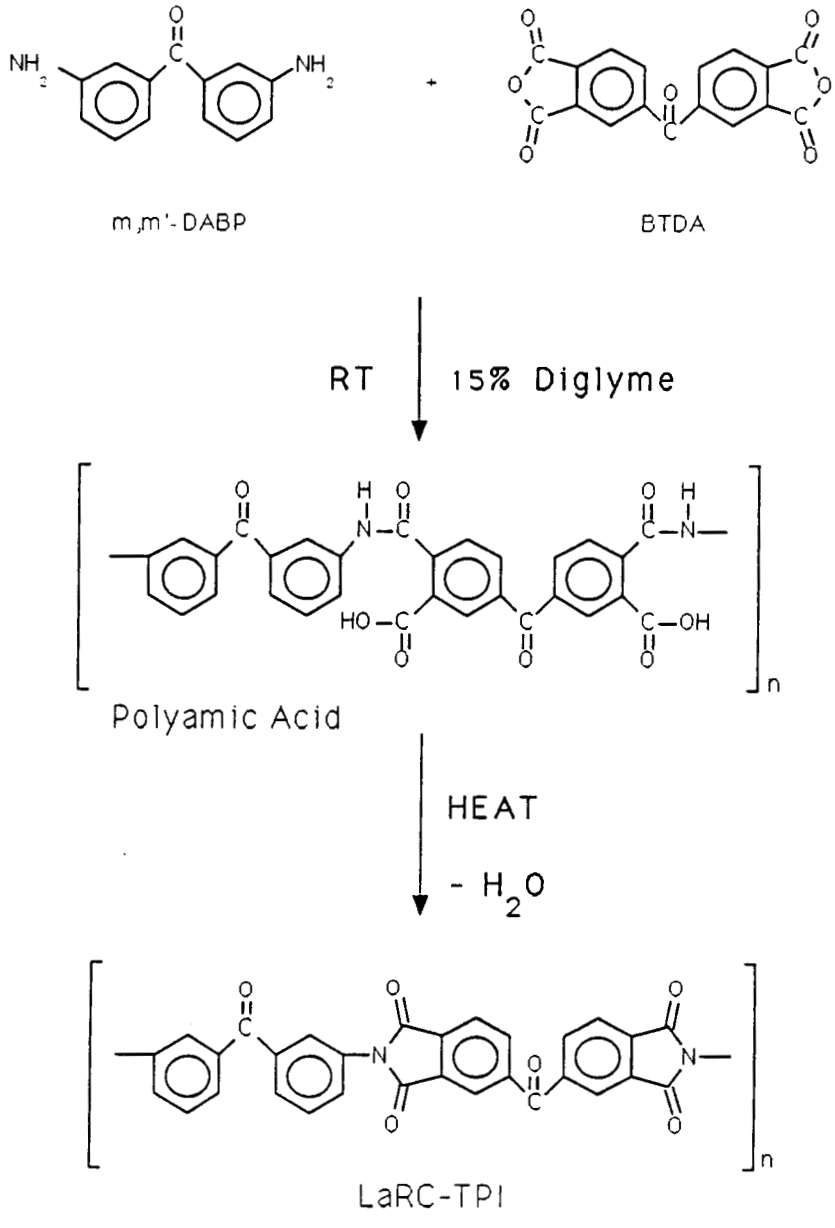

Figure 6. Chemical Reaction Scheme for the Preparation of LaRC-TPI

analysis of the Mitsui molding material (lot #72-501) showed that it was 91.9% imide, 5.8% amic acid, 3.1% isoimide. It had a 1.7% weight loss on drying (36).

Testing showed that the glass transition temperature, Tg, and the melt temperature, Tm, of the molding powder were low when initially melted. The initial Tg was approximately 210°C, and the initial Tm was 272°C. Infrared analysis of a number of samples which had been heated to different temperatures showed that the material was almost totally imidized . This conclusion was corroborated by thermo-gravimetric analysis which demonstrated less than 5% weight loss when samples were heated to 400°C (37).

However, when heated above 300°C, the characteristics of the material began to change immediately. A differential scanning calorimeter (DSC) study of the material showed that, when the MTC powder is heated above 300°C, both the Tg and the Tm begin to rise rapidly. This rise is irreversible and continues for about 60 minutes until an ultimate thermal condition is reached. This ultimate condition is a function of the temperature at which the material was annealed. Table 3 shows the values of Tg and Tm which can be reached after given times at different cure temperatures (35).

Three melt endotherms were observed on DSC for samples which were held at 280°C for extended periods. This indicates that a number of crystalline forms may be present in the polymer. The smaller endotherms on the DSC thermograms might also represent stressed crystalline structure at the interface between amorphous and crystalline regions (23). As the annealing temperature increased, the number of melting peaks decreased but the highest melt temperature increased (37). Samples annealed at 320°C for 60 minutes display only a single melt endotherm at 350°C.

Table 3. Effects of High Temperature Cure on LaRC-TPI Thermal Properties

Cure Temperature	Cure Time (minutes)			
	0	15	30	45
°C	Tg (Tm) °C	Tg (Tm) °C	Tg (Tm) °C	Tg (Tm) °C
300	210 (329)	211 (332)	216 (335)	221 (334)
310	215 (330)	221 (337)	227 (339)	231 (340)
320	214 (344)	226 (341)	237 (344)	241 (347)
330	215	232	243	249
340	216	239	244	251

Most of the melting temperature elevation is attributed to reorganization of the crystalline structure (37). It is likely that a chain extension reaction and an imide ring closure reaction also occur in the molten polymer (38). These chemical reactions have a strong effect on the Tg and a smaller effect on the Tm. The kinetics of the crystallization reaction may be controlled by an intermolecular oligomeric nucleation pathway (38). According to this hypothesis, pockets of oligomer or low molecular weight polymer form the seeds around which the crystalline regions grow. When the polymer is raised to a temperature above 300°C, these pockets begin to shrink as oligomers are incorporated in the chain extension reaction. Once the oligomer is exhausted, further crystallization proceeds very slowly. At temperatures above 320°C, the critical annealing temperature, no appreciable crystallization will take place in the MTC material, but any chemical reactions will occur at a high rate and increase the Tg. Other samples of LaRC-TPI, prepared at Langley Research Center, exhibit a critical annealing temperature of 340°C (39).

Both the polymerization reactions and the crystalline reorientation have a strong effect on the viscosity. This makes the melt viscosity quite time dependent, as illustrated in Figure 7 (35). This diagram shows the magnitude of complex viscosity as a function of cure time. The complex viscosity was determined at a frequency of 10 rad/sec which corresponds to a shear rate similar to that encountered during composite formation. Figure 7 also shows that there is a low viscosity induction period during which the transient crystalline state within the LaRC-TPI re-orients (35). If processed quickly so as to take advantage of this low viscosity state, LaRC-TPI could be effectively used to form composite matrix materials.

Further work is underway to improve the properties of LaRC-TPI. A new higher molecular weight molding powder has been synthesized by incorporating an organic base catalyst, triethylamine, in the reaction mixture before the cyclodehydration step (40). The primary advantage of this new material is that it can provide a Tg of about 250°C within a thirty minute annealing time. This higher Tg increases the use temperature of the polymer by about ten degrees Celsius when compared to the earlier material and, thus, it offers the possibility of improved matrix physical properties. The newer version has an initial melting temperature of 295°C and an initial crystallinity ranging from 40 to 50% (40).

Mixtures of LaRC-TPI and polyimide sulfones have been produced. These mixtures take advantage of the solvent resistance and lower viscosity of LaRC-TPI and the increased resin properties and higher Tg of the $PISO_2$. As the percentage of LaRC-TPI in the polymer blend is increased, the viscosity decreases (32, 41).

The possibility of plasticizing LaRC-TPI with a variety of materials has been explored (42, 5). One successful technique used 2.5% by weight of the bisamideacid from pyromellitic dianhydride and aniline complexed with N-methyl pyrrolidone (PMDA-An · 2 NMP) the structure of which is shown in Figure 8. Used in composite samples, this blend not only improved matrix distribution but resulted in a composite

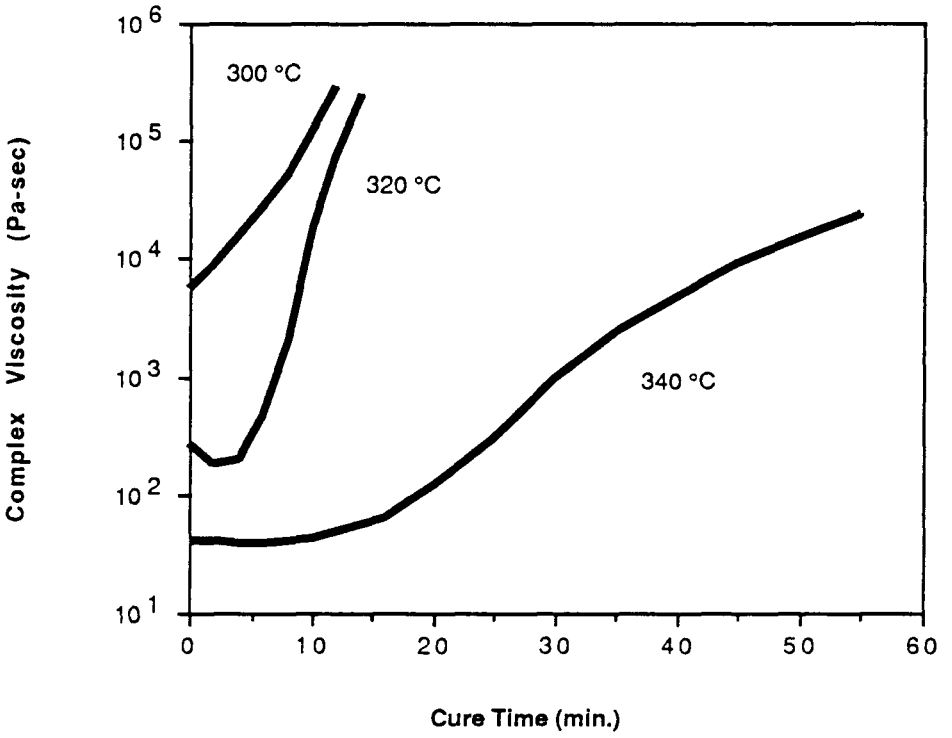

Figure 7. Complex Viscosity Versus Cure Time for LaRC-TPI at Three Temperatures

flexural strength of 1104 MPa (160 ksi) and a flexural modulus of 97 GPa (14.1 msi) at 205°C.

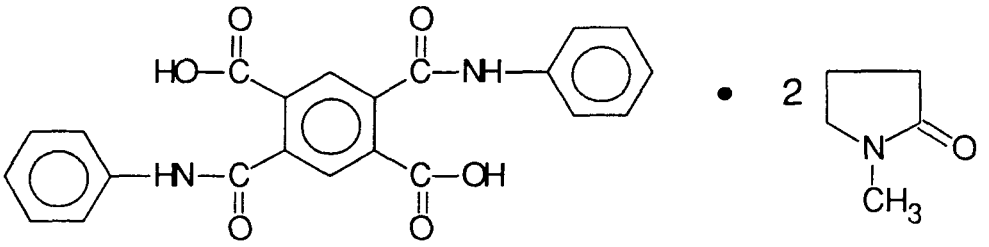

PMDA-An · 2 NMP

Figure 8. Chemical Structure of the Plasticizing Agent PMDA-An • 2NMP

Also, combinations of thermoplastic LaRC-TPI and thermoset acetylene-terminated LaRC-TPI, (AT-LaRC-TPI), have been produced and tested (43). These systems are called semi-2-interpenetrating networks or semi-2-IPN's (the "2" indicates that the thermoset network is formed second). The AT-LaRC-TPI oligomer plasticizes the LaRC-TPI, improving its processability and increasing its thermo-oxidative stability. Laminates were prepared using a solvent coating system by Egli, et al. (44). These laminates were consolidated at 300°C and 3.44 MPa (500 psi) into composite specimens that were nearly void-free. The biggest disadvantage of this technique may be a loss in toughness caused by the high degree of cross-linking.

CHAPTER III

PROCESS DEVELOPMENT

The high performance composite materials used in aerospace and military applications have been slow to move into commercial aviation, automotive, and consumer markets. Although many advantages would be gained by their use, often the price of such composites is prohibitive. Raw materials account for only about one third of this price, and the remainder may be attributed to processing costs. Therefore, the key to expanding the market for composite materials is developing improved, low cost processing methods.

Nearly all commercially available prepregs are produced using thermoset polymers. Carbon fiber bundles are impregnated with the uncured resin in a low molecular weight form to create the prepreg. Unfortunately, these thermoset prepregs tend to be tacky and difficult to work with, often making hand lay-up of composite parts necessary. Also, until cured, thermoset polymers are reactive, making refrigeration prior to use and during shipping necessary.

As discussed in Chapter I, a number of thermoplastic polymers are available today which have superior physical and thermal properties when used as a matrix material in carbon fiber composites. Prepregs incorporating these materials do not require refrigeration and are easier to handle than comparable thermoset prepregs. The major obstacle to the use of these promising new polymers is that carbon fiber tows are difficult to impregnate with these materials.

Previously, Gantt (2) showed that the thermoplastic matrix material can be applied to the carbon fiber tow using a powder coating technique. This technique eliminated the problem of melt impregnation and produced a coated fiber prepreg which was more flexible than traditional melt, solvent, or slurry coated tow. The

coated tow was quite flexible, making the product attractive for weaving, braiding or knitting into textile preforms, thus providing the potential for automated composite formation. However, the coating process developed in the initial research required continuous monitoring, and the thickness of the polymer coating varied considerably along the length of the prepreg product.

Therefore, the object of the present research was to develop an automated continuous process for coating carbon fiber with a thermoplastic polymer. While the coating thickness applied in the initial research was highly variable, the work did demonstrate that any continuous powder coating process would require a low-friction roller system to transport the yarn through the process, a carefully controlled yarn feed and take-up system, a device to spread the tow prior to coating, a device which applies an even coating of the thermoplastic powder, and an electrical heating system to melt the powder onto the spread fiber tow. The development of each of these is described in the following sections.

Roller Alignment System

At the beginning of the present research, a roller alignment system which ensured proper alignment of the rollers and allowed a great deal of design flexibility was constructed. Figure 9 shows this system which consisted of polished steel rods mounted on aluminum blocks. Other blocks with roller mounting posts slid along the steel rods and could be positioned as needed. Two types of rollers were used: a graphite roller to merely transport the fiber tow, and metal rollers for use in the electrical heating section of the system.

In order to provide the necessary low friction transport of the fiber tow, four smooth and four slotted 5.1 cm diameter graphite rollers were placed on 1.91 cm (3/4 inch) rods and attached to bearings in mounting blocks. In the initial design, 1.91 cm (3/4 inch) ID (inside diameter), 4.13 cm (1-5/8 inch) OD (outside diameter) bearings

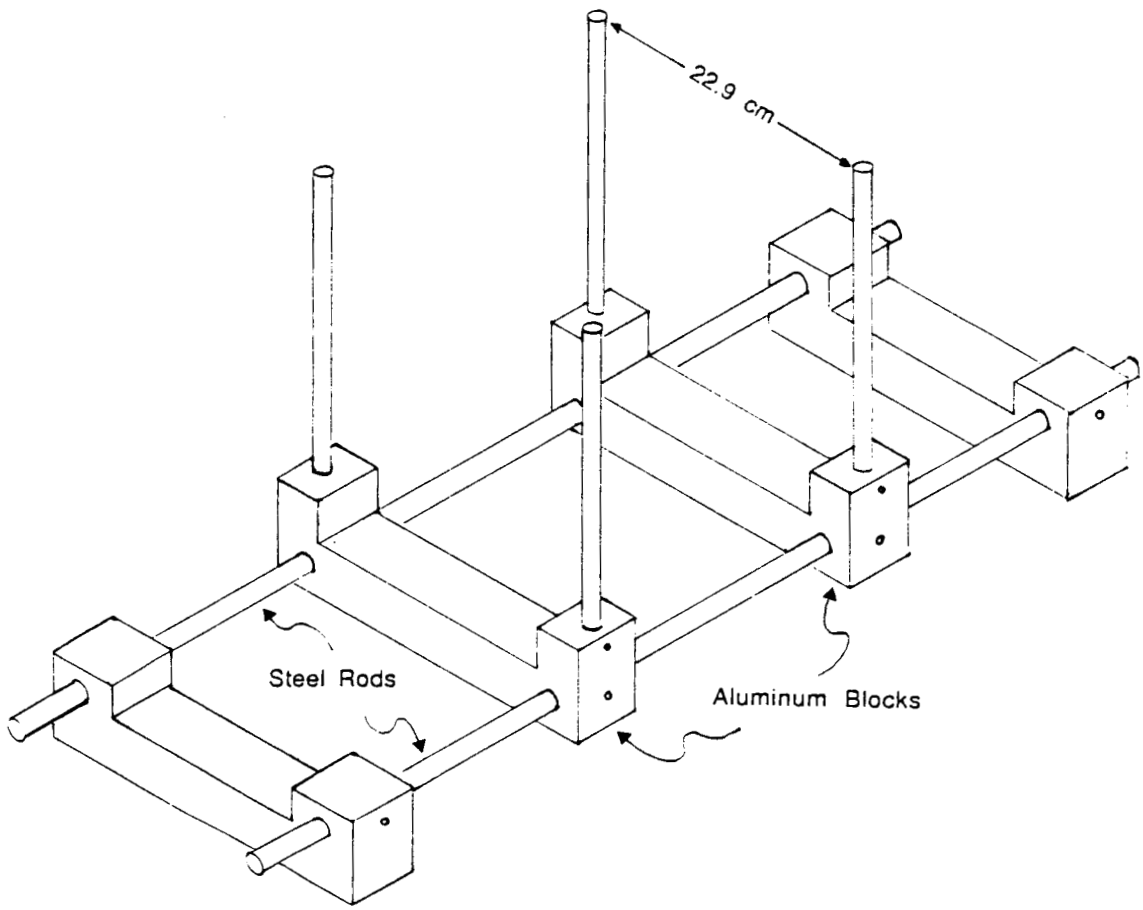

Figure 9. Schematic of Roller Alignment System

were used; however, even with the packing grease removed, these bearings did not turn freely. Several alternative systems were investigated including the use of high precision bearings or air bearings. It was found that smaller diameter bearings generated much less friction, and, therefore, 0.64 cm (1/4 inch) ID, 1.59 cm (5/8 inch) OD bearings were installed in mounting blocks as shown in Figure 10. During initial tests of the bearings and mounting blocks, it was found that the roller had to be absolutely level to guarantee alignment of the bearings and, thus, minimize friction.

For use in the electrical heating section of the coating apparatus, three large metal rollers were fabricated from sections of 8.89 cm (3-1/2 inch) OD stainless steel pipe and three were made using sections of 7.94 cm (3-1/8 inch) OD copper pipe for use in the carbon fiber heating section of the apparatus. These large hollow-metal rollers, shown in Figure 11, had aluminum end plates into which 1.59 cm (5/8 inch) OD bearings were press-fitted. Rubber tubing was pulled around the ends of the 0.64 cm (1/4 inch) mounting rods to help secure them in the mounting clamps and to electrically isolate the rollers when the fibers were electrically heated. This variety of roller was simple to fabricate, and bearing alignment proved to be less critical.

Tow Movement and Tension Control System

The previous research by Gantt (2) showed that, for the coating line to operate continuously, the coated tow would need to be traversed onto the take-up spool. The options available were either traversing the oncoming tow onto the spool, or holding the tow in place, laterally, and moving the spool from side to side. Although the first system would be easier to fabricate, it would require at least one additional contact roller and apply a large amount of lateral stress to the delicate prepreg, causing filament damage. Because of this, it was decided to traverse the spool rather than the prepreg.

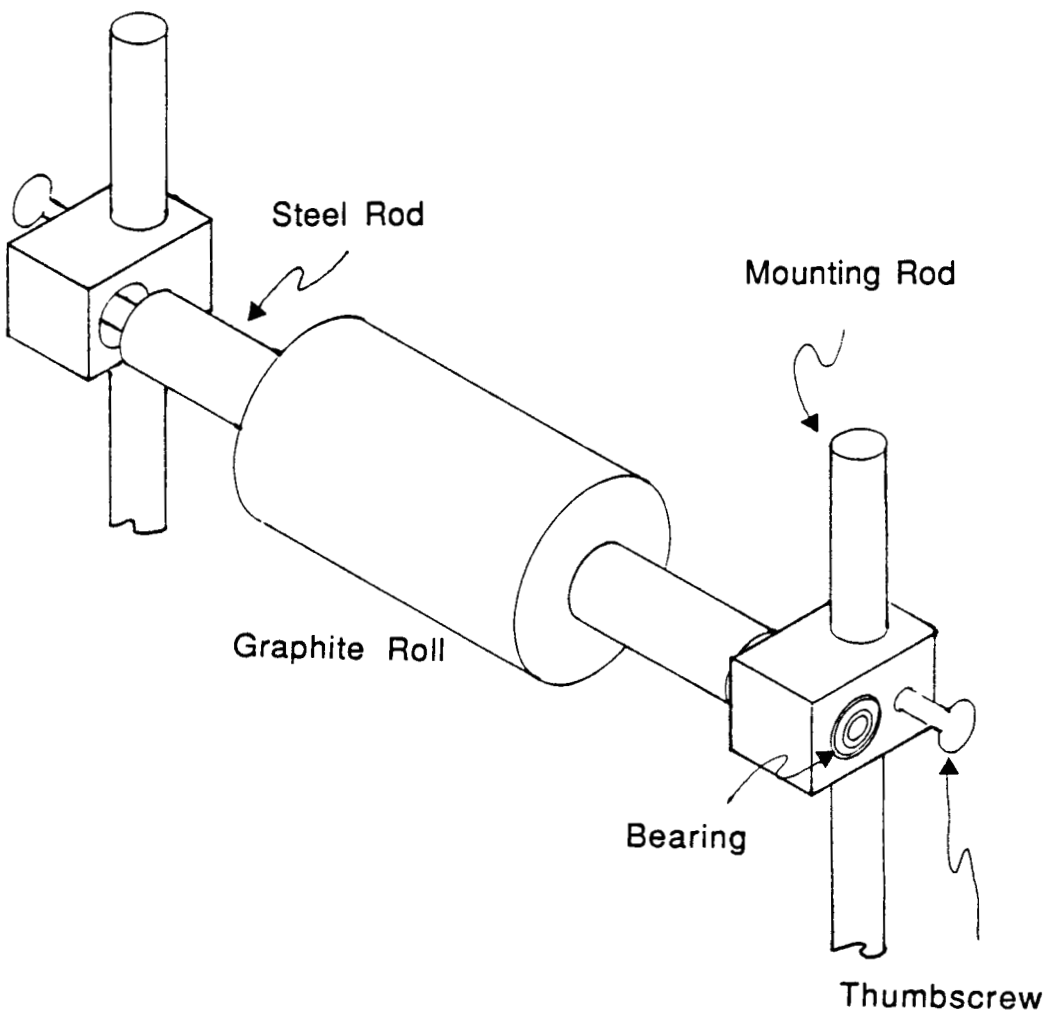

Figure 10. Graphite Roller

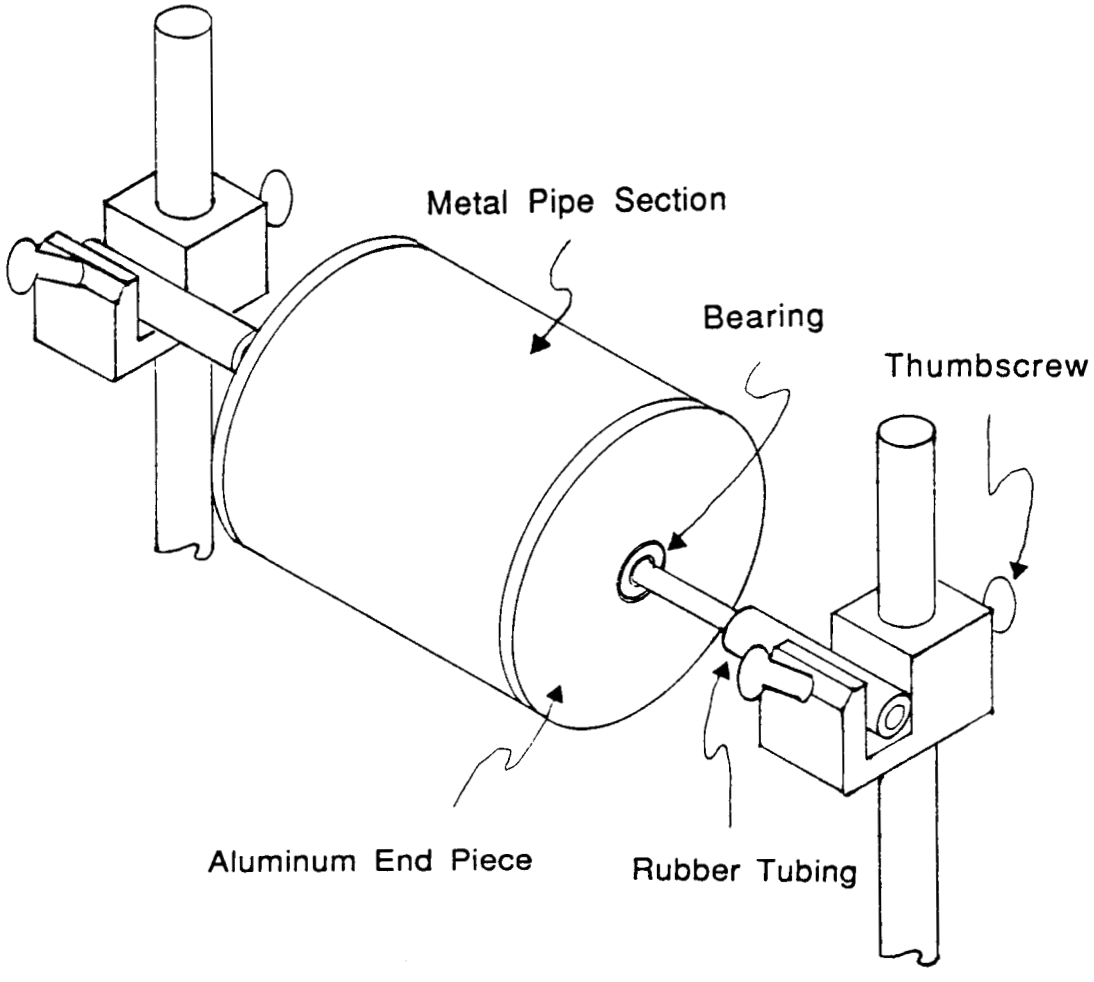

Figure 11. Roller Made from Metal Pipe Section

Several techniques for moving the spool from side to side were considered. A simple, flat eccentric cam could be employed. Also, the spool could be mounted on a threaded shaft. Thus, turning the shaft clockwise would drive the spool in one direction, and turning the shaft counterclockwise would return the spool to the original position. Although, both options would be easy to fabricate, both designs would wind a spool with a large quantity of material on the ends and a much smaller quantity in the middle.

Finally, a third technique, which employed a device called an interior worm cam, was selected. The 25.40 cm (10 inch) worm cam was cylindrical in shape and had a continuous "right-hand thread" slot which reversed at the ends to a "left-hand thread." A shoe riding in this slot pulled the spool back and forth as the cam rotated. The spool-mounting system (shown in Figure 12) consisted of two end pieces which were connected by three rods, a cam follower foot, and a bearing-mounted cam arm.

Next, a system to connect the spool to the rotating drive rod of the take-up was designed and fabricated. The spool had to be fixed in the direction of rotation but free to move along the shaft. Therefore, in order to allow the spool to slide along the shaft, a slot was machined into the wind-up shaft, and small brass keys were attached to the spool end pieces. Unfortunately, with this design excessive friction kept the spool from moving freely. It was obvious that a bearing mount was needed to minimize friction.

After examining several methods for fixing bearings to the shaft, it was decided to mount two 1.59 cm (5/8 inch) OD and 0.64 cm (1/4 inch) ID bearings to each of four 7.6 cm washers as shown in Figure 13. Two washer mounts were built in configuration "A" and two in configuration "B". These "A" and "B" washers were then alternated on the three threaded rods which held the spool ends together. The bearings on the washers were carefully positioned with the levelling screws to ride

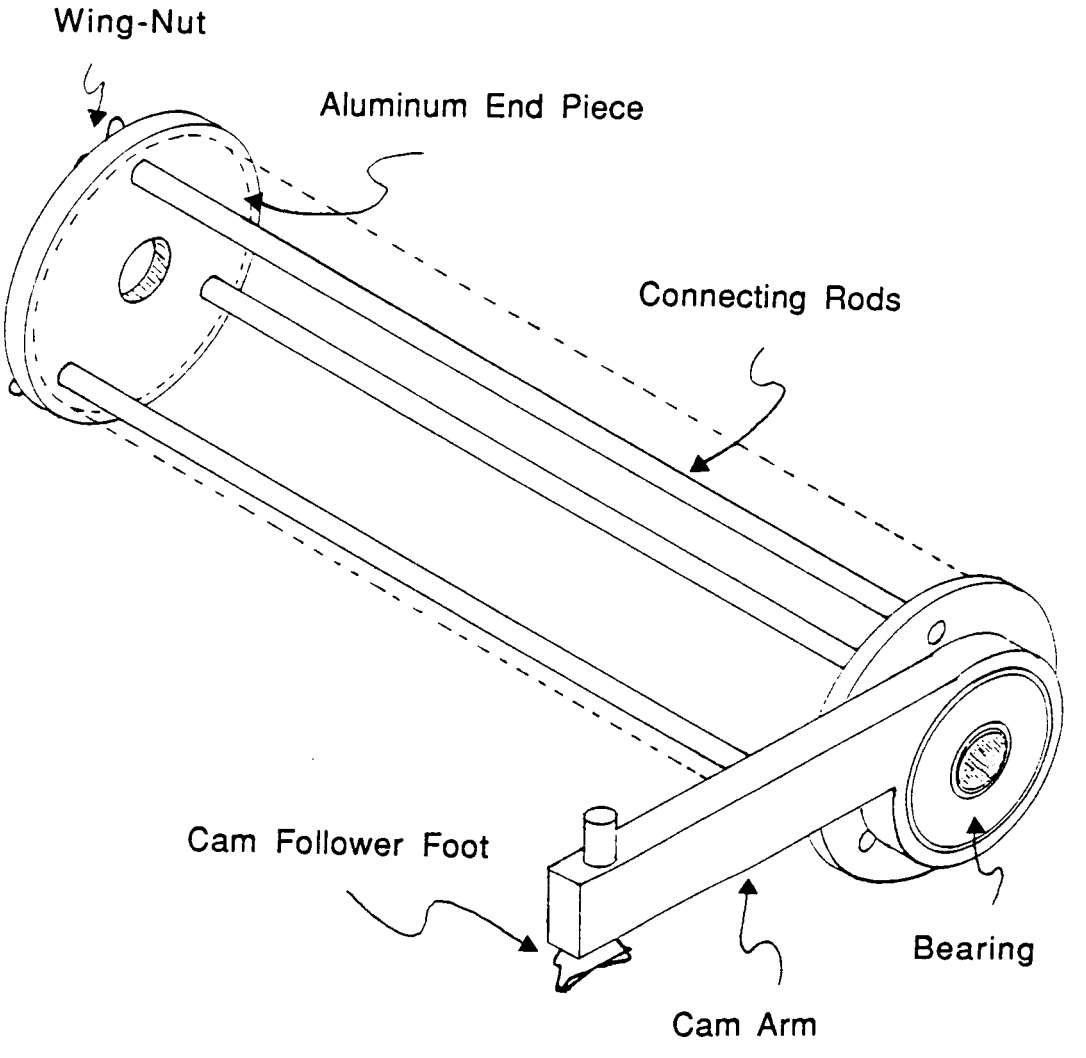

Figure 12. Spool Mounting Assembly

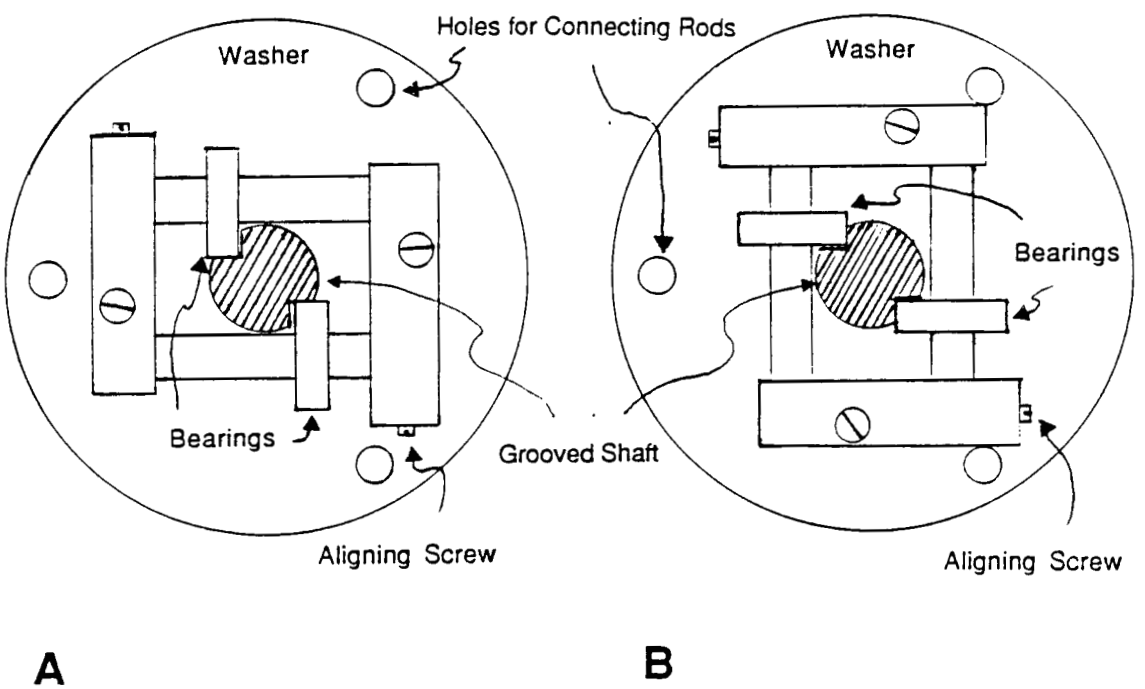

Figure 13. Bearing System for Traversing Take-Up Spool

along the flats in a grooved take-up shaft (see Figure 13). This apparatus provided excellent tangential stability and minimized friction.

The remainder of the take-up was assembled as shown in Figure 14. The power for both the wind-up and traverse was provided by a DC motor with an internal 33:1 worm gear reducer. An additional 50:1 gear reducer and a 4:1 v-belt pulley connection reduced the take-up speeds to the desired range of 0 to 3.8 m/min. The speed was controlled using a variable DC power supply. The traverse rate could be controlled independently with a variable gear reducer.

To keep the tow stationary as the spool traversed, a graphite fiber-guide wheel was fabricated and mounted on a low-friction separator roll. This guide wheel assembly was located 1.3 cm in front of the take-up spool.

Driven Take-off Spool and Dancer Arm

A spool mount similar to that shown in Figure 12 was used for the take-off, except that the take-off did not require a cam arm. Initially, the take-off was not driven. However, this undriven take-off could not provide the constant low tension needed to operate the spreader. This requirement made a drive and feedback motor synchronization system necessary.

A DC motor, identical to that powering the take-up, in conjunction with a 50:1 gear reducer and a 5:1 v-belt pulley connection, was purchased to drive the take-off system. Initially, a weighted pulley, which was able to move up and down to provide constant tension, was installed between the take-off roll and the first roller. During operation of the coating line, the take-off motor speed was adjusted manually to keep the pulley at a nearly constant level. Although the pulley did not provide motor speed control and damaged the fiber, it provided an interim solution to tension control and allowed work to be carried out with other aspects of the coating line.

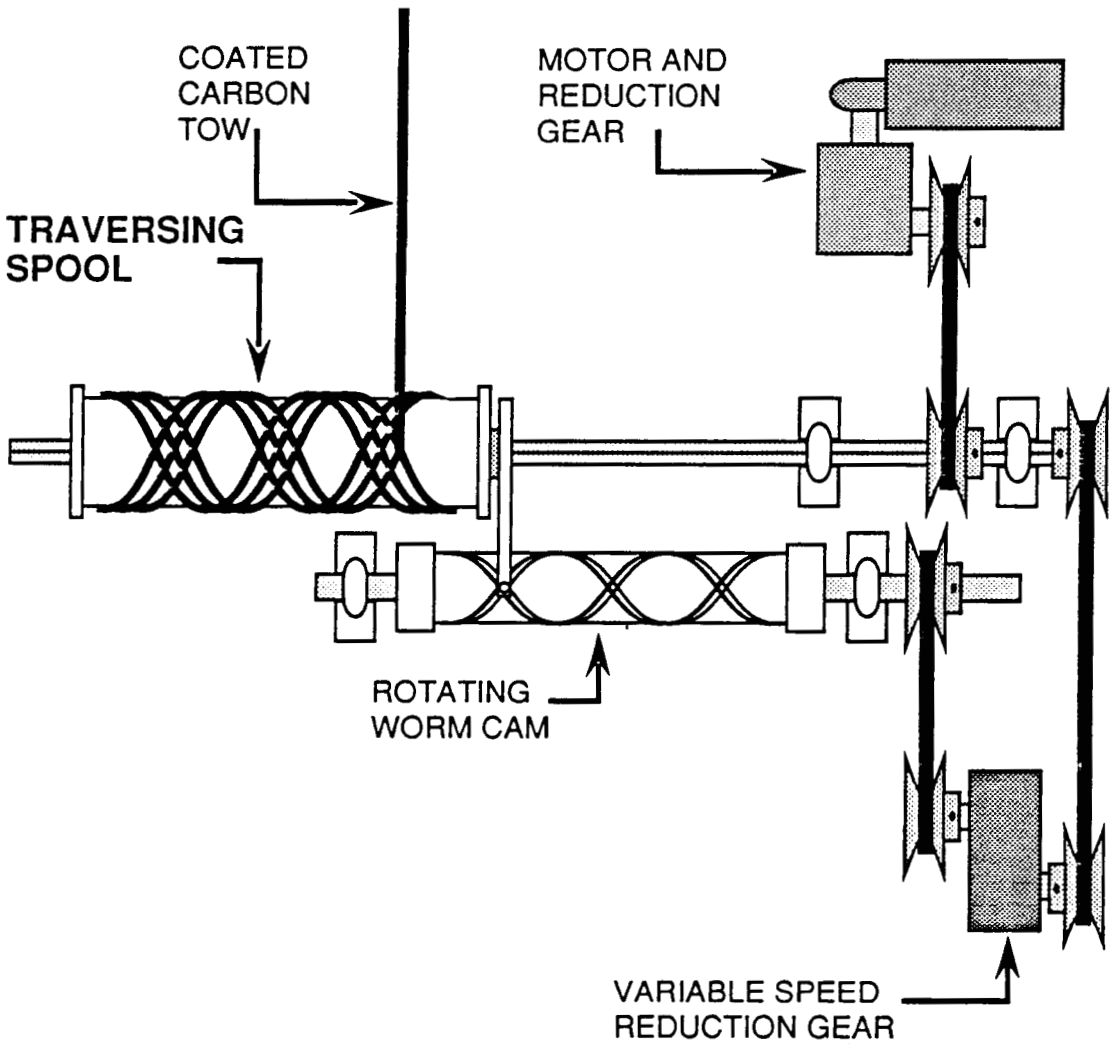

Figure 14. Schematic of Traversing Take-Up Apparatus

Eventually, the dancer arm control device, shown in Figures 15 and 16, was designed and installed. The dancer arm itself was mounted on a potentiometer which was connected to the take-off motor control circuit. The potentiometer sensed the position of the dancer arm and generated the signal used to control the speed of the take-off motor. If the motor was too slow with respect to the speed of the wind-up, the dancer arm would move downward. This rotated the knob on the potentiometer, increasing the take-off motor speed. Similarly, if the motor was turning too fast, the potentiometer adjusted its speed downward. The type of potentiometer used at the pivot determined the gain of the control system. If a potentiometer with a full-scale resistance of 5K ohms was used, a considerable movement in the dancer arm would be required to change the motor speed sufficiently. However, if the full-scale resistance were increased, much less movement in the arm would be needed to change the motor speed by the same amount. It was found that a 75K ohm potentiometer provided an appropriate gain for the control loop. The potentiometer was wired in series with the DC motor speed controller. The second potentiometer could then be used to adjust the steady-state position of the arm. The tension on the fiber tow could be changed by moving the 1 kg weight on the threaded rod of the arm. Thus, both the tensioning and motor synchronization could be controlled using the same device.

To minimize fiber damage, three graphite wheels with diameters of 8.26 cm were used on the dancer arm assembly. One wheel was mounted on two 0.95 cm (3/8 inch) OD bearings on the end of the arm, and the other two were attached to a single bearing-mounted shaft below the arm. The incoming fiber wound around one of the lower wheels and then passed up to the dancer arm and down around the second wheel (see Figures 15 and 16). By attaching both lower wheels to the same shaft, no work was lost turning a second shaft. The two lower wheels were fixed very loosely to the shaft, enabling them to rotate at different speeds as the position of the

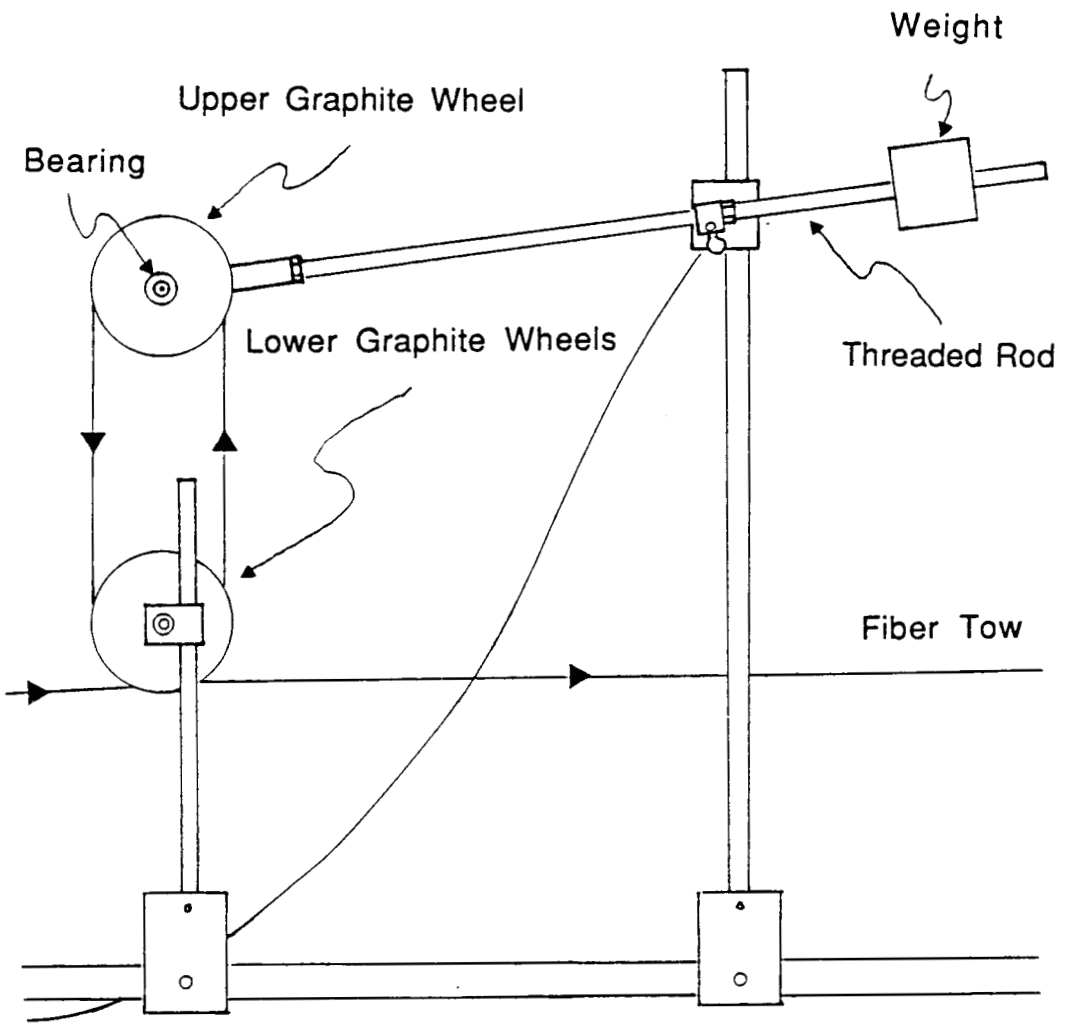

Figure 15. Front View of Dancer-Arm Tension Controller

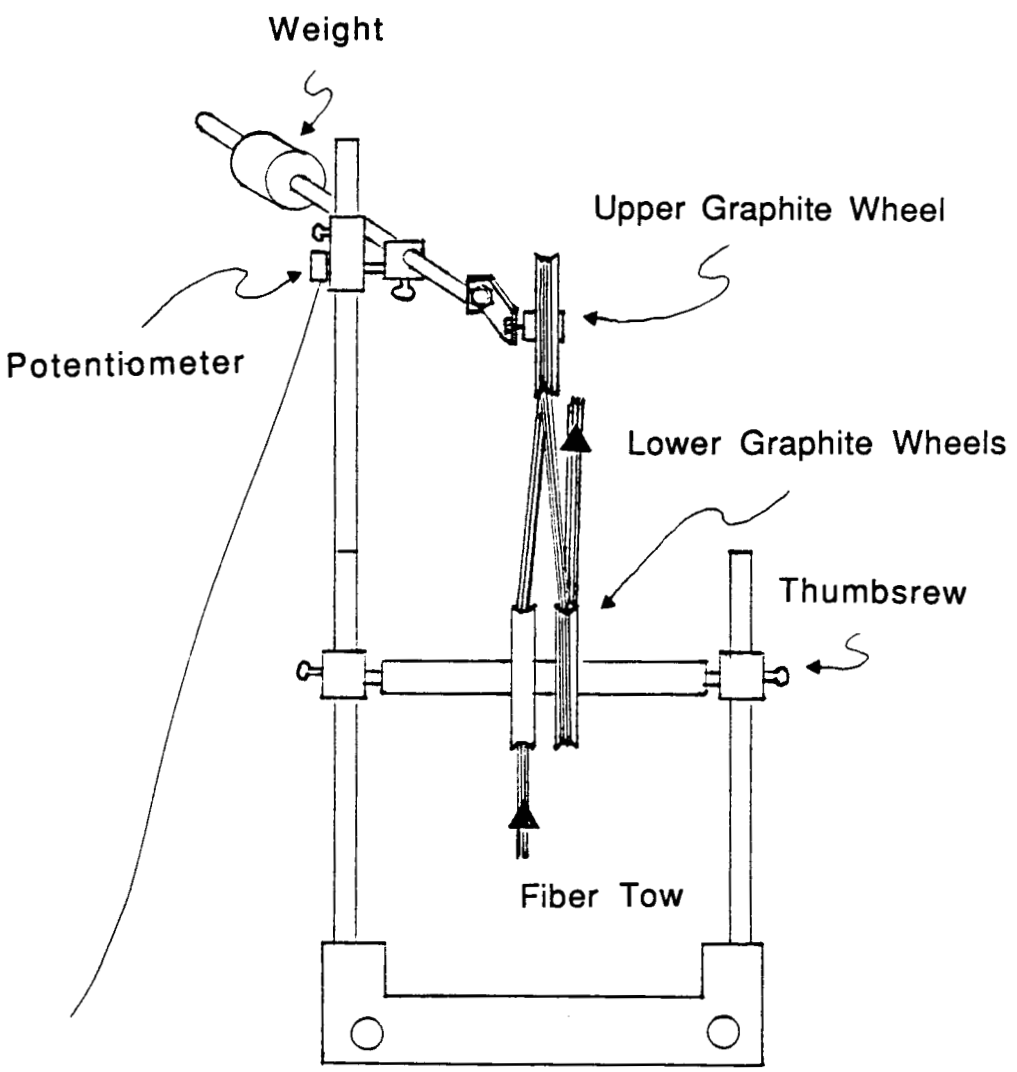

Figure 16. Side View of Dancer-Arm Tension Controller

dancer arm changed. Also, the lower wheels could be moved from side to side to center the tow on the coating line.

Fiber Spreading

Spreading carbon fiber tow for coating without damaging the individual filaments is a challenging problem. In work carried out by Gantt (2), convex rollers and consecutive s-wraps were used to spread the tow. While this technique did flatten the tow, the actual tow spreading was not adequate to allow the individual filaments to be subsequently coated with powder. The idea of splitting the tow with thin rollers or razor blades was considered; however, this would result in a great deal of fiber damage and still probably not adequately spread the tow. Finally, it was decided to use a pneumatic spreading technique developed by Kim and Gray (45) at the Naval Research Laboratory. The device designed by Kim and Gray spread a 12K tow to a width of 7.5 cm at a rate of 3 to 6 meters per minute. This was exactly the degree of spreading required for the powder coating line except that a smaller 3K tow would be used instead of a 12K tow. The spreader built by the Naval Research Laboratory, shown in Figure 17, had two slots. The first slot, S1, was about 20 cm long by 30 cm wide, and the second, S2, was 50 cm long by 30 cm wide. The vertical height of both slots was 0.64 cm. The device contained an air-tight chamber, L1, and a plenum, L2, from which air was drawn to a vacuum cleaner. The slot restrictors A, B, A', and B', were adjustable to control the degree of tow spreading. Air was drawn into the slots and forced to expand across the fiber path. This lateral air motion spread the fibers without damaging them excessively. To keep the fibers from being abraded, graphite was sprayed onto the surface of the slots.

In the present research, this general design was used for several experimental spreaders which were 46 cm long and 23 to 26 cm wide. It was found that no spreading occurred unless the vertical slot spacing was 0.64 cm or less. Initially, fans

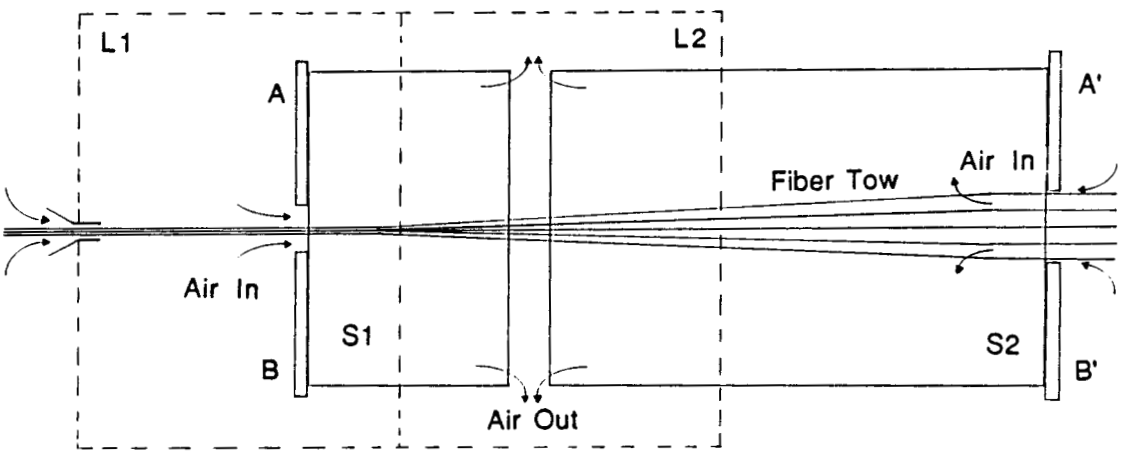

Figure 17. Schematic of the NRL Fiber Spreader Slot Configuration

were used to move air, but this proved unsuccessful. This failure was attributed to the low maximum pressure drop which could be maintained across a fan. Tests showed that a vacuum system would provide the pressure drop needed to spread the tow. However, during these initial tests it was also found that an important parameter for controlling the tow spreading was the tension on the fiber tow. Thus, no continuous spreading was possible until the dancer arm tension controller was in place. With the incorporation of the dancer arm and an adjustable speed vacuum cleaner, fine tuning of the final spreader design was possible.

Finally, the fiber spreader shown in Figure 18 was designed and constructed. This spreader was compact, easy to assemble, and versatile enough to permit evaluation of a number of different slot configurations. The framework shown in Figure 18 fixed the slot width at 25.5 cm or less and provided top and bottom attachments for a 10.2 cm (4 inch) dryer hose. A 10.2 cm (4 inch) PVC "T"-joint was used in conjunction with a number of reducers to allow the hose to be attached to the 5.1 cm nozzle of the vacuum system. The spreader walls were made from 0.64 cm (1/4 inch) Plexiglas.

After a slot with a constant height of 0.64 cm was installed, tests were conducted to determine the optimum slot length. If the entry section of the vertical slot was too long, the tow would divide into two bundles and destroy the spreading effect. However, if the entry section of the vertical slot was shortened to 10 cm or less, this tow splitting decreased. The exit section of the vertical slot was found to be the region in which the majority of the uniform and effective spreading took place. This section worked well at a length of 27 cm.

The center area through which the air entered the plenum chamber was found to create a destabilizing air flow which whipped the tow back and forth. A 5 cm wide enclosure was built to fit between the entry and exit section and protect the tow. The transparent rounded walls of this central isolation chamber were made from

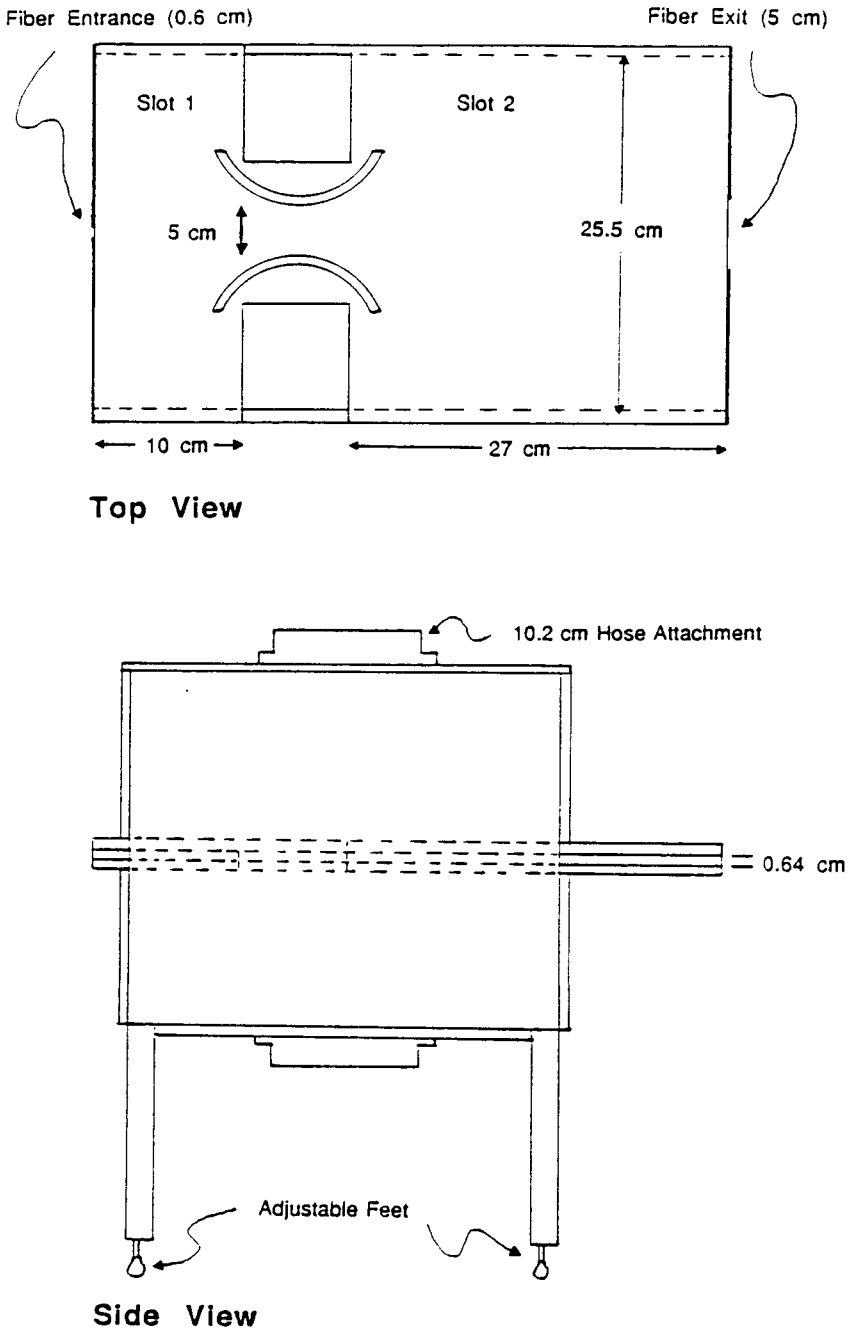

Figure 18. Schematic of Pneumatic Fiber Spreading Device

polyacrylate pipe. The enclosure also served to ensure that the tow did not divide in the entry section of the vertical slot and improved spreading in the exit section.

Finally, using these optimum slot sizes, a single piece Plexiglas top and bottom for the spreader section was fabricated. This could be easily removed for cleaning and had fewer sharp edges to abrade the tow. The inside surfaces were polished with a graphite powder which decreased the buildup of any static charges within the spreader. After extensive testing of the spreader, grey tape was used to narrow the entrance slot to 0.6 cm and the exit to 5 cm. Also, a ceramic pigtail guide was placed about 5 cm in front of the spreader to keep the tow in the center of the entrance slot.

This final design provided excellent tow spreading but, unfortunately, it was not possible to operate the spreader without supervision. There was a tendency for the tow to either split in two, pull together, or flip to one side. However, a slight increase in the tension on the tow was found to eliminate tow splitting or move the tow back to the center. Also, a slight decrease in the tension would reinitiate the spreading if the tow pulled together. During operation of the spreading device, these brief changes in tension were made by manually moving the tensioning arm either up or down. Also, spreading was not absolutely uniform. The spread tow tended to have a higher concentration of fibers at the edges than in the center. To alleviate this problem the tow was manually redistributed to the center every several minutes. To facilitate this manual readjustment of the tow, a large polished stainless steel roll was placed at the exit of the spreader. Upon leaving the stainless steel roll, the tow was s-wrapped around two graphite rolls to stabilize the spread. Also, this s-wrap isolated the low tension in the tow spreading section from the higher tension in the coating and melting sections of the line.

The proper airflow and tension for optimum spreading were determined by trial and error and varied with the line speed. The tension within the spreader was measured using a Rothschild Mini-Tens R-046 and was found to be less than 17

grams. However, the low tension made an accurate measurement difficult. The exact air flow rate for optimum spreading was not measured. However, it was found to be lower than that obtained by adjusting the 2.5 hp vacuum cleaner to its lowest speed setting. The speed of the vacuum motor was reduced below this level by plugging the motor into a variable autotransformer. During optimum spreading, this variable 125 V AC autotransformer was set at about 80% of full scale.

Recirculating Polymer Powder Deposition Chamber

Initial Trials

Because the method used to apply a polymer to a prepreg determines to a great extent the physical characteristics of the end-product, the coating section is a critical part of the process. During early trials, various slurry coating methods, such as the use of dip tanks or kiss rollers, were investigated. Since LaRC-TPI powder is slightly hydrophobic and will not form a slurry, small quantities of ammonium hydroxide or polyvinylalcohol were used as suspending agents. However, these suspending agents could not be removed by a simple heating step, making it likely that the end-product composites would contain these impurities. Also, since no highly volatile solvents will dissolve the near-fully imidized LaRC-TPI powder to any appreciable degree (32), solvent coating was not used.

The elimination of both solvent and slurry coating left dry powder coating as the only option. Previously, Gantt (2) had found that the dry polymer readily adhered to the fiber tow. At the start of the present research, three methods were considered for applying the dry coating to the spread fiber tow. The first was merely dumping the polymer powder onto the fiber. Another method was to press the powder into the tow using a wheel or kiss roller. The third technique was to coat the spread tow by passing it through a partially fluidized powder environment.

Since Gantt (2) found that the dumping technique produced a very non-uniform prepreg, this method for applying the powder was rejected. Initial trials showed that a kiss roller was not a reliable coating technique because only static electricity caused the powder to adhere to the metal kiss roller, so, the powder stopped adhering to the roll as soon as it charged to the same potential. Another problem was that the metal kiss roller caused additional fiber damage. With the elimination of the first two methods, the research concentrated on evaluating fluidized powder coating. Initial tests of fluidized coating appeared promising, but immediately it became obvious that for continuous operation an effective means of containing and fluidizing the powder would be required.

The powder used in the first evaluation trials was Eastabond FA 252. This powder had nearly the same consistency as LaRC-TPI but was much less expensive. The object of the initial fluidization tests was merely to determine the best method for fluidizing the powder. A clear plastic cup was used to contain the powder, and slots were cut in the cup to allow the fiber tow to pass through it. The top of the cup was covered with cellophane to decrease powder loss. In initial trials, a magnetic stirring bar was used to fluidize the powder. However, the stirrer power was barely enough to continuously rotate the bar, and any minor disruption stopped the rotation.

Next, a shaft-driven stirrer was installed through the cellophane in the top of the cup. The stirrer had four blades which were 8.9 cm in diameter and the blade pitch was just under 90°, or nearly vertical. Initially this stirrer formed a good cloud of polymer. But, during continuous operation, the powder fines stayed airborne while the larger particles of powder quickly separated and settled to the bottom of the cup. In the next series of trials, to provide more lift to the powder and better maintain the cloud, the pitch was reduced to approximately 45°. This stirrer pitch created an excellent powder cloud and cured the powder separation problem. However, when

the powder was thoroughly airborne, it quickly escaped from the poorly-sealed chamber. Therefore, the next step was to develop an improved fluidization chamber.

To better contain the fluidized powder, a small Plexiglas chamber was constructed. The chamber was approximately 12.7 cm high and 12.7 cm in diameter. In this design, the stirrer was mounted underneath the chamber, and the shaft passed through a bearing which was press-fit into the Plexiglas base-plate. This improved seal around the shaft reduced the powder leakage from the chamber. Since the stirrer was inverted, the pitch of the blades was reversed to provide the same powder lift obtained with the top-mounted stirrer. The top of the chamber consisted of two sections: the first was 20 cm square with a 7.6 cm diameter hole in the center, the second was 20 cm square with no hole. Semicircular spacers were used to hold the second square section 0.64 cm above the first. This formed a slot between the two sections through which the fiber could be passed.

With this chamber design, the stirrer acted much like a centrifugal pump and blew a continuous cloud of powder out the slot openings. Since the cloud of powder, if controlled, appeared to be a promising method for evenly coating the fiber tow, it was decided to incorporate a recirculating chamber with this type of fluidization system in the final coating line.

First Recirculating Chamber

Based on these results, the chamber shown in Figure 19 was constructed. The rounded walls were cut from 12.7 and 20.3 cm (5 and 8 inch) clear polyacrylate pipe sections. The smaller center section was removable to allow easy access to the inside of the chamber. The chamber sides were attached to the 0.64 cm polyacrylate ends and bottom with small screws. The aluminum base plate contained a hole into which a 2.22 cm (7/8 inch) OD, 0.95 cm (3/8 inch) ID bearing was pressed. The shaft of the brass stirring blade from the earlier work passed through this bearing and

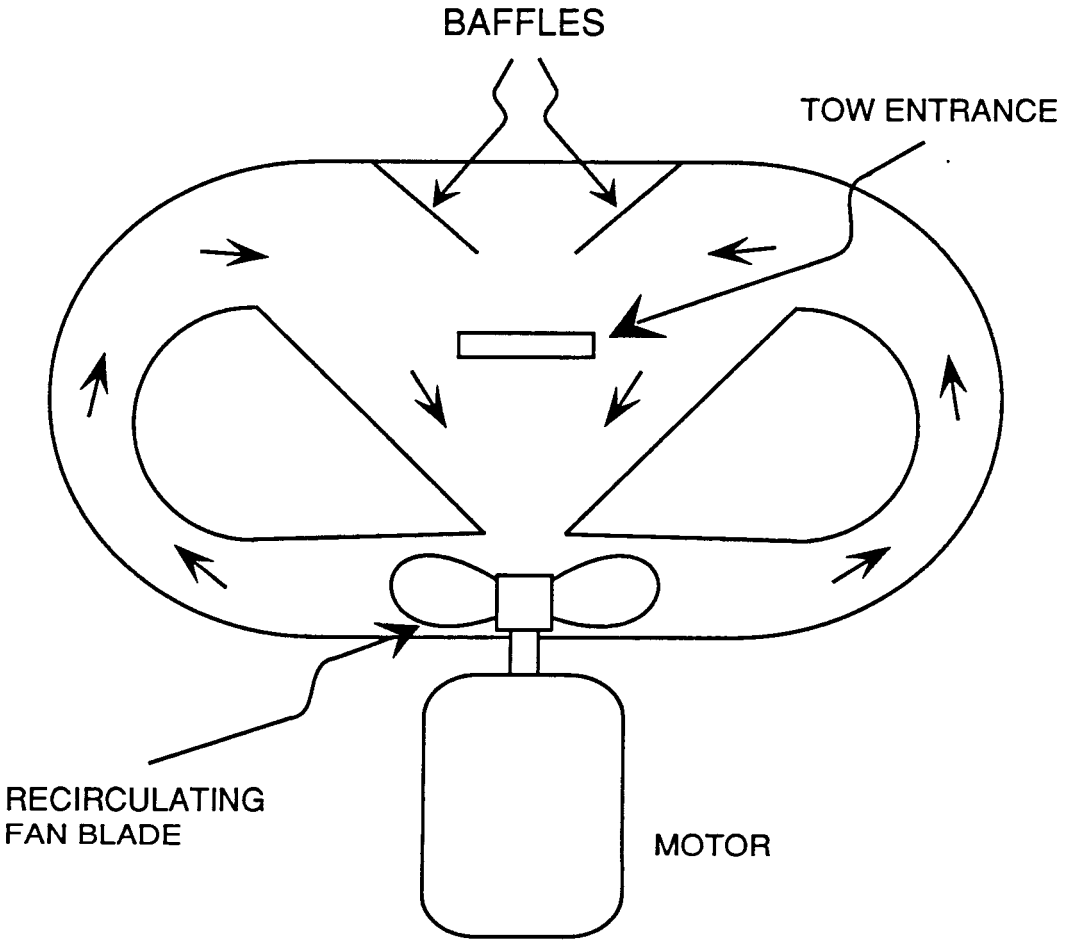

Figure 19. First Recirculating Polymer Coating Chamber

connected to the motor. The pitch on the blades was readjusted to about 75° from horizontal.

Fluidization of the powder was caused by an air stream which formed in the chamber during operation. While the smaller particles readily formed a fluidized cloud, a high air velocity was necessary to fluidize larger polymer particles. The deposition chamber design created a high air velocity which moved polymer particles up the outside of the chamber interior and allowed them to precipitate onto the fiber in a much lower velocity air stream at the chamber center. Fortunately, the design allowed the fiber tow to pass through this area of lower air velocity. This minimized fiber damage and maximized the polymer deposition on the tow. The high-velocity polymer-rich stream was projected onto a baffle at the top of the chamber to ensure that large moving particles would not directly impact the tow.

Although the chamber provided a very good recirculation of powder for coating, a great deal of powder was required to bring it to a steady-state, and much powder escaped from the fiber entrance and exit. In order to solve these problems, a number of changes were made to the deposition chamber before it was used to make substantial quantities of prepreg.

In an effort to reduce the amount of powder which accumulated in the box, a vibrator was added. This consisted of a simple eccentric weight attached to the stirring shaft which caused the stirrer to vibrate continuously during operation. In order to isolate the chamber vibration from the remainder of the coating line, rubber feet were installed on the chamber, and a piece of rubber tubing was used to connect the stirrer shaft to the motor. The vibration did decrease the powder accumulation within the chamber, but it eventually caused the aluminum around the press-fit shaft bearing to fail.

In order to further reduce the amount of powder required, vestibules were added to the entrance and exit openings. The vestibules were about 2.5 cm long and as

wide as the slits themselves. These vestibules provided a region of low air velocity, allowing the powder to precipitate from the exiting gas stream. Vent holes were cut in the top of each vestibule to ensure that the velocity of the gas stream decreased as it moved toward the exit of the chamber. This new technique dramatically reduced powder loss from the chamber.

For continuous long-term operation of the coating line, a powder feed system was needed for the coating chamber. It was decided to use a nitrogen gas stream to deliver this powder feed. The nitrogen would deliver powder effectively and ensure an oxygen-poor atmosphere inside the chamber. The nitrogen, supplied by a gas cylinder, was blown through a nozzle into a flask containing the powder feed. This fluidized the powder, allowing it to exit the flask with the gas stream. This powder-rich stream of nitrogen was introduced into the coating chamber at a point just below the fiber tow.

Unfortunately, this continuous stream of nitrogen carried powder with it as it exited the chamber through the vestibules, increasing the powder loss. In an attempt to decrease the velocity of the exiting nitrogen and, thus, the loss of powder from the chamber, vent holes were cut in the top of the chamber between the points of attachment of the baffles. It was felt that since this exiting gas stream would be forced to turn a sharp corner to exit upward between the baffles, it would carry very little polymer with it. These additional vent holes did decrease leakage, but the overall loss of powder from the chamber remained unacceptably high. Nevertheless, this showed that removing gas from the chamber would decrease powder loss.

A region of low polymer concentration in the chamber was near the center of the rotating fan shaft. Obviously, a gas stream removed at this location would contain a minimum amount of powder. To remove a stream of gas in this area of low powder concentration, the stirrer shaft seal was redesigned. A steel mount plate which could be tightened around the shaft bearing was fabricated. In order to provide a clearance

of 0.16 cm for the the 0.95 cm (3/8 inch) stirrer shaft, a 1.27 cm in diameter hole was drilled in a new aluminum chamber base plate. Then, the steel bearing mount plate was spaced 0.16 cm below this new base plate and screwed in place. The edges of the gap between the plates were sealed with putty and a hole was drilled in the bearing mount plate to allow the attachment of a suction line tap. Air could be drawn through the shaft clearance, between the two plates and out through the vacuum line. A hose, containing a 1.91 cm (3/4 inch) PVC valve for flow control, connected the line to the vacuum system used with the spreader.

Applying a vacuum to the chamber in conjunction with the vestibules decreased the loss of powder to an acceptable and controllable level. With these improvements, the chamber could continuously coat approximately 50 m of fiber. However, three problems still limited the useful life of the coating device. The first was that the polymer powder would accumulate in the vestibules. The second problem was that the air stream withdrawn from the bottom of the coating box contained enough powder to eventually clog the suction line. The third was that the nitrogen system tended to strip the feed flask of smaller particles of powder and would not fluidize the large particles. Also, the large number of flat surfaces within the coating box provided areas for polymer to build up, making it necessary to charge the chamber with at least one half pound of polymer before steady state could be reached. Since no alteration of the existing coating chamber would solve these problems, a new chamber was designed.

Final Coating Chamber

Using information gathered from the operation of the earlier coating chamber, a more effective powder coating apparatus, shown in Figure 20, was constructed. This device used a centrifugal, "squirrel cage", blower with a 9.53 cm blade to move the air and polymer. A flexible 3.13 cm (1-1/4 inch) ID Tygon tube delivered air at a much

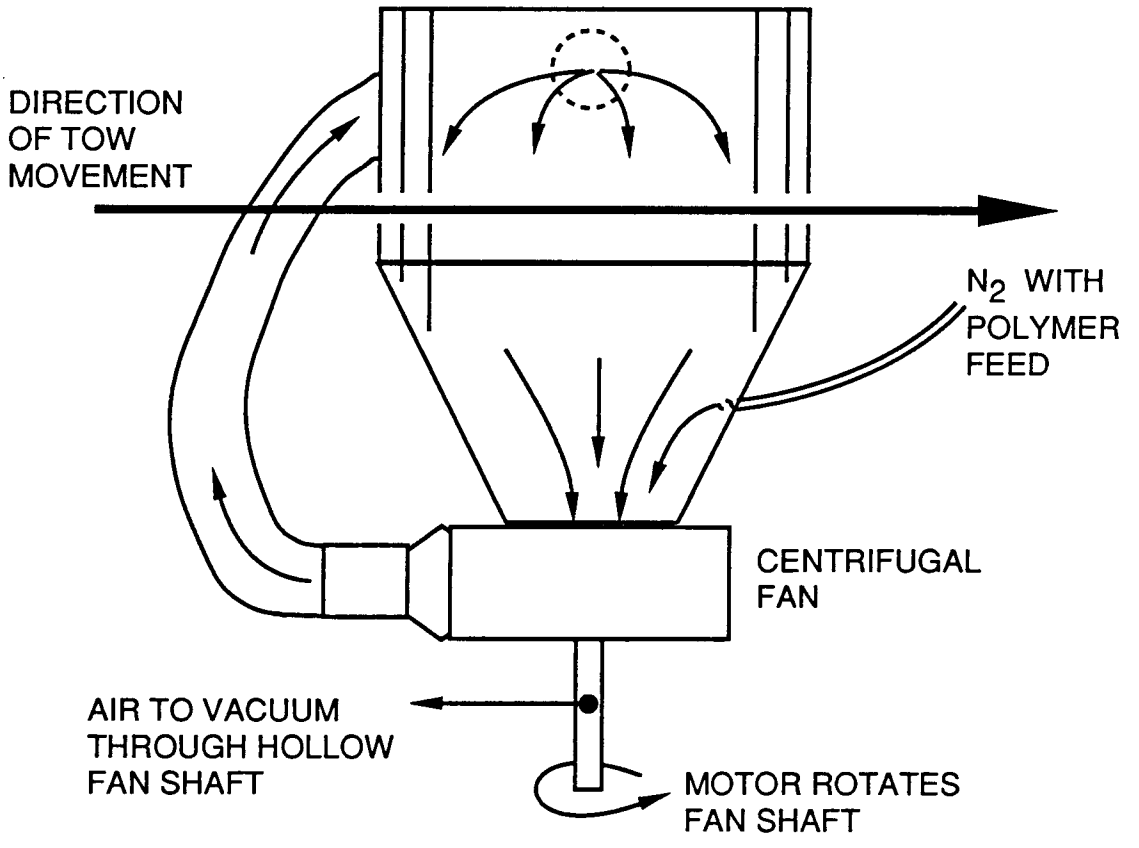

Figure 20. Improved Polymer Coating Chamber

higher velocity to the top of the chamber. The coating chamber was made entirely from Plexiglas and glued together with silicon rubber sealant. The top of the chamber was removable to allow easy inspection and fiber threading. The sides of the chamber formed an inverted pyramid to decrease powder build-up. The 5 cm square opening at the bottom of the pyramid-shaped sides channeled the powder to the center of the centrifugal fan at the bottom of the chamber. The Plexiglas slits through which the fiber passed were 0.5 cm high by 4.5 cm wide. There were a total of six such slits, including those of the vestibules. The four vestibules shown in Figure 20 were 1.3 cm long in the direction of the fiber movement. The problem of powder accumulation was eliminated by adding openings in the base of the vestibules for returning any stripped polymer to the recirculating stream. In order to minimize fiber abrasion, all the Plexiglas surfaces were well rounded and sanded to a smooth finish.

A moldable material, called Friendly Plastic, was used to form the fan-to-tubing and the tubing-to-chamber connections of the fluidized powder recirculating line shown in Figure 20. This fluidized powder recirculating line entered the top of the box horizontally so that no polymer particles would be directed at the delicate tow. The incoming stream blew against the front of the chamber, clearing the Plexiglas and allowing the inside of the chamber to be inspected during operation. Fiber damage was minimized by having the fiber pass through the widest part of the air path where air velocities would be the lowest.

Foam tape was placed between the removable chamber top and the body of the chamber. The weight of the top held it in place during operation. However, to guarantee proper alignment, the sides of the chamber top fit around the pieces which formed the vestibule walls, and four Plexiglas tabs were attached to the outside of the chamber top beside the tow entrance and exit openings. This method of aligning the lid ensured that it could be removed quickly and set back snugly into place.

A stream of nitrogen supplied powder feed to the coating chamber at a point which was near the fan inlet and below the fiber tow. This helped buffer the coating environment of the chamber from fluctuations in feed concentration.

To further reduce powder loss, an improved vacuum system was designed for the new chamber. The vacuum system of the previous chamber drew air around the rotating shaft of the fan. Therefore, it relied on the fan to clear polymer away from the inlet of the suction line. In the new design, the vacuum was drawn through the rotating fan shaft itself. This was accomplished by using the mechanism shown in Figure 21. A cap with holes perpendicular to the axis of rotation was placed on top of the hollowed fan shaft. Two sealed 0.95 cm (3/8 inch) ID bearings were installed above and below a vent hole in the hollow fan shaft. These bearings were held in place by two steel bearing mounts just like those used with the earlier chamber. The edges of the 0.64 cm space between the bearing mounts was sealed with putty and tapped for a plastic tubing connection. This allowed air to be drawn into the rotating holes, down through the hollowed fan shaft, and out a vent in the shaft into the air-tight region between the two bearing plates. This design would make it impossible for all but the finest polymer particles to enter the suction line. An Erlenmeyer bubbler flask was attached to the suction line to monitor the air flow rate from the powder coating chamber and to trap exiting polymer.

An electric dust vibrator was loosely mounted on the top of the chamber using a rubber sleeve. The speed of the vibrator was controlled by regulating the input voltage using a variable autotransformer. This vibrator proved very effective for decreasing the polymer needed to bring the chamber to steady state operation.

The fan at the base of the coating chamber was driven by an AC/DC series motor. Another AC variable autotransformer supplied the power for this motor and was used to regulate its speed. Since the desired fan speed was near the low end of the motor's operating range, a gear reducer between the motor and the fan blade

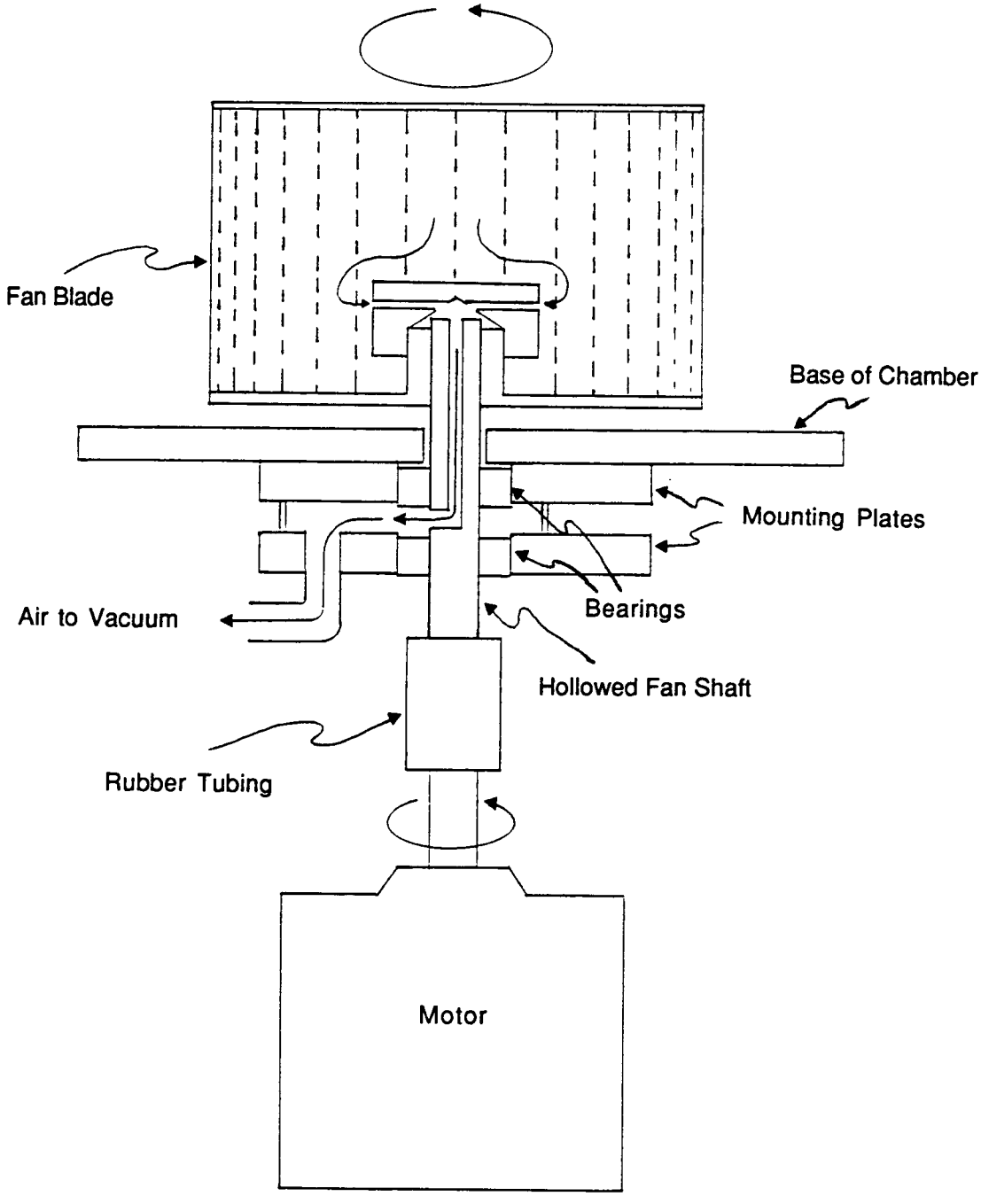

Figure 21. Schematic of Vacuum System At Base of Polymer Coating Chamber

might have improved the control of the system. Often the load on the motor was high enough to nearly stop the rotation of the motor shaft. This would make it necessary to temporarily increase the motor speed, creating intermittent high air velocities over the fiber tow. Obviously, the future addition of a gear reducer or a lower speed fan would improve long-term control of the coating chamber.

During initial testing of the new chamber, a vortex seemed to form inside the chamber just below the fiber path. This vortex was found to throw polymer up the sides, underneath the vestibules, and thus out the entrance or exit. This problem was solved using a simple cardboard baffle at the bottom of the pyramid-shaped section to disrupt the vortex.

Polymer Feed Extruder

Several different techniques, including stirring and vibration, were investigated to increase the effectiveness of the flask feed system used in the first recirculating chamber. After considerable study, it became clear that the wide variation in particle size of the LaRC-TPI would make it necessary to mechanically meter the powder to the feed system.

A dry powder extruder was considered the best alternative. However, no commercially produced powder extruders were available which delivered the low flow rate (less than one gram of powder per minute) required for the powder coating line. Therefore, one would have to be fabricated which could deliver powder from a feed hopper to the nitrogen feed stream at a flow rate which might range from 0.2 to 1.0 grams per minute.

The screw or auger itself was the most critical part of the extruder. In earlier work, Gantt (2) had used a simple drill bit to feed LaRC-TPI. However, over long periods of operation the flow rate from this extruder was not constant. This was because the fine powder would eventually pack the flight of the drill bit, changing the

extruder throughput. An alternative to the solid screw was to use a helical coil which would be rotated in the annular space between a stationary drive shaft and the exterior tube. Ideally, the coil would have a square or rectangular cross-section, large spaces (about 1 cm or more) between wraps, and very high stiffness. The spring-like, square cross-sectioned, auger material, called flighting, was commercially available only in large sizes which would deliver too much powder. Therefore, a stiff 1.59 cm (5/8 inch) OD spring with a left-handed thread was purchased. This spring was pulled onto a 1.27 cm (1/2 inch) bar and stretched to increase the spacing between the turns to 1.3 cm. This effectively increased the pitch of the coil and kept the polymer from wedging between turns and rotating with the auger. The spring was fixed to the end of the rod with epoxy glue to form the auger.

The final powder extruder, shown in Figure 22, consisted of a milled plastic bore section, a hopper, the auger, and a drive system. The 5.1 cm bore of the extruder barrel, as shown in Figure 23, opened to a tapered powder inlet at the top. The drive rod from the auger extended out the bottom of the bore section through a 1.27 cm hole. Since the bore was to be pressurized with nitrogen, the shaft exit at the bottom of the bore section was sealed with a rubber O-ring and grease.

Since the screw was mounted vertically, the hopper design was simplified. The top of the bore section was milled to 3.81 cm OD and connected to a 35.6 cm high, 3.81 cm (1-1/2 inch) OD PVC pipe section, which formed the hopper. Both the bore section and the hopper were inserted into a pipe coupling for easy assembly and disassembly. The central shaft around which the auger rotated was held stationary by a bar which ran through a hole near the top of the shaft and was fixed to the sides of the PVC hopper (see Figure 23). A pipe end cap with an O-ring sealed the top of the hopper, and the side was tapped for connection to 0.64 cm (1/4 inch) plastic tubing. This allowed the hopper to be pressurized with nitrogen during operation of the extruder.

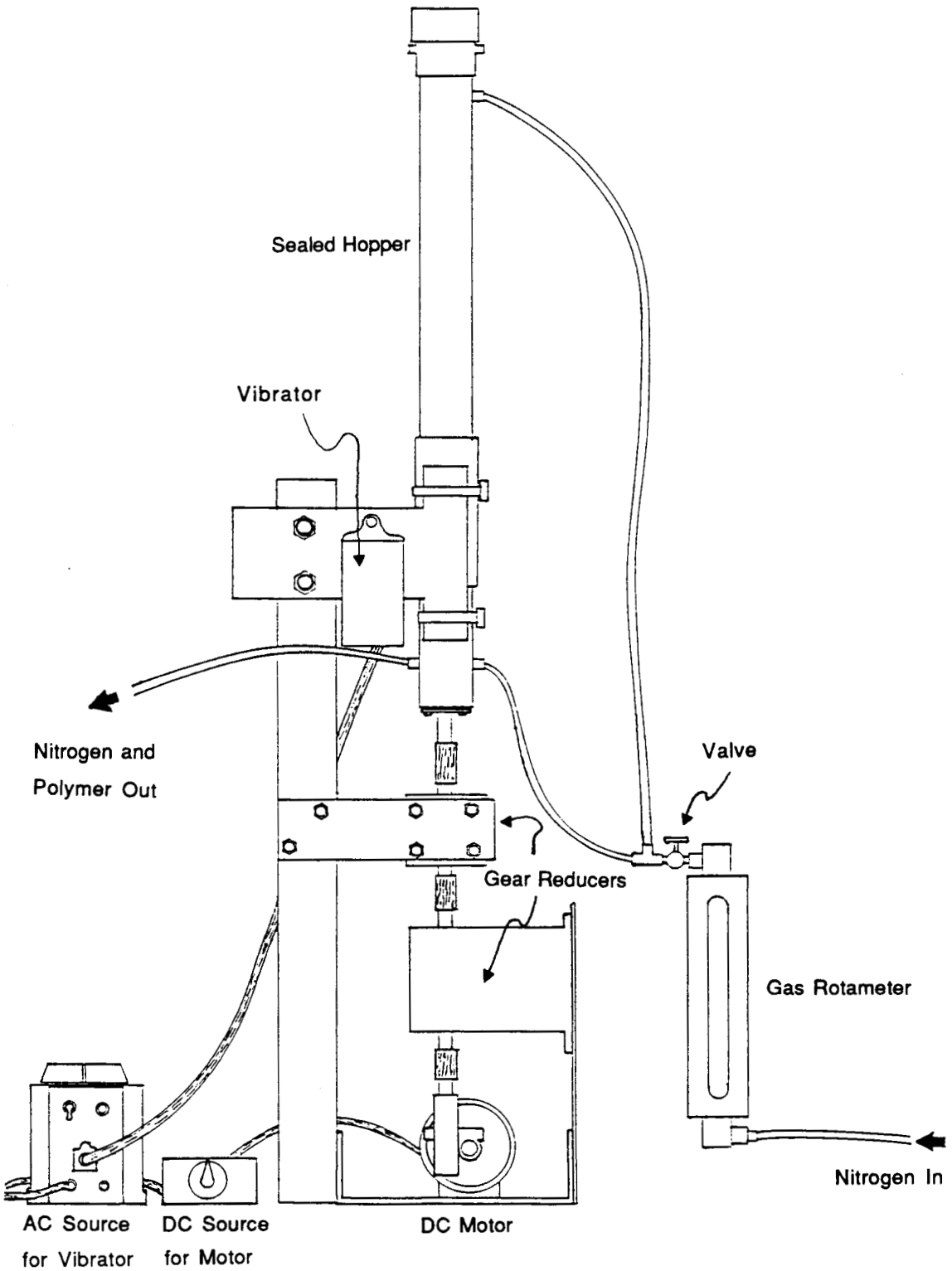

Figure 22. Schematic of Polymer Feed Extruder

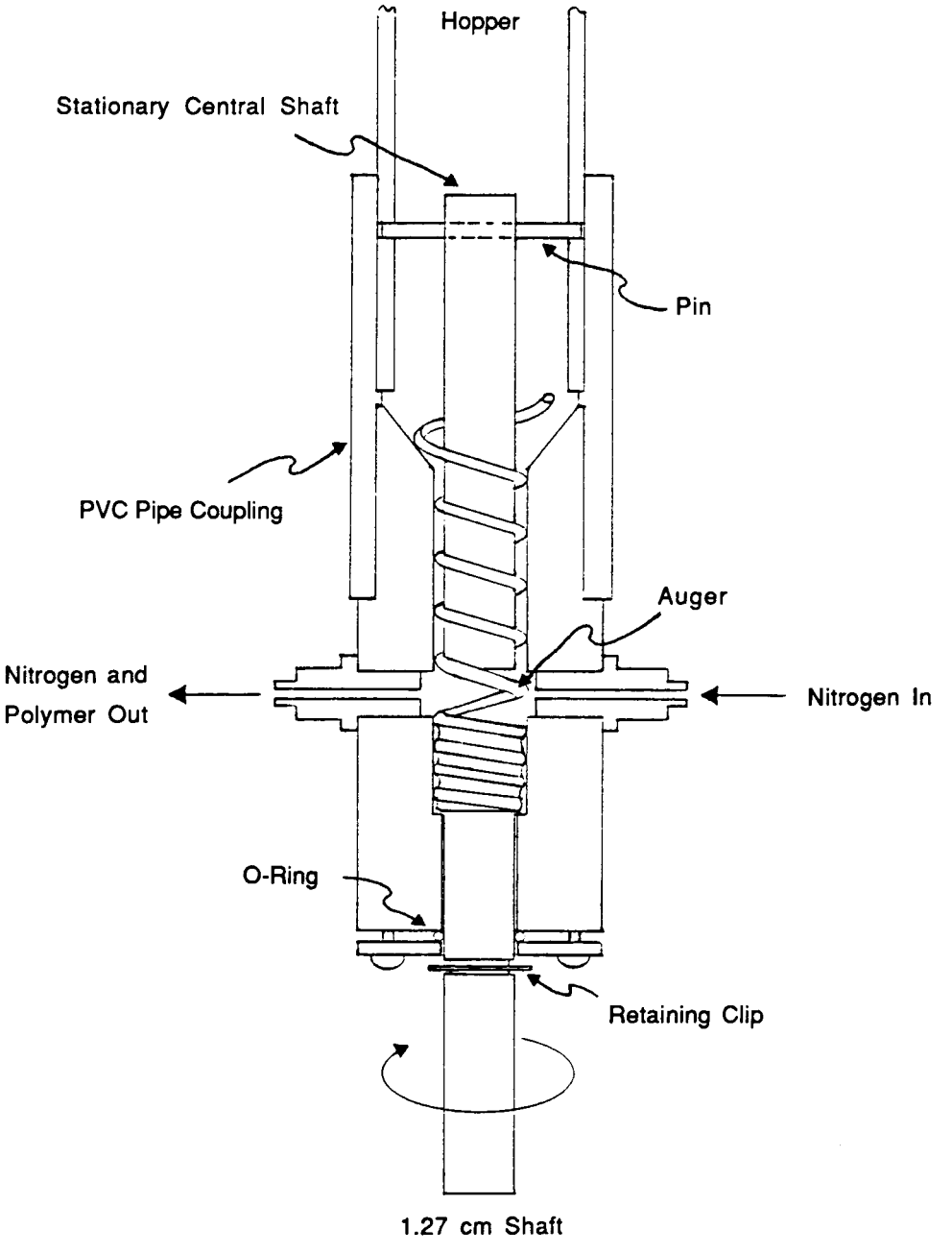

Figure 23. Extruder Bore Diagram

To ensure that the extruder and coating chamber conditions would be reproducible, a rotameter was installed on the nitrogen line. The rotameter was operated at 128.9 KPa (4 psig), and flow rate values were indicated in cubic feet per minute on a scale calibrated for air at 0°C and 101.3 KPa. A valve was installed after the rotameter to control the flow. A typical nitrogen flow rate during operation was 0.0023 m^3/min (0.08 cfm) (uncorrected).

The nitrogen was blown into the bottom of the extruder bore where it fluidized the polymer exiting the auger. This polymer rich nitrogen stream entered the coating chamber near the inlet of the fan. The hopper was also pressurized with nitrogen to prevent the blow-back of powder up the auger.

A vibrator, like that on the deposition chamber, was used with the extruder. This eliminated any powder clogging at the entrance to the extruder. Also, since the initial turns of the auger coil were larger in diameter, they tended to stir the feed powder. These two features eliminated polymer channeling in the hopper.

To provide the proper powder feed rate to the coating system, the auger needed to rotate at about 1 rpm. A small DC stirring motor connected to a two stage 400:1 gear reducer was used to drive the auger. Since good reproducibility was desired, this high gear reduction ratio was necessary to avoid operating at the low end of the DC motor's range. The motor typically operated at 30-40% of full-scale on a DC power source identical to those used for the tow wind-up and wind-off drive motors. The motor required at least 30 minutes to warm up before the speed became constant.

During evaluation tests of the powder feed system, the auger delivered powder at a constant rate for about ten minutes. At this point the powder would begin to stick in the extruder bore until the flow completely stopped. In an attempt to solve this problem, the bore of the extruder was widened from 1.67 cm to 1.83 cm. Unfortunately, not only did this not solve the problem, it increased the powder leaking around the auger. Finally, it was discovered that the sticking was caused by powder

gradually entering the section of the bore where the coil was connected to the 1.27 cm shaft. The drill-like shape of this connection pulled powder into this tight space, eventually stopping the auger. The intermittent flow stoppages were eliminated by filling in the spaces around the coil-shaft connection with more epoxy glue until the whole joint was smooth. But, the wider extruder bore now caused large, short-term fluctuations in the feed rate. Thus, this polymer feed extruder used on the final powder coating line provided an excellent control of polymer feed to the chamber but did not run with good reproducibility. Decreasing the extruder bore back to 1.67 cm should correct this problem.

Heating Section

Gantt (2) showed that, once the powder was coated onto the filaments of the tow, it could be melted to form a thermoplastic prepreg. However, since LaRC-TPI has a time-dependent melt-viscosity, it was important to minimize the heating time. The three heating methods which were investigated in the present research were electrical resistance heating, convection heating, and electromagnetic induction heating.

Previously, Gantt (2) found that a polymer does not wet a carbon fiber the same in electrical resistance heating and convection heating. If a powder coated carbon fiber was internally heated by the electrical resistance of the fiber, the polymer would tend to flow along the hot fiber surface. However, if the powder coated fiber was heated by hot air in a convection oven, the polymer would tend to form beads on the fiber and would fail to distribute uniformly. Gantt (2) found that a more flexible and uniform tow was obtained if the polymer was melted along the fiber using an interior heating technique such as electrical resistance or inductive heating.

Electrical Resistance and
Convective Heating

To heat the powder coated tow, Gantt (2) had used two small 3.18 cm diameter brass rollers mounted on 1.59 cm (5/8 inch) OD bearings. A DC voltage was applied to the fiber between these rollers, generating the heat required to melt the polymer powder. However, the small size of the rollers provided only a small electrical contact area. Also, since they rotate faster than larger rollers, the bearing friction of smaller rollers is normally higher. Both of these problems could be eliminated by increasing the size of the electrical rollers.

At the beginning of the present research, two smooth stainless steel rollers were made using 8.89 cm (3-1/2 inch) OD stainless pipe sections and aluminum end mounts (see Figure 11). Bearings with an OD of 1.59 cm (5/8 inch) were press-fit into the end mounts, and a 0.64 cm (1/4 inch) rod was passed through the center of the bearings. Rubber tubing was put on the central rods to electrically isolate them from the metal roller alignment assembly. Laboratory clamps were used to hold the two rollers in place on the vertical mounting rods which were approximately 30 cm apart. Alligator clips were attached to the central rods to apply a 30-45 volt potential difference between the rollers. The downline roller served as the ground. Initially, a DC power supply was used, but an AC variable autotransformer was soon substituted for safety and convenience.

During initial coating tests, the stainless steel rollers sparked excessively, leading to fiber damage and resulting in polymer build-up on the rollers. It was thought that the sparking was the result of intermittent electrical contact at the bearings, so the bearing grease was removed and a conductive graphite powder lubricant was substituted. This reduced the sparking slightly. Next, to further decrease the electrical resistance of the system, rollers of the same design were made from 7.94 cm (3-1/8 inch) OD copper tubing. These copper rolls were gold

coated to eliminate surface corrosion and decrease surface resistance. This coating decreased sparking still further and aided clean-up.

The next problem to be solved was that of polymer accumulation on the first charged roller. Interestingly, no polymer deposited on the second charged roller because at this point the polymer was well melted and adhered to the tow. Therefore, it was felt that preheating the tow prior to the first charged roller might reduce polymer deposition. To provide this heating, a small convection tube oven was constructed by wrapping a resistive wire around a 6.35 cm (2-1/2 inch) OD, 41 cm long ceramic tube. The oven was insulated with about 4 cm of fiberglass and wrapped with aluminum tape. The overall resistance of the oven was 11.1 ohms, and it was powered by an AC variable autotransformer. Its temperature versus voltage calibration curve is shown in Figure 24. The tow passed through the tube oven which was placed in the coating line between the powder coating chamber and the electrical resistance rollers. The oven was mounted on two laboratory jacks so that its height could be easily adjusted.

The tube oven required about 45 minutes to heat to 300°C, and at this temperature a gradient of from 20 to 40°C existed between the centerline of the tube and the wall. Even though the response of the oven was relatively slow, this gradient allowed the tow temperature to be quickly changed by merely adjusting the oven height. As the distance between the tow and the tube wall changed, the oven temperature gradient would change the tow temperature. After the polymer was partially melted by the tube oven, the powder coated tow passed over the first electrical roller. To further reduce accumulation on this roller, a low velocity compressed air stream was added to blow off any polymer which still adhered.

During prepreg production, convection heating of the coated tow was always kept at the minimum necessary to avoid polymer accumulation on the first electrical roller. This caused the electrical resistance heating to do the majority of the polymer

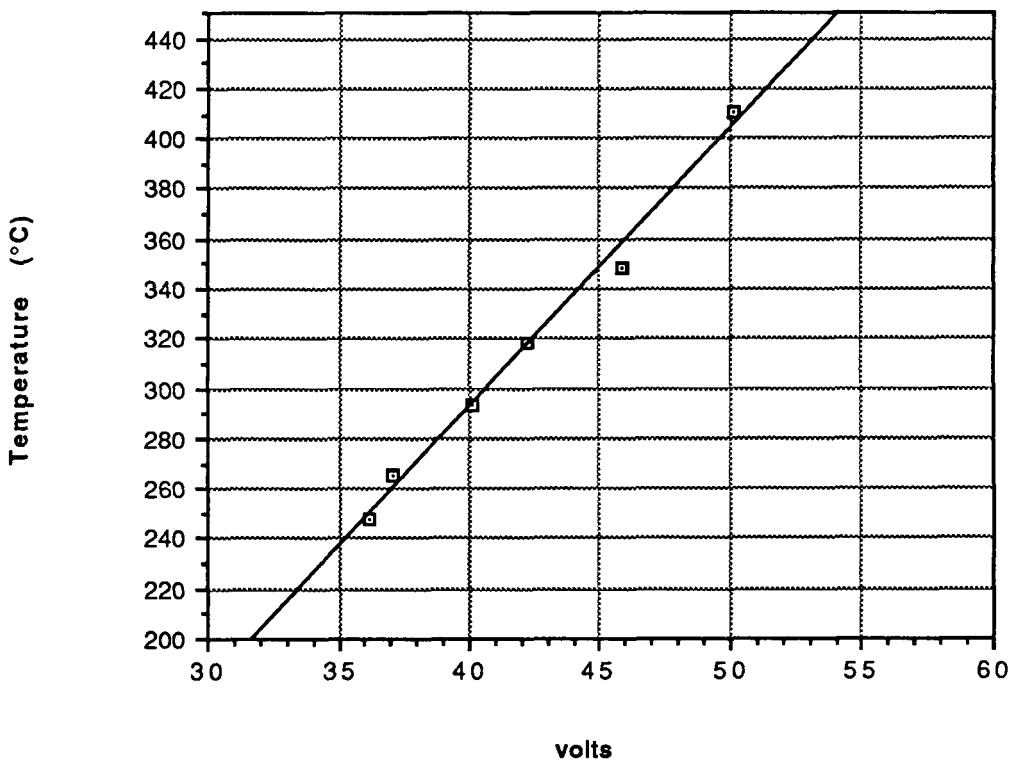

Figure 24. Convection Oven Center-Line Temperature Versus Applied Voltage

melting and increased flexibility of the final coated tow product. The dual-stage heating section is shown in Figure 25.

Inductive Heating

Electromagnetic induction heating of conductive materials is very similar to direct electrical resistance heating in that the heat is produced as a result of resistive losses. However, induction heating relies on an oscillating electromagnetic field to induce potential differences between regions of the conductive material and, thus, cause current flow. The major advantage of induction heating is that heat can be transported rapidly to a material without physical contact. This would be a significant benefit in carbon fiber prepreg manufacture because physical contact often results in fiber damage.

Inductive heating will occur in a conductive medium if the electromagnetic field oscillates at a frequency appropriate for the size of the load. The wavelength of the radiation in a conductive media will be many times smaller than the wavelength within air (46). The diameter of the material to be heated should be greater than the wavelength of the radiation within the given conductive media (47,48). The wavelength within the media is given by

$$\lambda = \frac{2\pi}{\sqrt{f\pi\mu\sigma}}, \qquad (1)$$

where

λ = wavelength (m),

f = frequency (Hz),

μ = permeability ($\mu H\ m^{-1}$) $\cong$ 1.26 for graphite (diamagnetic),

σ = conductivity (Mmho m^{-1}) $\cong$ 0.1 for graphite.

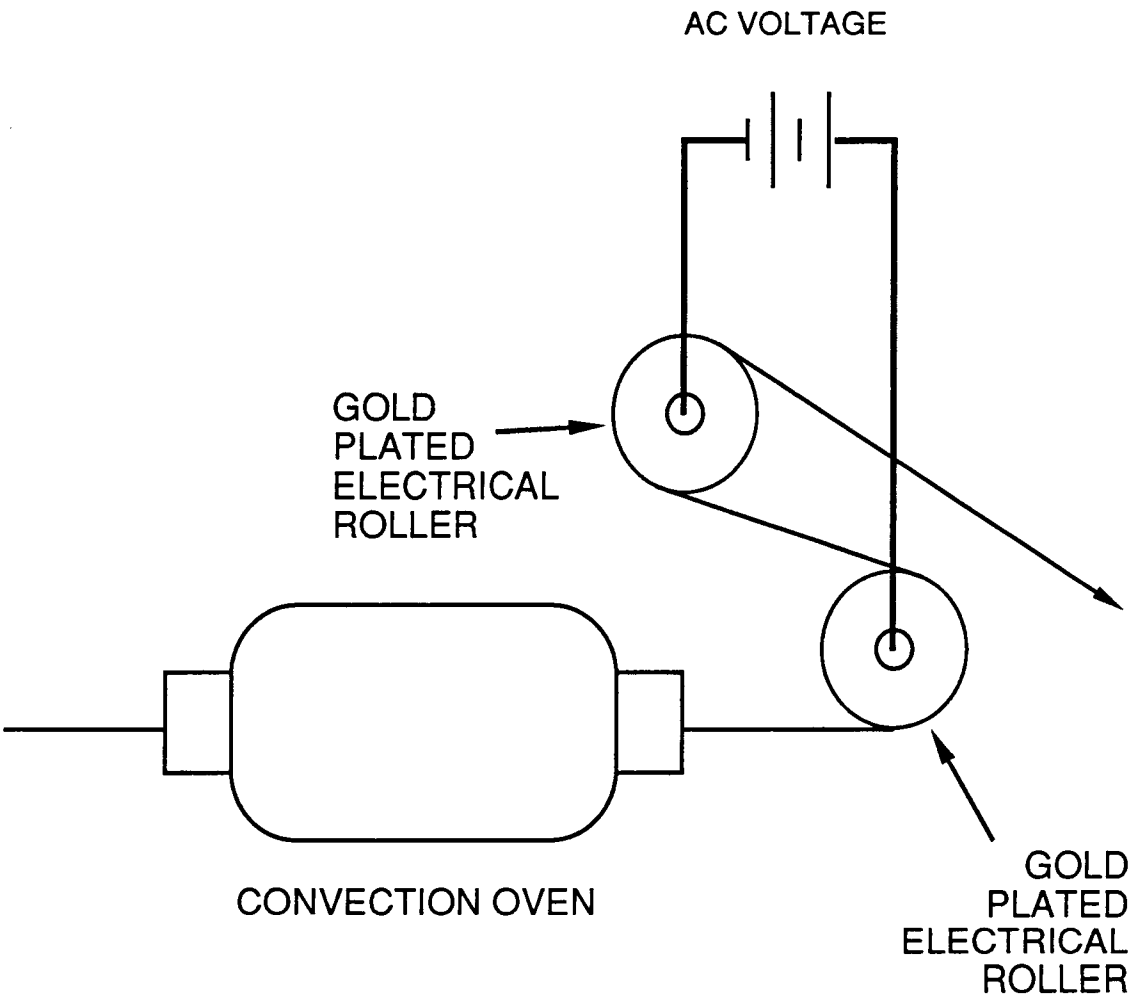

Figure 25. Dual-Stage Heating System

If the diameter of the material is less than about one third the wavelength of the given radiation, no appreciable heating will occur.

In earlier work Gantt (2) was unsuccessful in attempts to heat a tow bundle of seven micron diameter carbon fibers using a 10 KHz power source attached to an induction coil. Using equation 1, the wavelength in graphite for this frequency is found to be 10 cm, which corroborates Gantt's finding that inductive heating will not occur. From equation 1, the frequency which would produce a wavelength of seven microns is 2035 MHz, which is quite close to 2450 MHz, the frequency of a standard microwave oven (48). Since the higher frequency of the microwave oven will produce a wavelength slightly shorter than seven microns, it should heat the fibers very well.

To determine if 2450 MHz radiation would heat individual fibers in the tow, experiments were carried out with carbon fibers in a microwave oven. A large beaker of water was placed inside the oven during all heating trials to absorb excess radiation and avoid magnetron burn-out. When the oven was turned on, the fibers were found to glow red almost instantly. This meant that the heating was so effective that it raised the fibers to about 1000°C within one second.

A 1000 W solid state dimmer was used to cut back the oven power to a more appropriate level for a single fiber tow. A 200 W light bulb was wired in parallel to the oven to provide a constant resistive load which improved the operation of the dimmer. Polymer coated tow could be very effectively heated with this reduced power oven to provide a flexible and uniform product. This investigation of microwave heating was exploratory. Since the results appeared promising, this method will be pursued in future research.

CHAPTER IV

PROCEDURE

In this chapter the procedure used to assemble the coating line using the wind-up, wind-off, dancer arm, coating chamber, convection tube-oven, and electrical resistance heating rollers will be detailed. Once the assembly has been described, the operation of the line will be explained. The procedure used to fabricate unidirectional composite specimens from the coated tow will be described. Finally, the testing of the composite specimens will be discussed.

Assembly of Coating Line

The coating line was assembled on a counter top 5.8 m long by 0.7 m wide. Fortunately, the fan motor for the coating chamber fit into a space in the center of the counter. The assembled coating line is shown in Figure 26. The line was assembled according to the instructions given below.

1. Position the wind-up and the wind-off so that there is at least 4.5 m between the rods which hold the fiber spools.
2. Place the two sections of the roller alignment assembly between the wind-up and the wind-off.
3. Mount the two lower tensioning wheels on the alignment assembly about 1.2 m from the wind-off spool.
4. Mount the dancer arm on a rod about 38 cm downline from the lower tensioning wheels, so that the pulley on the arm is just above the wheels.
5. Wire the potentiometer of the tensioning system in series with the take-off motor speed controller.
6. Mount the pigtail guide 0.9 m downline from the tensioning wheels.
7. Place the spreader 6 cm downline from the pigtail guide, with the longer slot opening downline.

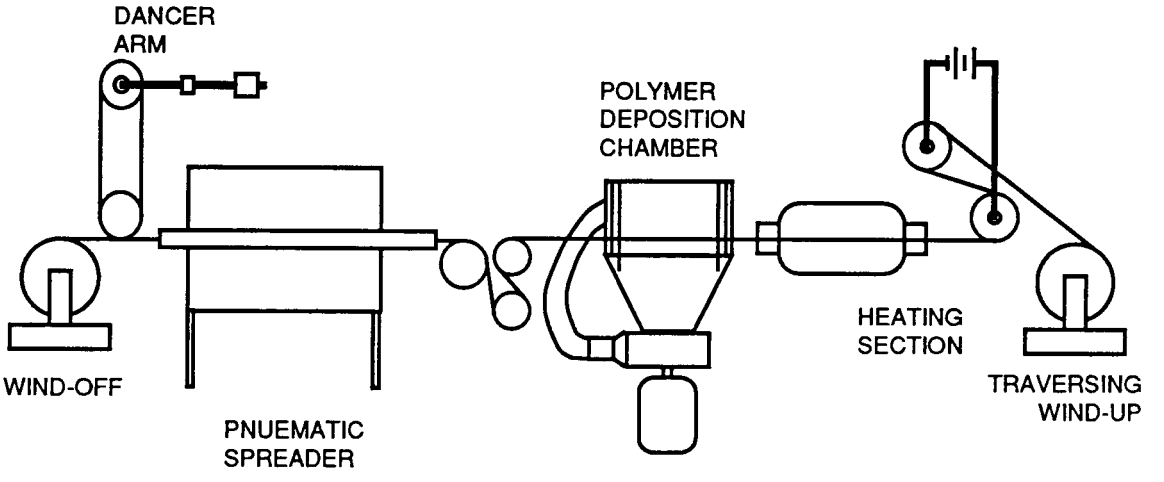

Figure 26. Schematic of Carbon Fiber Coating Line

8. Place a 10.2 cm (4 inch) PVC "T" next to the spreader. Attach one end of a 60 cm section of dryer hose to the bottom of the spreader, then the other end to one leg of the "T" joint. Attach a 90 cm section of hose to the top of the spreader and then to the other leg of the joint.

9. Connect a coupling and two reducers to the base of the "T" joint.

10. Attach a 6 cm long section of 5.1 cm (2 inch) ID PVC pipe to the reducer.

11. Connect one leg of a 5.1 cm (2 inch) PVC "T" to the pipe section.

12. Apply several layers of tape to the nozzle on the 5.1 cm ID vacuum hose. Insert this nozzle into one leg of the 5.1 cm "T" joint.

13. Place reducers in the base of the 5.1 cm "T" to allow a 1.9 cm (3/4 inch) threaded PVC pipe section to be screwed into place.

14. Attach a 1.9 cm (3/4 inch) ball valve to the pipe section.

15. Mount a large polished stainless steel roller 1 cm from the exit slot of the spreader and just beneath the top of the slot opening.

16. Place two graphite rollers on the same alignment rods, one over the other, about 3 cm downline from stainless steel roller.

17. Place the powder deposition chamber mounting blocks on the roller alignment rods over the inset sink in the counter top.

18. Attach the motor to the underside of the downline mounting block using the screw clamp.

19. Place the coating chamber on the mounting blocks and attach the fan to the motor shaft using thick-walled tubing.

20. Place the powder vibrator with rubber tubing on the retaining screw that extends upward from the coating chamber lid.

21. Attach 1.5 m of Tygon tubing to the vacuum draw-off which is located underneath the coating chamber and near the shaft.

22. Fill a 1000 ml suction flask (which has a side spout) with about 200 ml of water and place the flask next to a 1.9 cm (3/4 inch) PVC valve on the suction line.

23. Seal the top of the flask with a large rubber stopper. The stopper should have a single hole into which a section of glass tubing long enough to reach the bottom of the flask should be inserted.

24. Attach a 60 cm section of Tygon tubing to the side spout on the erlenmeyer flask.

25. Insert the other end of the tubing into a rubber stopper and place the stopper into the opening in the 1.9 cm PVC valve.

26. Connect the tubing from the base of the coating chamber to the glass tube in the top of the bubbler flask.

27. Position the oven elevator platforms as close as possible to the deposition chamber exit.

28. Place the notched firebrick oven holders on the elevator platforms.

29. Place the tube oven with its ceramic ends in the firebrick notches. The wire leads should extend out and downward.

30. Position the mounting clamps for charged rollers on separate pairs of rods; the first pair even with the oven outlet and the second pair about 20 cm downline.

31. Secure rubber tubing on the charged roller shafts to ensure that they are electrically insulated.

32. Place the rollers in mounts as shown in the heating section diagram.

33. Attach the alligator clips from the variable autotransformer, which controls the roller potential difference, to the metal ends of the roller shafts. The downline or higher roller is the grounded one.

34. Insert the feed tube from the polymer extruder into the smaller hole in the lid of the coating chamber. The tubing should extend into the chamber far enough so that it can be positioned at the bottom of the pyramid shaped section, well below the fiber path.

Coating Line Operating Procedure

The coating line was operated by two people. One person observed the operation of the fiber spreader and, if necessary, adjusted it. The other person monitored the amount of polymer and heat applied to the tow, and made any needed adjustments. The line is operated by following the steps outlined below.

1. Preheat the tube oven to a midline temperature of 260°C by adjusting the AC variable autotransformer to 27% of 140 volt full-scale which corresponds to a potential of 37.1 volts.

2. Place an 28 by 30 cm piece of paper around the 27.9 cm long by 7.6 cm diameter take-up spool. Be sure that the paper is taped to itself and not directly to the spool, so that the paper may be removed easily from the spool after the prepreg is in place.

3. Slide the take-up spool onto the take-up mount; friction will hold it in place.

4. Place an uncoated, unsized, zero-twist carbon fiber spool onto the take-off mount by inserting the three threaded rods through the spool and into the end-piece. The spool should be placed so that the fiber leaves from the top of the spool rather than from the bottom. Once the screws are tightened, the spool mount will stay in place on the take-off shaft. The spool may be centered on the rod by slowly sliding it to the appropriate position.

5. The cut end of the tow should be held together by a small piece of tape to avoid splitting.

6. Rotate the take-off spool a number of times to produce about 1 meter of slack. Thread the tow around the tensioning arm and roller as shown in Figures 15 and 16. A piece of tape may be used to attach the tow to the counter, since the tensioning arm will tend to pull it back.

7. Attach the tow to a 60 cm long rod using tape. Pass the rod through the opening in the shorter slot of the spreader and out the opening in the longer slot. The take-off spool should be manually rotated whenever more slack is needed.

8. Pass the tow over the large stainless steel roller and around the graphite roller s-wrap.

9. The tow should then be taped to a stationary rod mount so that the top of the powder deposition chamber can be lifted. Remove the lid of the coating chamber and pull the tow over the slot openings. Replace the chamber lid.

10. Pass the 60 cm rod to which the tow is attached through the convection tube oven taking care not to touch the hot oven surfaces.

11. Remove the tow from the rod and pass it around the gold-plated electrical rollers. The power to the rollers must be off when this is done.

12. Pass the fibers under the graphite guide roller on the wind-up assembly and tape them to the paper which is wrapped around the spool.

13. Unscrew the cap on the polymer feed hopper and charge the extruder with a known amount of polymer powder. Reseal the hopper.

14. With the nitrogen flow control valve positioned above the gas rotameter and turned off, open the valve on the nitrogen tank and adjust the nitrogen line pressure to 128.9 KPa (4 psig).

15. Using a carpenter's level, adjust to position of the gold-plated rolls. Turn on the take-off and take-up motors and observe the tow movement over the various rollers. If any of the graphite rollers are not turning, level them to relieve stress on the bearings.

16. While the tow is moving, adjust the lateral position of the two graphite wheels below the dancer arm so that the tow passes through the center of the spreader. Once the tow is centered in the spreader, pull it into the ceramic pig-tail just in front of the spreader opening.

17. Turn the second potentiometer knob on the aluminum box to the desired line speed. Then adjust the position of the dancer arm to the horizontal using the first knob on the control box. Watch the dancer arm to ensure that it is not moving slowly up or down. If it is, readjust its position with the control knob.

18. Close the valve on the powder chamber vacuum line and turn on the vacuum cleaner. Once the vacuum is on, manually adjust the fiber to the desired spreading, and correct the tension on the dancer arm to maintain the spreading. Adjust the power level on the vacuum cleaner to the appropriate suction using the switch on the vacuum and the AC variable autotransformer if necessary.

19. Open the nitrogen control valve and adjust the flow rate to read 0.08 cfm on the rotameter. Turn on the polymer extruder motor.

20. Turn on the chamber vibrator then the blower motor. Adjust the speed of the blower using the variable autotransformer on the control table.

21. Turn on the variable autotransformer which powers the charged rollers. Adjust the voltage level to 30 volts which is about 21% of 140 volt full scale.

22. Open the vacuum line to the polymer chamber. Observe the airflow by watching the bubbler flask.

23. Carefully adjust the height of the convection tube oven, so that the polymer melts only enough to avoid build-up on the first charged roller.

24. Turn on the compressed air flow so that it blows lightly on the first roller and eliminates any build-up.

25. When coating begins to become uniform, attach a piece of tape to the tow as a marker and start a stopwatch to time the run.

26. Whenever necessary, adjust the spreader tension to maintain spreading and the polymer extruder flow rate to ensure coating uniformity.

27. When the run is complete, stop the stopwatch and mark the tow end with tape.

28. Close the suction line to the polymer chamber.

29. Turn off the polymer coating chamber.

30. Turn off the polymer extruder and close the nitrogen valve on the tank.

31. Turn off the main switch, which stops the vacuum cleaner, the tow movement system, and the electrically charged rollers.

32. Turn off the convection tube oven.

33. Wrap tape around the tow near the wind-up and cut through the tape. Tape the end of the tow to the base of the wind-up.

34. Remove the spool of prepreg from the mount on the wind-up.

35. Remove and clean the gold coated surfaces of the electrically charged rollers with soap and water. Try to avoid wetting the bearings. Allow the rollers to dry and return them to the line.

36. Clean the spreader slots with cotton on a wire to remove any fiber that may have accumulated inside. Clean the polymer build up from around the oven and the coating chamber.

37. Empty and weigh the polymer in the extruder hopper.

Composite Formation Procedure

The prepreg line was used to make several long sample sections to determine if the coated fiber tow could be effectively molded into composite parts. Two sets of composite specimens were produced for testing, each set of specimens was made from a single continuous sample of prepreg. Because the two prepreg sections had different properties, the two different composite formation procedures were used. The first spool of prepreg was quite boardy and, therefore, it was cut into sections and placed into the mold for composite formation. Because the second prepreg sample

was quite flexible, it was formed into composites samples using a wrapping technique.

Mold Lay-Up and Composite Formation
using the Boardy Prepreg

1. Extend a steel tape measure to a length of 1.7 m and tape it to a wood cutting board.

2. Mount the spool of coated prepreg on the take-off assembly from the coating apparatus, and disconnect the drive belt from the take-off shaft to make it free spinning.

3. Place the cutting board in front of the spool, in line with the fiber.

4. Pull the end of the coated prepreg along the cutting board and secure it to the far end of the board using a weight.

5. Align the coated prepreg with the tape measure on the board and, making sure the prepreg is pulled tight, secure the other end with a weight.

6. Using the tape measure as a guide, cut a 1.524 m section of the tow.

7. Weigh this piece of the tow to the nearest 0.0001 g and use the calculation procedure shown in Appendix A to determine the fiber volume fraction. Because it must be folded this section of prepreg is discarded after being weighed.

8. Cut 26 more 1.524 m sections of prepreg using the steps 4-6 above. Lay the cut tow sections out on sheets of paper about 2 cm apart so that they can be separated later.

9. Weigh the 26th piece and calculate the fiber volume fraction. Discard this piece after weighing.

10. Repeat steps 8-9 above once to give a total of 50 prepreg sections.

11. Calculate the average of the three fiber volume fractions.

12. Calculate the number of prepregs necessary to form a 0.158 by 1.27 cm (1/16 by 1/2 inch) sample with this fiber volume fraction using the procedure in Appendix A.

13. The number of prepreg sections calculated in step 12 plus an additional five sections (to account for any prepreg non-uniformity) will be incorporated into each composite sample.

14. Take the number of samples calculated in 13 above, subtract 100 and divide by two. This is the number of additional 1.524 m strips which must be cut.

15. Cut all necessary additional strips.

16. Take two 1.524 m sections and lay them on the cutting board. Secure the ends with weights.

17. The 1.524 m sections are now cut into six 25.4 cm sections.

18. Make three different stacks of prepreg. In order to maintain the homogeneity of the composite samples to be made, two 25.4 cm sections from each 1.524 m section are put in each prepreg stack. The stacks should be kept neat so that better orientation is possible in the composite specimens.

19. Cut and distribute all the 1.524 m sections this way.

20. Record the weight of each final stack.

21. Remove the plunger bars from five sections of the mold shown in Figure 27.

22. Spray the bottoms of three of these plungers and the insides of the center three mold cavities with Frekote FRP mold release agent. Wipe away the excess and allow to dry for five minutes. Repeat this procedure four times to build up a thin layer of release agent.

23. Place the mold on the base plate which contains the K-type thermocouple lead. Carefully slide the lead into the hole in the base of the mold.

24. Put one stack of prepreg sections carefully into each of the three center cavities in the mold.

25. Slide the plungers into the cavities and press them down as much as possible.

26. Place two 0.159 by 0.635 by 20.32 cm (1/16 by 1/4 by 8 inch) spacer bars in the cavities next to the cavities which contain the samples. These spacers will ensure that the plungers will not crush the samples should the pressure be too high.

27. Insert the plungers into the cavities with the spacer bars. Tighten the wedge clamp to close the mold.

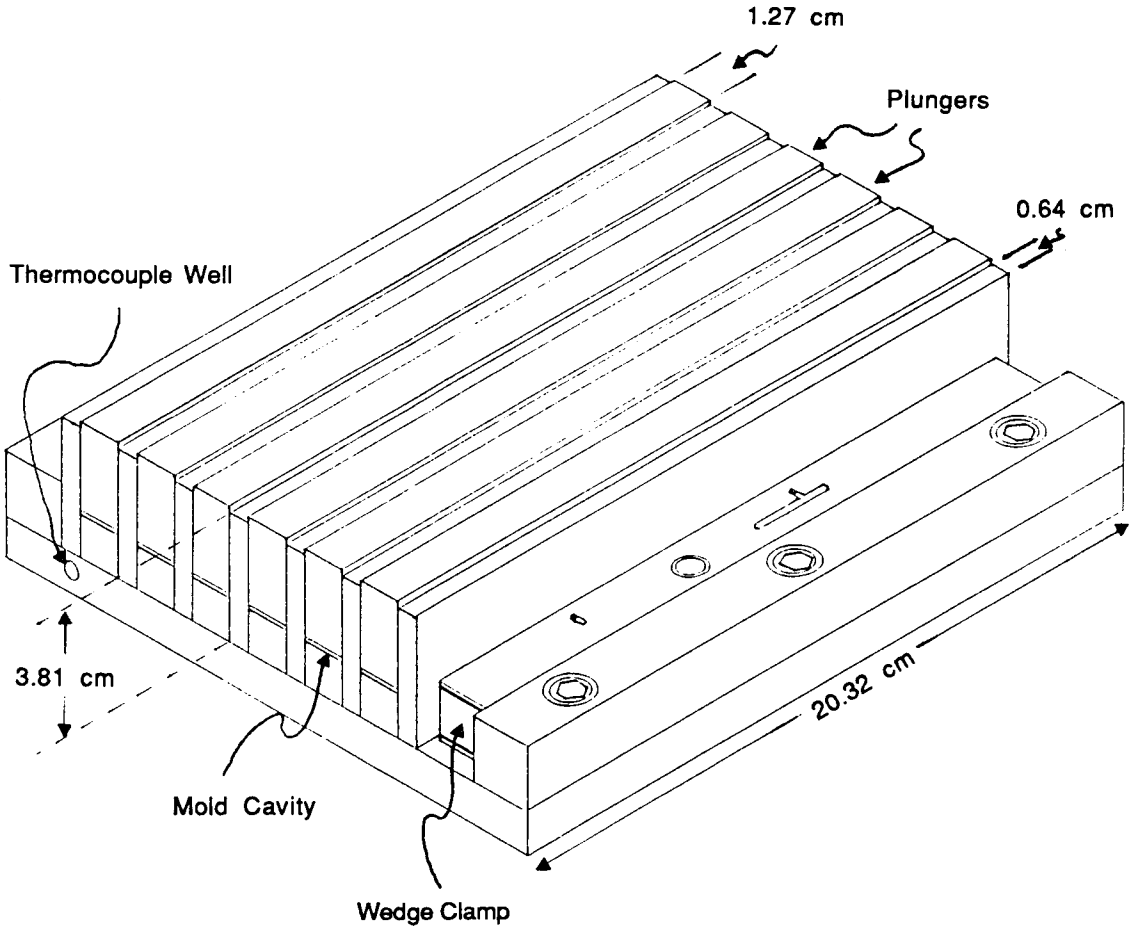

Figure 27. Mold Used to Produce Composite Specimens from Prepreg

28. Apply a strip of high temperature sealant tape to the base of the aluminum dike shown in Figure 28. Place the dike around the mold. Insert the screws through the base plate and secure the dike in place.

29. Place a piece of Kevlar cloth over the mold inside the dike.

30. Place an aluminum plate with side flaps over the mold and inside the edges of the dike.

31. Place a strip of sealant tape around the top edge of the dike.

32. Cut a 30 by 38 cm piece of film and press it down onto the sealant tape.

33. Insert the screws of the sealing bracket into the tabs which are connected to the dike.

34. Make folds in the four corners of the film to eliminate crimping. Insert small pieces of sealing tape into the folds to avoid leaks.

35. Place a 22.9 cm section of 0.64 cm (1/4 inch) OD copper tubing along each long edge of the dike.

36. Fold the edge of the film around the bar on the two long edges and put the folded edge back under the sealing bracket.

37. Tighten the screws to seat the sealing bracket making sure that the folded edges of the film remain underneath.

38. Attach the vacuum hose to the stainless steel tubing which is connected to the dike.

39. Start the vacuum pump and evacuate the mold.

40. Watch the vacuum gauge to ensure that the pump is drawing no less than 90 KPa of vacuum.

41. If the gauge indicates that the mold is leaking, find the leak and seal with sealant tape.

42. Allow the mold to stand under vacuum for 20 minutes.

43. Place two 0.32 cm thick aluminum plates on the bottom platen to protect the surfaces of the press.

44. Close the press.

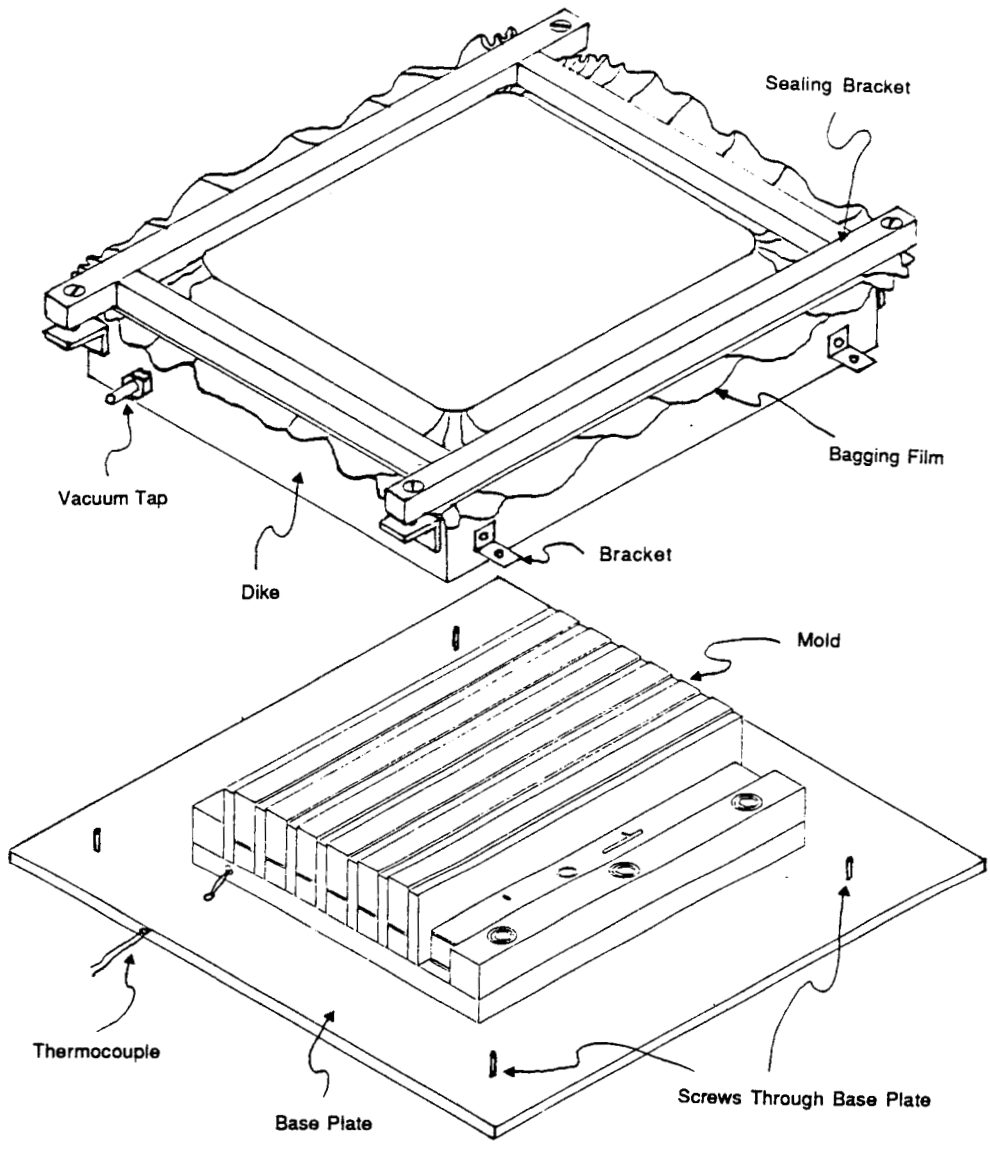

Figure 28. System Used to Apply Vacuum to Mold

45. Preheat the bottom platen of the high temperature press to a temperature at least 50°C higher than the desired processing temperature or to about 393°C. The top platen should not be heated above 370°C to avoid degradation of the vacuum film.

46. Attach the K-type thermocouple wires extending out from the base of the mold to the leads from the temperature chart recorder.

47. As soon as the press reaches the set point temperature, lower the bottom platen and remove one aluminum plate.

48. Using heavy insulated gloves place the mold on the lower platen and slide it into place.

49. Center a 12.7 by 20.3 by 0.9 cm thick steel plate over the plungers of the mold and then place the preheated aluminum plate over this plate.

50. Set the automatic pressure control on the press to approximately 100 kg.

51. Close the press.

52. Reset the temperature set point of the bottom platen to 374°C.

53. Allow the mold to heat up until the thermocouple indicates that it has reached 300°C.

54. Increase the pressure to 10,000 kg using the automatic pressure controller.

55. When the thermocouple indicates that the mold has reached 343°C set the heating timer to 40 minutes and start the timer.

56. After about 50 minutes, when the press has finished its automatic quench cycle, lower the bottom platen and remove the mold.

57. Disconnect the thermocouple leads.

58. Turn off the vacuum pump and remove the vacuum tube from the mold.

59. Allow the mold to cool.

60. Unscrew the dike and lift it off of the mold with the film intact. This film often may be reused.

61. Loosen the wedge clamp and remove the plungers.

62. Remove the composite bars from the mold.

63. Record the weight of the bars.

Mold Lay-Up Using Flexible Prepreg

1. Mount the flexible prepreg spool on the take-off assembly and disconnect the drive belt from the take-off shaft.

2. Stick semicircular pieces of moldable high temperature sealant tape to the ends of the rotating lay-up frame shown in Figure 29. These pieces of sealant will ensure that when prepreg is wrapped onto the frame it will not be damaged by being bent around the 90° corners of the frame.
3. Apply a coating of mold release to all four mold cavities, and wipe off the excess.

4. Allow this coating to dry and repeat until a total of five coats of release have been applied.

5. Weigh the lay-up frame and record its weight.

6. Insert a 25 cm long piece of 0.64 cm rod into the center pivot of the lay-up frame.

7. Mount the lay-up frame on the roller alignment assembly of the coating line.

8. Cut and weigh a 1.524 m section of coated tow. Determine the fiber volume fraction of the prepreg using the calculation procedure in Appendix A. Discard this section after weighing it.

9. Weigh a small piece of masking tape. Tape the end of the prepreg to the sealant tape at the end of one of the cavities on the lay-up frame with this piece of tape.

10. Rotate the lay-up frame so that one strip of prepreg is applied to the edge of one of the cavities.

11. Continue to rotate the frame and apply strips of prepreg to the cavity. The strips should be gradually moved across the space inside the cavity so that the area is uniformly filled.

12. Apply a total of 50 strips of prepreg to the cavity.

13. Weigh another small piece of tape and use it to secure the 50 layers of prepreg. Cut the tow. Remove a 1.524 m section of tow and record its weight. Then determine its fiber volume fraction fiber.

14. Repeat steps 7-11 until a total of 100 strips have been applied.

15. Average the three fiber volume fractions. Calculate the number of prepreg pieces necessary to form a 1.27 by 0.16 cm (1/2 by 1/16 inch) composite sample using the procedure in Appendix A.

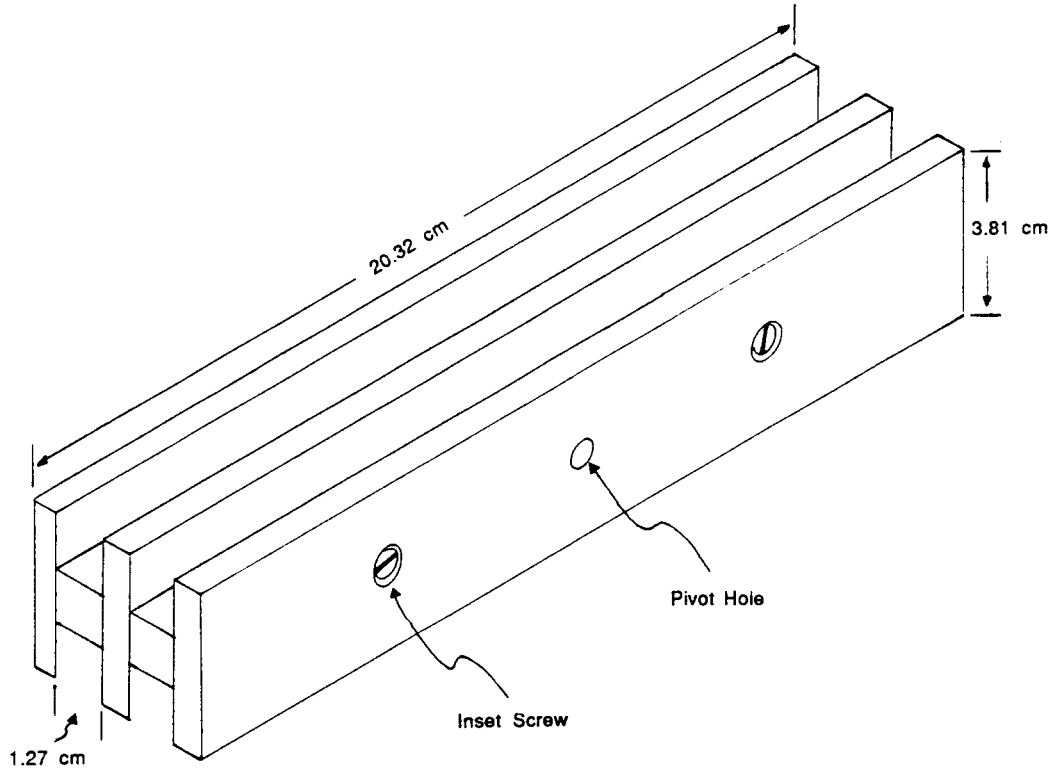

Figure 29. Mold Section Used to Form Composite Specimens from Flexible Prepreg

16. To account for possible prepreg non-uniformity, add 5 to the number of requisite prepreg strips determined in step 13 above. Subtract 100 from this number and apply the remaining number of prepreg strips to the cavity.

17. Hold the last prepreg section in place with a weighed section of tape.

18. Weigh the frame lay-up and prepreg.

19. Repeat steps 4-15 to fill the second cavity with prepreg.

20. Weigh the lay-up frame.

21. The composites can now be formed using the same procedure described for boardy prepregs starting from step 25.

Composite Test Specimen Preparation Procedure

Before the composite specimens which could be tested, all mold flash was removed and the non-uniform ends were cut off. Mold flash is the small quantity of material which is pressed into the cracks or gaps of the mold cavity. This flash must be removed to accurately measure the cross-sectional area of each specimen, and to eliminate any non-uniformity. The flash was removed by carefully shaving the edges of each specimen with a razor blade. The rough ends of the specimens were removed using a ceramic bladed cut-off saw. Since the side flash in each sample represented less than half of one percent of the total amount of material in the sample, it was neglected when determining the number of fibers in the specimen cross-section.

The specimen was carefully weighed after removing the ends and flash. The length, width and thickness of the specimen were also carefully determined using a micrometer. Since the most critical dimension was the thickness, this was measured at both ends and at the center of the specimen. The smallest thickness measured was used to calculate the tensile strength while the average thickness was used to determine the void volume and density of the specimen.

Strain gages were applied to the specimens in order to accurately determine the tensile modulus during testing. The strain gages used had a resistance of 120 ohms, a gauge factor of 2.04 and a gauge length of 0.95 cm (3/8 inch). The strain gages were applied using materials from an M-line accessories kit purchased from Measurement Groups Inc., Romulus Michigan. The procedure used to apply the gages was similar to that described in the product literature and is described below (49).

1. Apply a small quantity of acetone to a tissue and quickly wipe the center of the specimen.
2. Again, wipe the specimen with a dry tissue.
3. Lightly abrade the specimen surface with 320 grit silicone carbide paper.
4. Apply several drops of M-Prep Conditioner A to the surface and wipe with tissue.
5. Apply several drops of M-Prep Neutralizer 5 and wipe away with a tissue.
6. Wipe the surface with a dry tissue.
7. Measure 0.64 cm over from the side and mark with a pencil at both ends of the specimen. Connect these two marks with a light pencil line which runs the length of the specimen.
8. Using tweezers remove a gauge from the package and place it bond-side down on an empty gauge box. Place a solder terminal next to the gauge.
9. Attach a short length of clear plastic tape to the gauge and solder terminal. Remove the gauge and solder terminal with the tape.
10. Position the gauge on the sample so that the aligning marks correspond to the center line drawn on the specimen. Attach the tape to the specimen.
11. Remove one side of the tape so that the terminal and gauge are lifted with it.
12. Coat the specimen surface, the back of the gauge, and the terminal with M-Bond 600 adhesive. Allow to air dry for 5 minutes.
13. Return the gauge assembly to its original position over the alignment marks. Press down on the gauge to smooth the adhesive coating.

14. Place rubber pads on the front and back of the specimen around the gauge, and clamp in place.

15. Place the specimen in a cool oven. Heat the oven slowly to 120°C and allow it to stand for two hours. Turn off the oven heat and allow the specimen to cool slowly.

16. Take the specimen out of the oven and remove the clamp.

17. Slowly peel the tape from the specimen.

18. Apply several drops of M-Flux AR to the copper surface of the terminals, and wipe them clean with a tissue after a few moments.

19. Strip two 2 cm sections of fine wire.

20. Solder one end of each wire to the terminals on the gauge. Solder the other end of each wire to a copper surface on the terminal strip.

21. Cut a section of three conductor cable 1.2 m in length. Strip both ends of each wire.

22. Solder one wire to one of the copper surfaces on the terminal strip. Solder the other two wires to the remaining terminal.

23. Wrap the wire around the specimen and set it aside for testing.

Specimen Testing Procedure

The tensile strength and the tensile modulus of six composite specimens were determined by the Materials Testing Laboratory at NASA Langley Research Center. Glass fiber reinforced end-tabs were glued to the specimens by the technicians at NASA. The epoxy glue used to attach the tabs contained fine glass spheres to improve adhesion. Figure 30 shows a sample with the tabs and strain gauge.

The samples were tested on an Instron tensile testing unit. The load cell used had a capacity of 10,000 kg. The strain gauge of each specimen was wired to a strain measurement device which gave a plot of strain percent versus load. All specimens were tested to failure at room temperature.

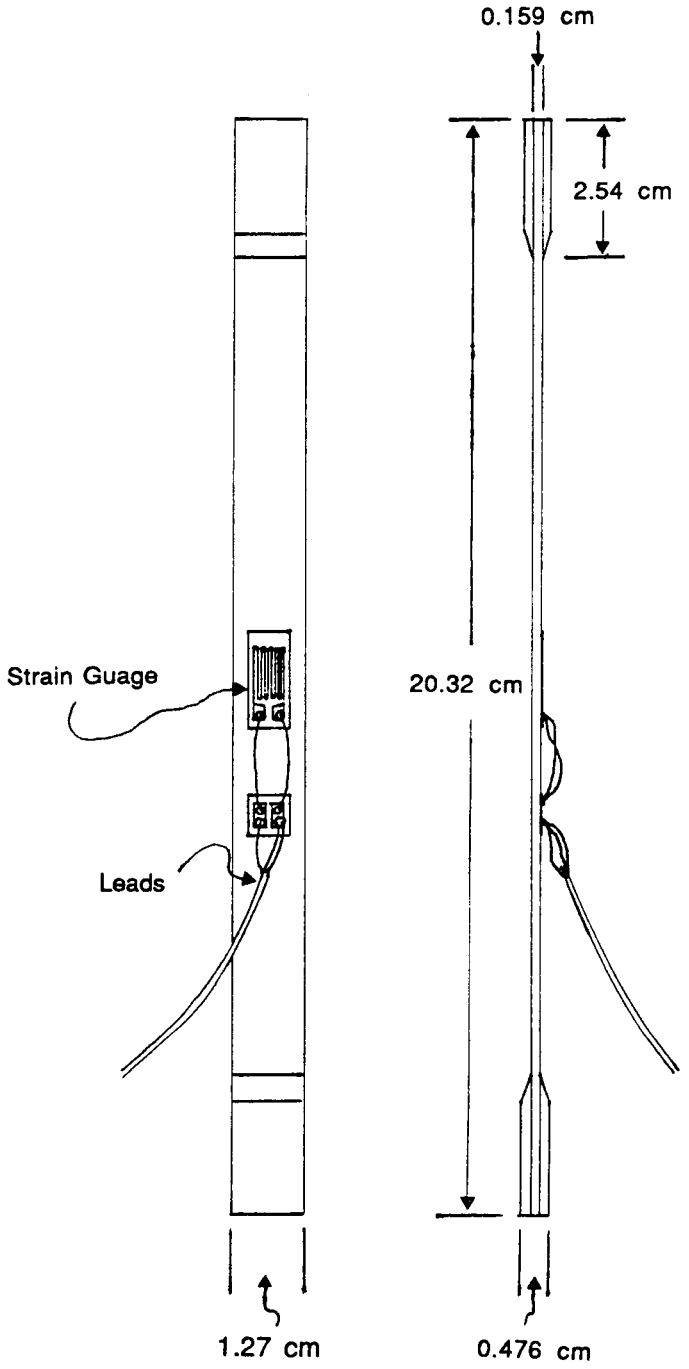

Figure 30. Composite Test Specimen

CHAPTER V

RESULTS AND DISCUSSION

Once the powder coating process was developed, it was operated continuously to produce several coated tow sections with lengths of up to 275 m. This continuous operation allowed the reliability of the various sections of the coating line to be evaluated and provided coated prepreg. The prepreg was subsequently formed into composite specimens using the procedure described in the previous chapter. This chapter will discuss these evaluation trials, the problems encountered in forming the composite specimens, and the final properties of the composite specimens formed from the coated tow. Amoco T-300 (3K, unsized, no twist, surface treated) carbon fiber tow and LaRC-TPI polymer powder (Mitsui Toatsu Chemicals) were used for all trials.

Coating Line Operation

The coating line was operated following the procedure detailed in Chapter III. As mentioned, two people were required to operate the line. One person monitored the operation of the fiber spreader and, if necessary, adjusted it. This allowed the second person to monitor the amount of polymer and heat applied to the tow, and to make any needed adjustments to these sections of the process.

During continuous operation of the coating line, the primary control parameters of the coating line were found to be:

1. electrical potential applied to the charged rollers,
2. line speed,
3. tow tension,
4. tow temperature within the convection oven,
5. feed rate of polymer to the coating chamber.

Only the electrical potential applied to the charged rollers could be absolutely fixed. The line speed was established by fixing the rotational velocity of the take-up roller at the start of the run. The take-up spool diameter would increase from 8.7 cm to about 10.0 cm as prepreg was wound onto the spool. This resulted in a 16% increase in line speed after about 250 m of prepreg had been produced. Table 4 gives the electrical potential and initial line speed values used for the continuous coating trials.

Table 4. Run Conditions for Prepreg Trials

Trial #	Roller Electrical Potential	Initial Line Speed	Convection Oven Centerline Temp.	Extruder Motor Setting
	volts	m/min	°C	Scale 1-10
1	43.0	1.6	255	*
2	42.0	1.6	255	*
3	37.0	1.6	242	*
4	41.0	1.6	292	*
5	34.7	1.6	312	*
6	44.2	1.6	300	*
7	38.5	2.8	296	**
8	48.4	2.8	260	4.2
9	35.7	2.8/3.8 ***	260	3.5
10	35.7	3.2	260	4.5

*The polymer feed extruder was not operated during this trial.
**The polymer feed extruder jammed and clogged during this trial.
***The line speed was changed during trial.

No accurate values for tow tension, tow temperature in the convection oven, or polymer feed rate could be obtained while the line was operating. The effects these values had on the operation of the coating line was observed visually and the values were adjusted accordingly. The centerline temperature of the oven as well as the average setting used for the polymer feed extruder motor are given in Table 4.

Prior to the continuous coating trials, the convection tube oven was heated to a centerline temperature of approximately 260°C. As mentioned in Chapter II, the temperature of the tow was adjusted during the trial by raising or lowering the oven. This adjustment was made during the first few minutes of each continuous trial and then kept constant for the remainder of the test. This initial heating was necessary to avoid polymer build-up on the first charged roller.

The take-up motor speed and the voltage between the charged rollers were fixed at the start of each coating trial. These values were not changed as the trial progressed.

The evaluation trials showed that the polymer extruder feed rate was inconsistent. Because of this, it was necessary to adjust the speed of the extruder motor approximately every 5 minutes to maintain an even polymer coating on the tow. This adjustment was made by visually observing the amount of polymer which was applied to the tow and changing the extruder motor speed accordingly.

The tension on the fiber tow was found to be critical for proper operation of the fiber spreader. Often the individual fibers would pull together, slip to one side, or split into two sections in the tow spreader after approximately one minute of continuous operation. If the fibers pulled together, the spreading could be restarted by briefly lifting the weight on the dancer arm, decreasing the tension on the tow. If the tow split or pulled to one side, briefly increasing the tension by pulling the dancer arm weight downward would reinitiate tow spreading. If a large number of fibers grouped into a single bundle, the spreading was reinitiated by manually respreading

the tow on the large stainless steel roller at the spreader exit. These periodic adjustments could be easily made by the one operator during continuous line operation. However, this critical interaction between tension and spreading means that further automation of the spreader may require additional refinement in the feedback control of the tow tension.

The polymer feed extruder could hold enough polymer to coat about 1000 m of prepreg. However, broken fibers tended to collect in the spreader and interfere with its operation. Continual contact with this buildup of broken filaments eventually caused knots and twists to form in the tow, and, after processing about 250 m of tow, these decreased the efficiency of the spreader noticeably. The knots also decreased the consistency of the polymer coating and lowered the flexibility of the final coated prepreg. Thus, the length of the coated tow produced during these evaluation trials was limited to 275 m.

The evaluation trials showed that the coating line was capable of applying a maximum of 50 volume percent polymer to the tow. The quantity of polymer applied to the tow could be altered by changing either the line speed or the concentration of polymer in the recirculating deposition chamber. When higher levels of coating were attempted, the air flow in the chamber would blow the additional powder off of the tow before it exited the coating chamber. However, by reducing the concentration of polymer in the chamber, the volume percent polymer applied to the coated tow could be reduced to nearly zero. Thus, a wide range of coating levels could be produced.

The operation of the coating chamber also was affected by the average particle size and the particle size distribution of the polymer powder. Scanning electron micrographs of a LaRC-TPI powder showed that the particle size distribution is bimodal (see Figure 31). It primarily consists of smooth, 4 μm diameter polymer particles and particles smaller than 1μm which have agglomerated to form large 50 to 100 μm clumps of powder. At start-up, the smaller 4 μm particles appeared to

ORIGINAL PAGE
BLACK AND WHITE PHOTOGRAPH

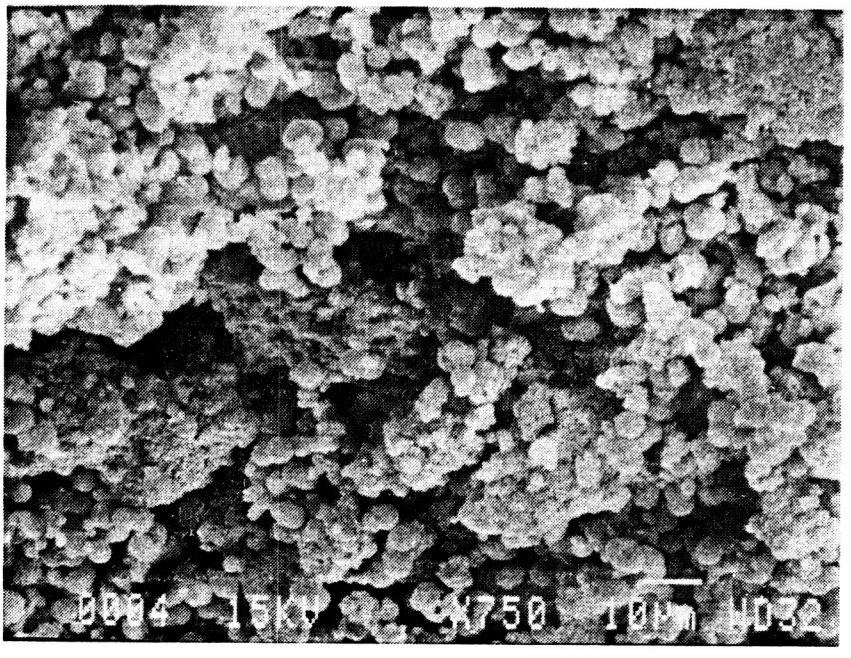

Figure 31. Scanning Electron Micrograph of LaRC-TPI Powder

selectively coat onto the fiber, which caused the concentration of the large clumps in the recirculating deposition chamber to increase. Then, as the coating line continued to operate, these larger particles also began to coat the fiber, and eventually a steady state was reached.

The large clumps created two problems during the continuous coating trials. Because their large size made the clumps difficult to fluidize, it was necessary during the trials to maintain a high air velocity in the coating chamber. This high air velocity increased fiber damage and blew polymer off of the coated tow, decreasing the total amount of coating on the tow. Also, it was very difficult to evenly distribute these large 50 to 100 μm particles on the individual 7 μm carbon fibers. Because of this, the coated prepreg product often had a non-uniform, mottled appearance.

Despite these problems and the uneven feed rate of the polymer feed extruder, the overall uniformity of the coating applied to the fiber was very good. To test this uniformity, a continuous length of prepreg from Trial #10 was cut into thirty 60.96 cm (24 inch) sections. These sections were weighed and their volume fraction of polymer was determined using the procedure detailed in Appendix A. These data and calculated volume fractions are given in Table 5. The average volume percent fiber in these samples was 53.5 % with a standard deviation of only 3.3 %.

The overall coating efficiency of the process, defined as the percentage of polymer fed to the system which was eventually coated onto the fiber, was estimated in trial #10. Before the trial, a known quantity of polymer was added to the feed hopper of the polymer extruder and, at the end of the trial, the amount remaining in the hopper was determined. The difference in these masses yielded the approximate feed rate of the polymer to the coating line. The average mass of polymer per unit length was multiplied by the length of prepreg produced to yield the quantity of polymer which was coated onto the fiber. Dividing the quantity of polymer in the prepreg by that fed to the system gave the efficiency. This calculation, shown in

Table 5. Uniformity in Consecutive 60.96 cm (24 inch) Prepreg Samples (Trial #10)

Sample	Mass of Prepreg, g	Mass of Polymer, g	Volume Percent Fiber
1	0.1993	0.0787	55.0
2	0.2075	0.0869	52.5
3	0.2072	0.0865	52.6
4	0.2145	0.0939	50.5
5	0.2106	0.0899	51.6
6	0.1939	0.0733	56.7
7	0.2067	0.0861	52.7
8	0.2036	0.0829	53.6
9	0.1915	0.0709	57.5
10	0.1792	0.0586	62.1
11	0.1962	0.0755	56.0
12	0.1947	0.0741	56.4
13	0.1950	0.0743	56.4
14	0.2181	0.0975	49.6
15	0.2180	0.0974	49.6
16	0.2228	0.1021	48.4
17	0.2114	0.0908	51.4
18	0.2184	0.0978	49.5
19	0.2157	0.0950	50.2
20	0.2082	0.0876	52.3
21	0.2131	0.0924	50.9
22	0.2189	0.0983	49.4
23	0.1921	0.0715	57.3
24	0.1982	0.0775	55.3
25	0.1964	0.0758	55.9
26	0.2150	0.0943	50.4
27	0.1882	0.0680	58.7
28	0.1983	0.0777	55.3
29	0.2021	0.0814	54.1
30	0.2109	0.0903	51.5
		avg.	53.5
		std. dev.	3.3

Appendix A, yielded a coating efficiency of 93%. However, since this does not account for the amount of polymer lost during weighing or for the difference between the amount of powder in the coating chamber at the beginning and end of the run, it should only be considered an estimate.

Only a small fraction leaked from the entrance and exit of the chamber. The majority of the 7% polymer lost in Trial #10 fell off before it was melted in the convection tube oven. A few lumps of polymer briefly adhered to the first electrical roller and then were blown off by the compressed air stream. There was no loss of powder from the sealed polymer extruder. Once the coated tow was heated by the electrical resistance heating section, the amount of polymer which fell off of the fiber tow was negligible.

Prepreg Flexibility and Characteristics

The 40 to 50% by volume LaRC-TPI prepreg produced during these trials was nearly as flexible as uncoated carbon fiber tow. This particular prepreg could be bent into a loop 5 mm in diameter without crimping or breaking, compared to 3 mm for the uncoated tow. The coating actually improved the bundle cohesion and made the tow easier to handle. Even though some small polymer particles were visible on the surface of the prepreg, they didn't rub off during handling. Table 6 lists the properties of the prepreg produced during each of the trials.

During the evaluation trials, several tests were conducted to determine the amount of heat required to properly melt the powder onto the tow. In the initial tests, a large amount of heat was applied to the fiber tow. During these tests it was noticed that, when the convection oven temperature exceeded 310°C, the polymer would degrade as it melted on the tow. Also, if the potential difference applied to the electrical rollers exceeded 50 volts, the melting was excessive and the spread tow

would contract into a single, stiff, coated strand. This strand crimped as it cooled around the second charged roller, giving the coated product a curled or spring-like shape. This coated product was brittle and broke easily if bent.

Table 6. Properties of Prepreg

Trial #	Length (m)	Approx. % by Vol. Fib.	LaRC-TPI Lot. #	Comments
1	16.5	74.2	92-708	poor uniformity, curled, inflexible
2	51.0	47.1	92-708	poor uniformity, curled, inflexible
3	34.6	89.6	92-708	good uniformity, flexible
4	24.7	58.3	786001	bad uniformity, very stiff
5	49.4	*	786001	burned by oven,bad uniformity
6	65.8	85.0	786001	fair spreading, uniformity, and flex.
7	110.9	*	782101	extruder failure, very non-uniform
8	110.9	73.6	782101	uniform, boardy, well spread
9	228.6	64.6/57.2**	782101	excellent flex., mottled but uniform
10	275.2	53.5	782101	excellent flex., mottled but uniform

*Volume fraction was not obtained.
**Line speed and, therefore, fiber volume fraction were changed during trial.

To avoid these problems, the heat applied in both the convection oven and the electrical heating section was gradually reduced. The best coating results were obtained when the the convection tube oven barely melted the polymer powder. This partial melting firmly attached the polymer particles to the fibers but did not affect their distribution. This eliminated polymer build-up on the first electrically charged

roller and allowed the resistance heating section to operate more efficiently and melt the particles onto the individual filaments.

The voltage between the electrical rollers could be adjusted to heat the coated carbon fiber tow to a wide range of temperatures. However, the current and, therefore, the heat were not always evenly distributed across the tow. When tow spreading was poor and fibers grouped together, the current would preferentially flow through this grouped part of the tow. When this occurred, the filaments would briefly glow red, indicating that the filament surface was well above the degradation temperature of the polymer. This rapidly melted the grouped fibers into a single strand. This interaction between tow spreading and filament temperature showed that, in the final continuous coating line, the effectiveness of the electrical heating section was dependent on the reliability of the spreader.

Initially, it was thought each individual fiber could be encapsulated in a sheath of polymer. Completely melting the polymer required a great deal of heating between the electrical rollers. However, to evaluate a tow in which the coating polymer has been thoroughly melted by electrical resistance heating, a continuous section of prepreg (trial #8) was produced which was 110.9 m in length. The process conditions for this trial are listed in Table 4. The resulting prepreg was referred to as "boardy" due to its stiffness. A scanning electron micrograph (SEM) of a portion of this tow is shown in Figure 32. The figure illustrates that, again, increased heating causes the carbon filaments to agglomerate within the coated tow. Nevertheless, in order to evaluate the physical properties of this prepreg, it was formed into three composite specimens.

In a subsequent evaluation trial, in order to reduce this agglomeration of filaments, the amount of heat supplied to the tow during the electrical heating section was reduced. During this trial, the melting of the powder was barely noticeable. The only evidence was a slight darkening of the prepreg caused by more fiber becoming

ORIGINAL PAGE
BLACK AND WHITE PHOTOGRAPH

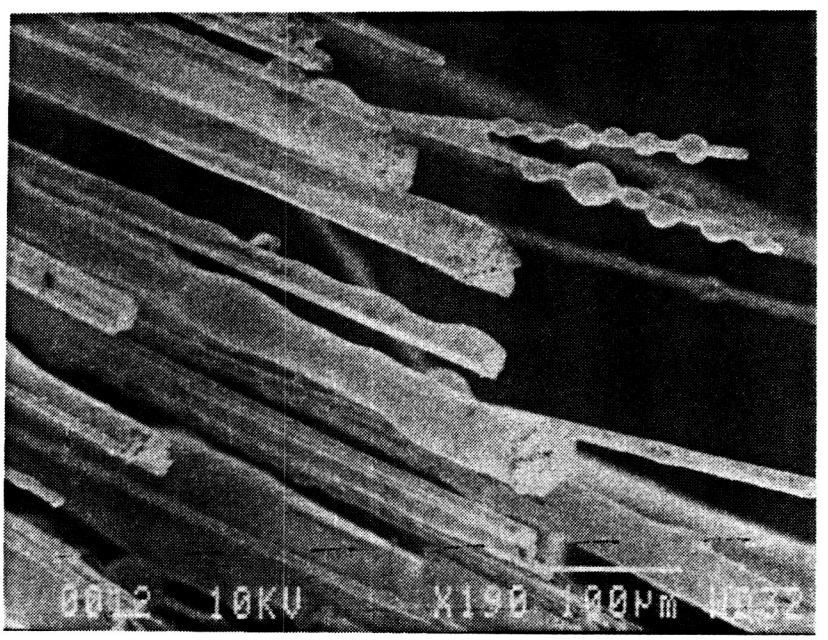

Figure 32. Scanning Electron Micrograph of "Boardy" Prepreg from Trial #8

visible as small particles of powder melted during heating. The tow produced by this process (trial #9) was exceptionally flexible, indicating that only a few filaments were firmly bonded together by the melted polymer. Figure 33 shows an SEM which confirms this observation. The Figure shows that the filaments are linked by droplets of slightly melted polymer, but they are not bonded rigidly by the polymer.

The effect of particle size distribution can be seen from Figure 33. Several small particles are visible which have been completely melted onto the side of one fiber, while the larger particles bridge between fibers, holding them together. It appears that the larger particles may actually contribute to the flexibility of the final tow by holding the filaments apart until the small particles melt.

Operating Parameters for Prepreg Production and Composite Formation

After the tows of Amoco T-300 carbon fiber had been coated with LaRC-TPI polymer powder, they were formed into composites using the procedure described in Chapter III. To determine the influence of polymer melting on final composite performance, two different groups of composites were fabricated and tested. Each group was made from a single length of prepreg. Prepreg from trial #8, the"boardy" prepreg, was selected to form one set of composite specimens, since high melting temperatures were used in this coating trial. The second set of composite specimens was fabricated from prepreg produced during trial #9, since a low melting temperature was employed and the coated tow was very flexible.

To develop a successful composite formation technique, prepreg produced during trial #6 was used to form a composite specimen in a high temperature press. Forming this composite (specimen #1) allowed the necessary press preheat to be determined. It also permitted the accuracy of the mold thermocouple to be checked.

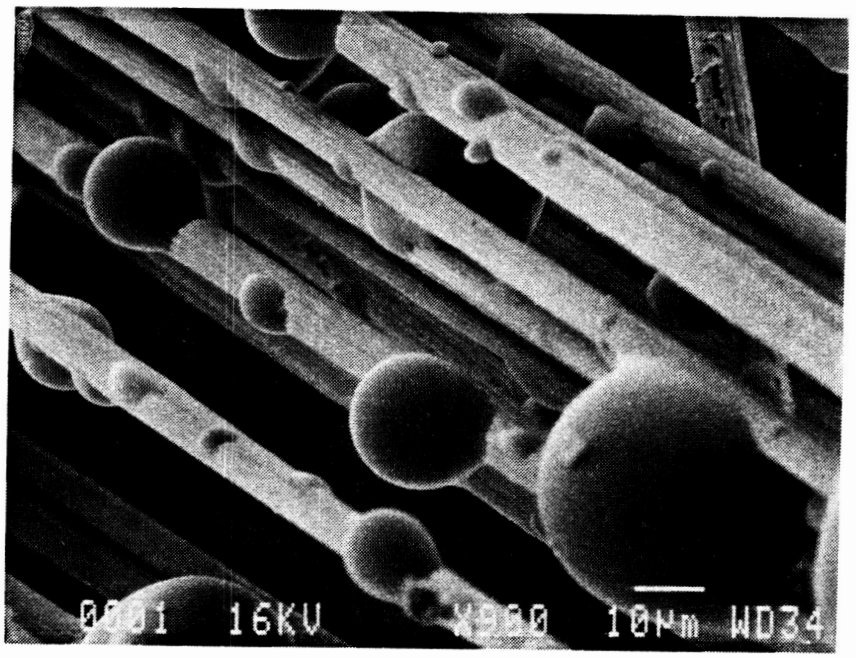

Figure 33. Scanning Electron Micrograph of Flexible Prepreg from Trial #9

Using information gained from the formation of composite specimen #1 prepreg produced during trial #8 was formed into composites which were 68 volume percent fiber. Prepreg from trial #9 was then made into 62 and 57 volume percent fiber composites. The two formation techniques are described in Chapter III. Prepreg from trial #8 (the "boardy" prepreg) was cut into small sections and laid into a mold, whereas the more flexible prepreg produced in trial #9 was wrapped around a mold during fabrication of the composite specimen. The composites were consolidated under vacuum to minimize the formation of voids and to remove any gases caused by further reaction of the polyimide. Because LaRC-TPI has a time dependent melt viscosity, the thermal history of the composite specimen was recorded on a strip chart during formation. Figure 34 shows the temperature of the mold during the processing of the "boardy" prepreg produced in trial #8.

After the first three composite specimens were fabricated using the trial #8 prepreg (the "boardy" prepreg), it was found that they had compacted to a thickness of only 0.180 cm, instead of the 0.159 cm (1/16 inch) expected for a 74 volume percent fiber composite. These samples were placed back in the mold and pressed under vacuum at higher pressure. After being removed from the mold, measurements showed that they had not been further compacted by the reprocessing. It was suspected that the LaRC-TPI was too viscous to redistribute within the specimens and fill the voids during processing.

The sections of the flexible tow produced in trial #9 were laid-up in two wraps which formed four composite specimens, as described in Chapter III. Then these parts were also pressed under vacuum. The thermal history of the flexible tow composites is given in Figure 35.

The composites made from the prepreg produced in trial #8 (the "boardy" prepreg) averaged 0.42% weight loss during formation, while those made from trial #9 prepreg (the flexible prepreg) averaged 1.15% weight loss. It is likely that this

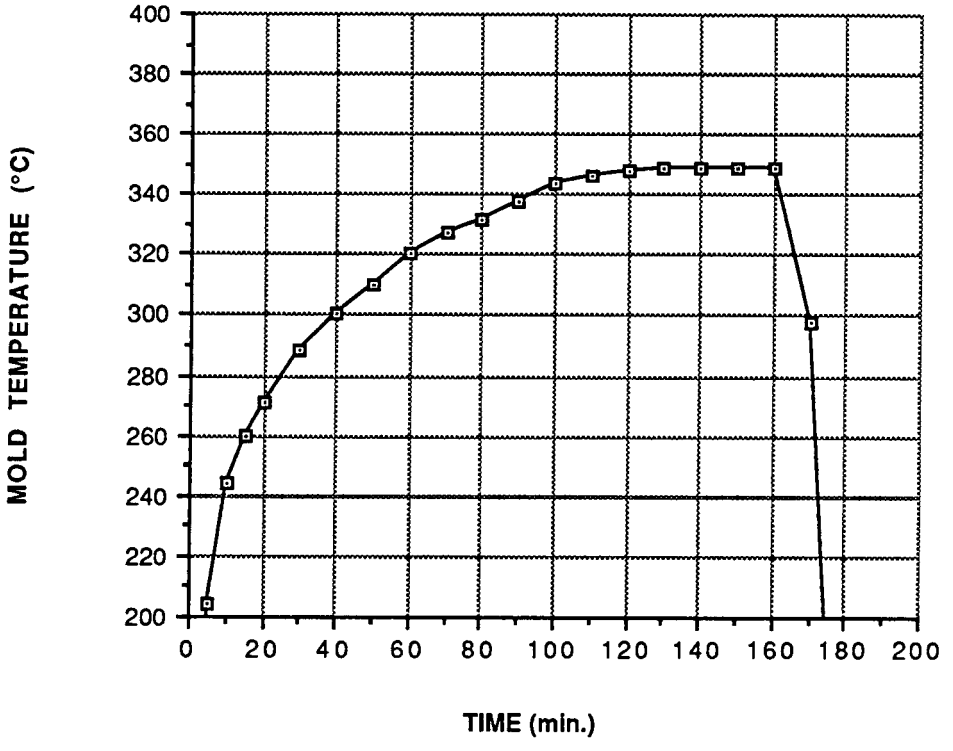

Figure 34. Thermal History of Composite Specimens 2, 3, and 4 (Processed at 11.5 MPa)

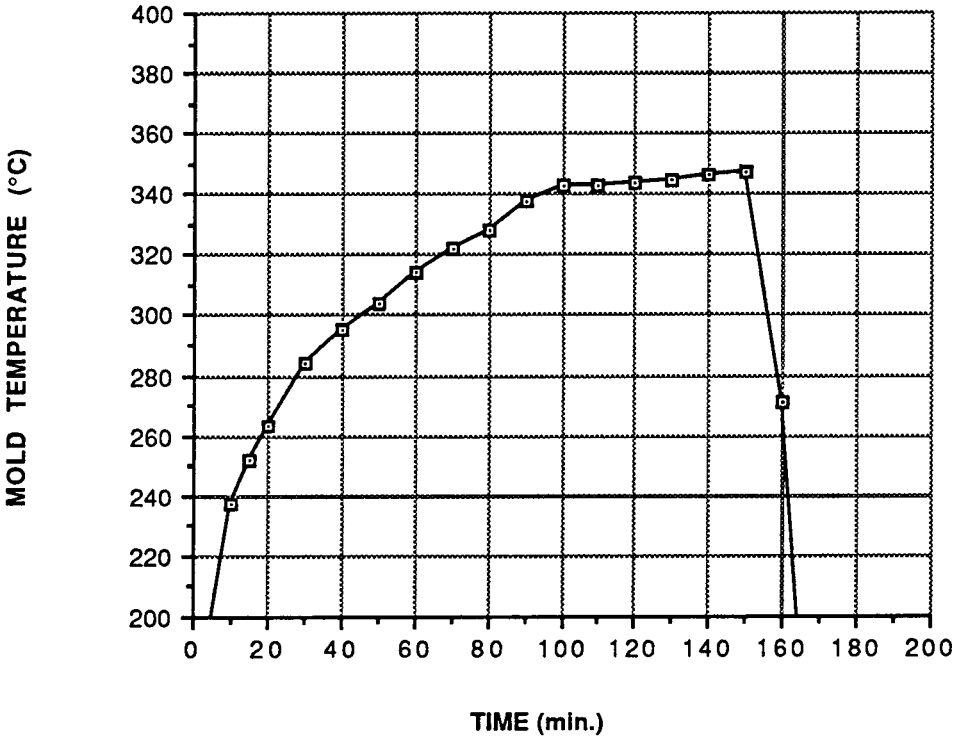

Figure 35. Thermal History of Composite Specimens 5, 6, 7, and 8 (Processed at 17.3 MPa)

weight loss is caused by volatiles given off from the completion of the imidization reaction during composite consolidation. Since the same LaRC-TPI was used to form both prepreg samples, one would expect both to yield a similar total weight loss. Thus, the lower weight loss of the composites fabricated from trial #8 prepreg probably indicates that more of this reaction took place as the powder melted during prepreg formation. Since a higher melting temperature was employed, this is, indeed, likely. If the polyimide was more fully reacted its viscosity would be higher, making composite consolidation more difficult.

Composite Test Results and Observations

Composite Specimen #1 was tensile tested in the Textile Department testing laboratory to gain experience with testing techniques. Tensile tests on composites specimens #3-8 were carried out by the Materials Research Group at NASA Langley Research Center. The tests were conducted according to the ASTM D3039 standard procedure, except that the end tabs were shorter and thinner than those recommended. Strain gauges were applied to the specimens to provide information on tensile modulus. Figure 30 in Chapter IV shows the dimensions of the composite specimens, end tabs and the approximate location of the strain gages. The test results are given in Table 7. The fiber volume fraction and the void volume fraction were calculated from density measurements using the procedure which is outlined in Appendix A.

The tensile modulus of the unidirectional composite samples clearly increases as the fiber volume fraction increases. Since the tensile modulus of LaRC-TPI is much lower than that of the T-300 carbon fibers, this certainly would be expected. Reference 50 reports the tensile modulus for composites fabricated from approximately 62 volume percent T-300 carbon fiber in a matrix of LaRC-TPI polymer

to be 138 GPa (20 Msi). The two composite specimens tested which had fiber volume fractions of 62% were found to have modulus values equivalent to this.

Table 7 shows that the tensile strength of all of the composite samples tested was quite low. Reference 50 reports the tensile strength for composites fabricated from approximately 62 volume percent T-300 carbon fiber in an epoxy matrix to be 1.72 GPa. The tensile strength of the composite samples produced in the present research ranges from only 0.71 to 0.89 GPa.. The trend of the tensile strength appears to follow no consistent pattern. Surprisingly, the samples with the lowest fiber volume fraction and 8% void content were found to have a tensile strength considerably higher than the other samples.

Table 7. Physical Characteristics of Composite Specimens

Specimen #	Prepreg Used	% by Vol. Fiber	% by Vol. Voids	Tensile Strength	Tensile Modulus
				MPa (ksi)	GPa (Msi)
1	#6	59	5	710 (103)	*
2	#8	69	11	*	*
3	#8	68	13	760 (111)	150 (22)
4	#8	67	13	850 (124)	150 (22)
5	#9	62	6	770 (112)	150 (22)
6	#9	62	6	840 (122)	140 (20)
7	#9	56	8	850 (120)	130 (18)
8	#9	57	7	890 (130)	130 (18)

*Specimen was not tested

A number of factors may have contributed to the low tensile strength of the composite specimens. One factor was the high void volume of the specimens. This high void volume was probably caused by the composite consolidation procedure. The mold used to form the specimens was quite large, weighing slightly more than 10 kg, therefore, a lengthy heat-up time was required. LaRC-TPI has a time dependent melt viscosity (see Figure 7). Its viscosity remains low only for about 10 minutes and then rapidly increases by several orders of magnitude. This rise in viscosity begins at a melt temperature of approximately 300°C. Because of this the mold must be heated from the melt temperature to the processing temperature in less than 10 minutes. Figure 36 shows a temperature versus time plot for the specimens. It can be seen from the figure that heating the samples from 300°C to 343°C took, in all cases, more than 30 minutes. It is likely that this extended time allowed the chain extension reaction and crystalline reorientation to increase the melt viscosity (38) before the matrix was fully distributed.

Another factor which probably contributed to the low tensile values for specimens fabricated from prepreg produced during trial #8 (specimens 3 and 4) was the excessive fiber and polymer heating during this evaluation trial. Visual examination of these failed composite test specimens showed that many fibers pulled out of the matrix at failure. This indicates that poor fiber/matrix adhesion may have lead to premature failure of the composite specimen. Since heating was excessive during the preparation of prepreg from trial #8, it is likely that the polymer at the interface of the fiber was degraded, leading to the early failure of these composite specimens. The fracture surfaces of the other composite test specimens produced from prepreg produced during trial #9 showed no evidence of this failure mode. Figure 37 is an SEM of the fracture surface of specimen #1 which was also made from flexible prepreg. The fact that no matrix delamination occurred with any of the samples made from flexible prepreg indicates that matrix adhesion for these samples

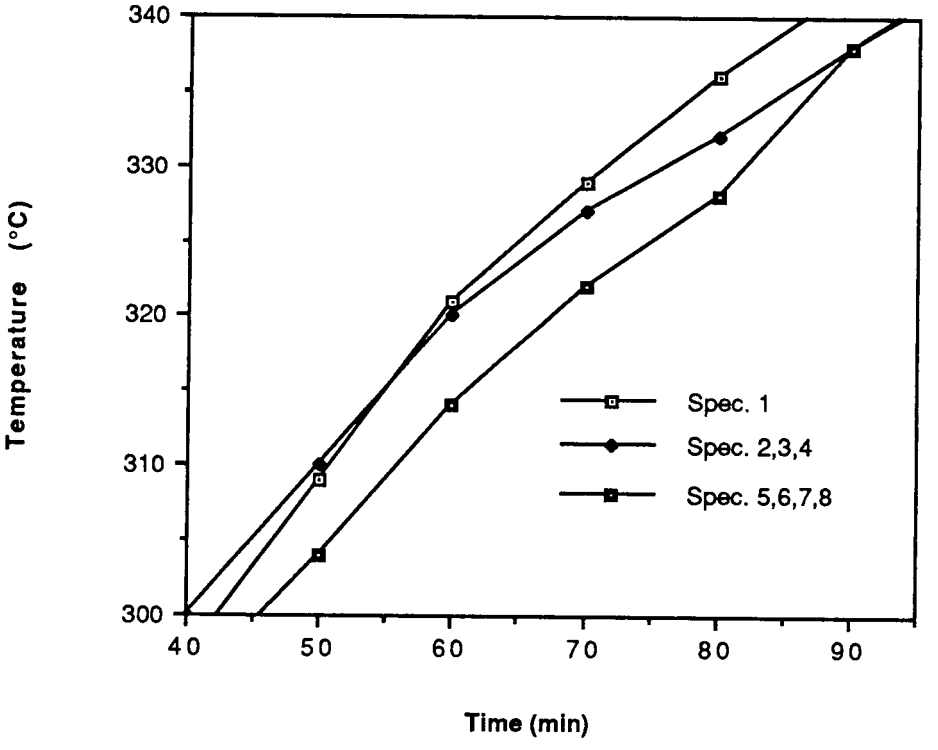

Figure 36. Mold Temperature Versus Time within LaRC-TPI Increasing Viscosity Region

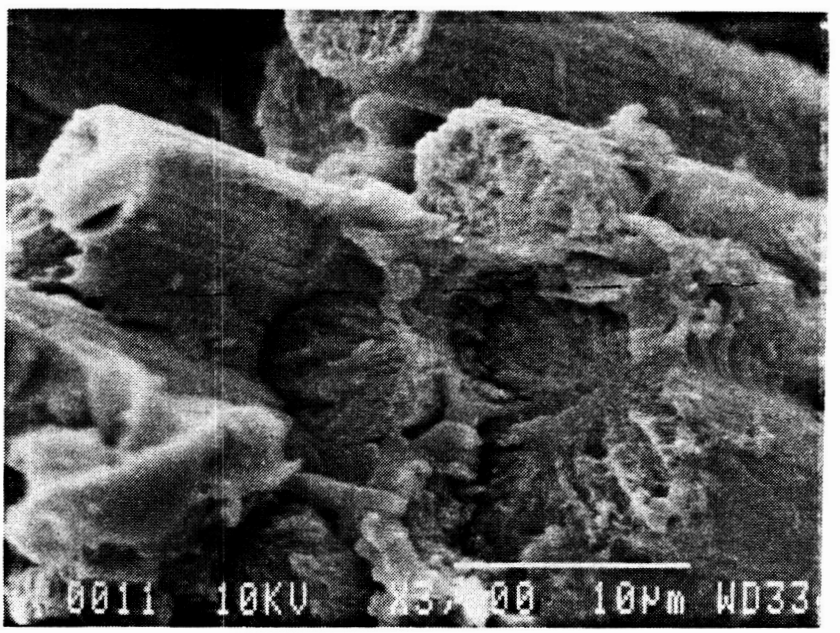

Figure 37. Scanning Electron Micrograph of the Fracture Surface of Specimen #1

However, even though the tensile strength of the composite specimens was low, the matrix distribution was quite good. Figures 38 and 39 show photomicrographs of cross-sections of several of the composite specimens. It is clear from the micrographs that there are no large areas of undistributed polymer. Since the powder coating process coats the individual fibers in the tow, good matrix distribution in the final part is assured. As might be expected, the specimen formed at a pressure of 17.3 MPa (Figure 38) has a larger number of voids than the specimen formed under a pressure of 34.5 MPa (Figure 39).

Commercially produced composites are typically formed with a pressure of less than 5 MPa. However, the high viscosity of the molten LaRC-TPI made the much higher pressures necessary. If the specimens could have been heated faster during processing, the viscosity would have been reduced and lower consolidation pressures may have been adequate.

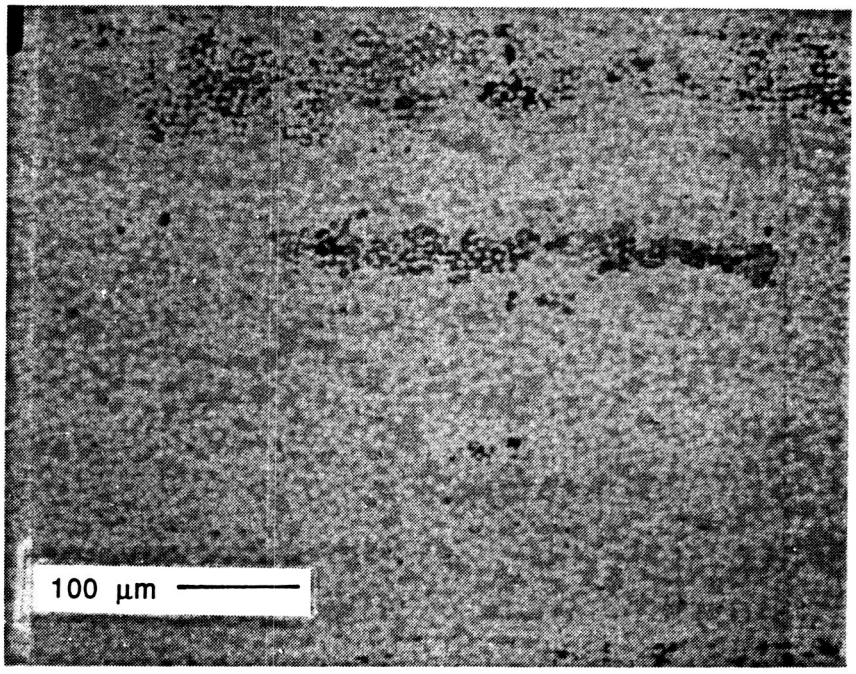

Figure 38. Photomicrograph of a Cross-Section of Specimen #7 (Processed at 17.3 MPa)

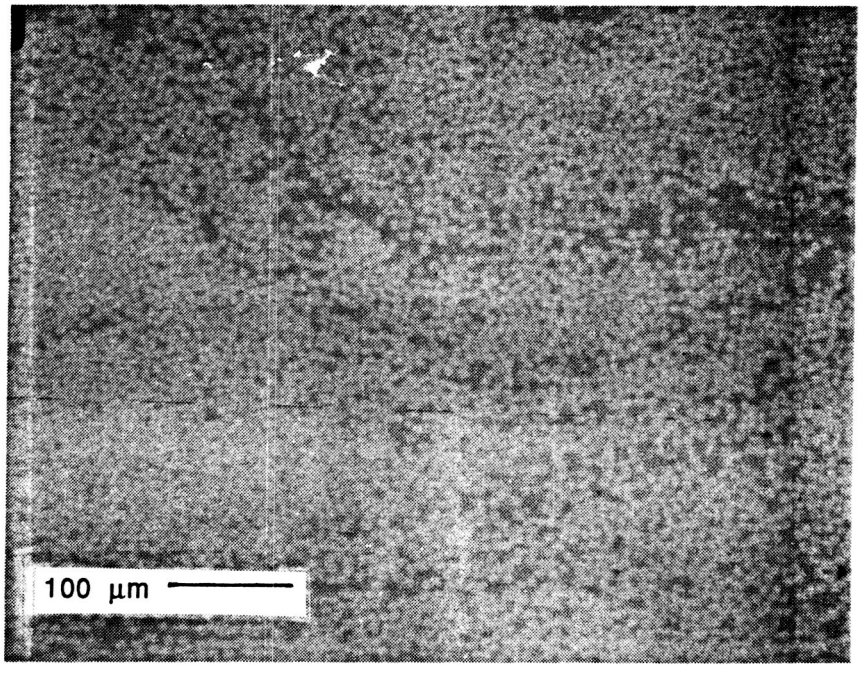

Figure 39. Photomicrograph of a Cross-Section of Sample #1 (Processed at 34.5 MPa)

CHAPTER VI

CONCLUSIONS

The following conclusions may be drawn from the results of this investigation:

1. The polymer powder coating technique developed in this research produces a uniform prepreg with flexibility approaching that of uncoated fiber. The high flexibility of this prepreg should allow it to be braided, woven or knitted into a preimpregnated composite form.

2. Unlike some other powder coating techniques, this process has negligible powder loss. This low loss is a result of the recirculating nature of the polymer coating chamber. The vestibule design and the use of a vacuum on the coating chamber further reduced powder loss.

3. The low tensile strength of the composite specimens may have been caused by either voids or poor interfacial bonding.

4. Excessive electrical resistance heating of prepreg during processing can reduce the interfacial strength of carbon fiber/LaRC-TPI composites due to polymer degradation.

5. The performance of the pneumatic spreader limited the length of a prepreg section to less than 300 m. The degree of tow spreading prior to polymer application directly affected the coating uniformity and prepreg flexibility.

CHAPTER VII

RECOMMENDATIONS

The following recommendations are made for future work in this area:

1. A more thorough investigation of the pneumatic spreading of carbon fibers should be conducted. This study should investigate the use of compressed air instead of a vacuum system, as well as the use of a multi-stage pneumatic spreader.

2. Microwave frequency induction heating of the coated carbon fiber tow should be examined to see if greater control of tow heating can be achieved. Since this method of heating does not rely on physical contact with the fibers, it may prove to be less damaging to the prepreg and less dependent on the operation of the pneumatic spreader than direct electrical resistance heating.

3. This polymer coating method should be tried with a number of other thermoplastic polymer powders.

4. A new composite mold should be designed which would allow rapid heating of the prepreg during part consolidation.

5. The polymer feed extrusion system should be improved.

APPENDICES

Appendix A

Sample Calculations

The following sample calculations were used to determine prepreg characteristics and the physical properties of composite specimens. These sample calculations are for prepreg trial #8 and composite specimen #4. The calculation of coating efficiency was done for trial #10. The density used for LaRC-TPI is 1.40 g/cm3 and is for the initial molding powder (31). This value provides only an estimate of the density of the polymer phase after processing, due to changes in degree of crystallinity, so for calculations involving composite specimens it will be rounded to 1.4 g/cm3. The reported density for unsized, surface treated, 3K Amoco T-300 carbon fiber is 1.76 g/cm3 (50).

Uncoated Tow Linear Density. The mass of a small aluminum weighing dish was recorded. A known length of uncoated tow which had been run through the spreader on the coating line was cut. The tow sample was placed in the dish and the mass of sample and pan was determined. The mass of the fiber sample, m_t, was determined as follows

m_t = (mass sample and pan) - (mass pan),

m_t = 2.2043 g - 1.3900 g,

m_t = 0.8142 g.

The uncoated tow linear density, d_{ln}, was then calculated from

$$d_{ln} = \frac{m_t}{l},$$

where

m_t = uncoated tow mass, g,

l = length of tow, cm,

$$d_{ln} = \frac{0.8142\ g}{411.5\ cm},$$

$d_{ln} = 1.979 \times 10^{-3}$ g/cm.

Prepreg volume fraction fiber. A length of polymer coated carbon fiber prepreg was cut and placed in an aluminum weighing dish. The mass of the sample of prepreg, m_p, was determined by

m_p = (mass of prepreg and pan) - (mass of pan),

m_p = 1.7821 g - 1.3900 g,

m_p = 0.3921 g.

The mass of fiber in the prepreg, m_f, was then found from

$m_f = d_{ln} \times l$,

where

d_{ln} = linear density of the uncoated tow, g/cm,

l = length of prepreg sample, cm,

$m_f = (1.979 \times 10^{-3}\ g/cm) \times (152.4\ cm)$,

m_f = 0.3016 g.

The mass fraction fiber in the sample, X_{fm}, was then found by

$$X_{fm} = \frac{m_f}{m_p},$$

where

m_f = mass of fiber in prepreg, g,

m_p = mass of prepreg, g,

$$X_{fm} = \frac{0.3016\ g}{0.3921\ g},$$

$$X_{fm} = 0.7692.$$

The fiber volume fraction in the prepreg, X_{fv}, was then determined from

$$X_{fv} = 1 - \left(\frac{\left(\frac{1}{X_{fm}} - 1 \right)}{\left(\frac{1}{X_{fm}} - 1 \right) + \frac{d_p}{d_f}} \right),$$

where

X_{fm} = fiber mass fraction,

d_p = density of polymer, g/cm3,

d_f = density of fiber, g/cm3,

$$X_{fv} = 1 - \left(\frac{\left(\frac{1}{0.7692} - 1 \right)}{\left(\frac{1}{0.7692} - 1 \right) + \frac{1.40\ g/cm^3}{1.76\ g/cm^3}} \right),$$

$$X_{fv} = 0.726.$$

Efficiency of polymer use. The calculation of efficiency was done for prepreg trial #10. The average polymer mass fraction of the prepreg, X'_{pm}, was calculated as follows

$$X'_{pm} = 1 - X'_{fm},$$

where

X'_{fm} = fiber mass fraction,

$X'_{pm} = 1 - 0.589$

$X'_{pm} = 0.411.$

The mass of polymer coated onto the fiber, m_c, was then determined from

$$m_c = \frac{(X'_{pm})\, m'_p\, (s_l)\, t_r}{l},$$

where

X'_{pm} = average mass fraction polymer,

m'_p = average mass of prepreg sample section, g,

s_l = line speed during prepreg trial, m/min,

t_r = run time for prepreg trial, min,

l = length of prepreg sample section, m,

$$m_c = \frac{(0.411)\, 0.2048 \text{ g } (3.2 \text{ m/min})\, 86 \text{ min}}{0.610 \text{ m}},$$

m_c = 38 g.

The coating efficiency, η, was then found using

$$\eta = \frac{m_c}{m_i},$$

where

m_c = mass of polymer coated onto fiber, g,

m_i = mass of polymer fed to system, g,

$$\eta = \frac{38 \text{ g}}{40.8 \text{ g}},$$

η = 0.93

Number of prepreg strips used for a composite part. The volume of the mold cavity, V_m, was determined as follows:

$V_m = L \times T \times W,$

where

L = length of mold cavity, cm,

T = thickness of mold cavity, cm,

W = width of mold cavity, cm,

$V_m = (20.32\ cm) \times (0.159\ cm) \times (1.270\ cm),$

$V_m = 4.10\ cm^3.$

The required fiber volume, V_{fr}, is determined by

$V_{fr} = X'_{fv} \times V_m,$

where

X'_{fv} = the average fiber volume fraction of three lengths of prepreg,

V_m = volume of mold cavity, cm^3,

$V_{fr} = (0.740) \times (4.10\ cm^3),$

$V_{fr} = 3.03\ cm^3.$

The minimum number of prepreg sections required, N_m, was then found by

$$N_m = \frac{V_{fr}(d_f)}{L(d_{ln})},$$

where

V_{fr} = required fiber volume, cm^3,

d_f = density of fiber, g/cm^3,

L = length of mold cavity, cm,

d_{ln} = linear density of uncoated tow, g/cm,

$$N_m = \frac{3.03\ cm^3\left(1.76\ g/cm^3\right)}{20.32\ cm\left(1.979 \times 10^{-3}\ g/cm\right)},$$

$$N_m = 133.$$

The number of prepreg sections used for the composite specimen, N_p was then determined by

$$N_p = N_m + 5,$$

where

N_m = minimum number of prepreg sections required,

$$N_p = 133 + 5,$$

$$N_p = 138.$$

Fiber volume fraction in composite part. The volume of fiber in the part, V_f, was calculated from

$$V_f = \frac{N_p(L_p)\,d_{ln}}{d_f},$$

where

N_p = number of prepreg specimens in part,

L_p = length of part, cm,

d_{ln} = linear density of uncoated tow, g/cm,

$$V_f = \frac{138\,(20.08\ cm)\,1.979 \times 10^{-3}\ g/cm}{1.76\ g/cm^3},$$

$$V_f = 3.12\ cm^3.$$

The volume of the part, V_p, was then determined using

$$V_p = L_p \times W_p \times T_p,$$

where

L_p = length of part, cm,

W_p = width of part, cm,

T_p = average thickness of part, cm,

V_p = 20.08 cm x 1.273 cm x 0.182 cm,

V_p = 4.65 cm^3.

The fiber volume fraction, X_{fv}, of the part was then calculated by

$$X_{fv} = \frac{V_f}{V_p},$$

where

V_f = volume of fiber in part, cm^3,

V_p = volume of part, cm^3,

$$X_{fv} = \frac{3.12\ cm^3}{4.65\ cm^3},$$

X_{fv} = 0.67.

Void fraction in composite specimens. The estimation of void fraction in the composite specimens was based on measurements of part mass and volume and on the density of LaRC-TPI and T-300 carbon fibers found in the literature. The mass of fiber in the part, m_{fp}, was found from

$$m_{fp} = N_p \times L_p \times d_{ln},$$

where

N_p = number of prepreg sections in part,

L_p = length of part, cm,

d_{ln}, = linear density of fiber, g/cm,

m_{fp} = (138) x (20.08 cm) x (1.979×10^{-3} g/cm),

m_{fp} = 5.484 g.

The volume of the LaRC-TPI in the part, V_{pp}, was found from

$$V_{pp} = \frac{m_p - m_{fp}}{d_p},$$

where

m_p = mass of part, g,

m_{fp} = mass of fiber in part, g,

d_p = density of LaRC-TPI (31), g/cm^3,

$$V_{pp} = \frac{6.803 \text{ g} - 5.484 \text{ g}}{1.4 \text{ g/cm}^3},$$

V_{pp} = 0.94 cm^3.

The void volume fraction of the part, X_{vp}, was then calculated by

$$X_{vp} = \frac{V_p - V_{fp} - V_{pp}}{V_p},$$

where

V_p = volume of part, cm^3,

V_{fp} = volume of fiber in part, cm^3,

V_{pp} = volume of LaRC-TPI in part, cm^3,

$$X_{vp} = \frac{4.65 \text{ cm}^3 - 3.12 \text{ cm}^3 - 0.94 \text{ cm}^3}{4.65 \text{ cm}^3},$$

$X_{vp} = 0.13.$

Tensile strength of a composite specimen. The ultimate tensile strengths of composite specimens # 3 through 8 were tested by the Materials Research Group at NASA Langley Research Center. The cross-sectional area of the sample, A_{cx}, was first determined at the point of minimum height on the part by

$$A_{cx} = W_p \times T_{pm},$$

where

W_p = width of part, cm,

T_{pm} = minimum thickness of part, cm,

A_{cx} = (1.273 cm) x (0.180 cm),

$A_{cx} = 0.229\ cm^2.$

The tensile load at failure was then taken from the plot of load versus strain ratio for the specimen. The tensile strength, σ, was then calculated from

$$\sigma = \frac{Ld\,(g)}{A_{cx}}\left(\frac{100\ cm}{m}\right)^2,$$

where

Ld = maximum tensile load, kg,

g = acceleration of gravity, 9.81 m/s^2,

A_{cx} = cross-sectional area at minimum height, cm^2,

$$\sigma = \frac{1980\ kg\left(9.81\ m/s^2\right)}{0.229\ cm^2}\left(\frac{100\ cm}{m}\right)^2,$$

$\sigma = 850$ MPa.

The strain ratio at failure was taken from the tensile load versus strain ratio plot. The tensile modulus, E, was determined by

$$E = \frac{\sigma}{X_{st}},$$

where

σ = tensile strength, Pa,

X_{st} = strain ratio,

$$E = \frac{850\ \text{MPa}}{5.6 \times 10^{-3}},$$

$$E = 15\ \text{GPa}.$$

Appendix B

Materials

Carbon fiber. Thornel T-300 3K, un-sized, zero-twist, surface treated, 3 lb nom. wgt., manufactured by Amoco Performance Products, Inc., Greenville, SC. Used in all prepreg.

Polymer powder. Eastabond FA 252, hot melt adhesive, manufactured by Eastman Chemical Products, Inc., Kingsport, TN. Used to develop powder coating techniques.

Polyimide powder. LaRC-TPI, #2000, lot #'s 92-708, 786001, and 782101, supplied by NASA Langley Research Center, Hampton, VA, manufactured by Mitsui Toatsu Chemicals, Inc., Tokyo, Japan. Used as polymer matrix in all prepreg.

Mold release. Frekote FRP aerosol, 400 ml, manufactured by Hysol Div. of the Dexter Corp., Seabrook, NH. Used on composite mold surfaces to avoid sticking.
Bagging film. Thermalide, 0.0076 cm thickness, 30.5 cm wide roll, manufactured by International Plastic Products Inc., Carson, CA. Used to bag composite mold during specimen formation.

Vacuum bag sealant tape. A800 G3, manufactured by Airtech Intl. Inc., Carson, CA. Used to seal mold.

Strain gauges. EA-06-375BG-120, 120 ohms, 0.953 cm gauge length, manufactured by Micromeasurements Inc., Romulus, MI. Used to measure strain while testing samples.

Strain gauge application accessories. M-Bond 600 adhesive, M-Prep Conditioner A (dilute phosphoric acid), M-Prep Neutralizer S (dilute ammonium hydroxide), 330-DFV 3-conductor cable, CEG-AST bondable terminals, M-Flux AR flux, manufactured by Micromeasurements Inc., Romulus, MI. Used to apply strain gauges.

Appendix C

Equipment

Prepreging apparatus. Custom design, including wind-off, dancer-arm tension control, fiber spreader, recirculating polymer deposition chamber, polymer extruder, convection tube oven, electrical resistance heating rollers, and wind-up. Fabricated by the author, and Clemson University Engineering Services. Used to make carbon fiber prepregs.

High temperature press. Carver Laboratory Press Model #2529, Clemson ID #173985, located in room #12, Earle Hall, manufactured by Fred S. Carver Inc., Menomone Falls, WI. Used to apply heat and pressure when making composite specimens.

Composite mold. Custom design shown in Figure 27. Fabricated by Clemson University Engineering Services. Used to form composite specimens.

Variable Autotransformer. Powerstat model #3PN1165, manufactured by Superior Electric, Bristol, CN. Used to supply variable AC power to the vibrator on the polymer extruder.

Variable Autotransformer. Powerstat model #3PN1165, manufactured by Superior Electric, Bristol, CN. Used to supply variable AC power to the vibrator on the recirculating polymer deposition chamber.

Variable Autotransformer. Model #3PN1010, manufactured by Staco Inc., Dayton, OH. Used to supply variable AC power to the electrically charged rollers when coating fiber.

Variable Autotransformer. Model #3PN1010, manufactured by Staco Inc., Dayton, OH. Used to supply variable AC power to the convection tube oven when coating fiber.

Variable Autotransformer. Model #3PN1010, manufactured by Staco Inc., Dayton, OH. Used to supply variable AC power to the fan motor on the recirculating deposition chamber.

Variable Autotransformer. Powerstat model #2PF136, manufactured by Superior Electric, Bristol, CN. Used to supply variable AC power to the vacuum cleaner.

Variable DC power supply. Model 15DC25-1, manufactured by Dart Industries, Zionsville, IN. Used to control speed of wind-up motor.

Variable DC power supply. Model 15DC25-1, manufactured by Dart Industries, Zionsville, IN. Used to control speed of wind-off motor.

Variable DC power supply. Model 15DC25-1, manufactured by Dart Industries, Zionsville, IN. Used to control speed of polymer extruder motor.

Electric vibrator. Syntron, model #V-4, serial #0795, manufactured by Syntron Co., Homer, PA. Used to vibrate polymer extruder.

Electric vibrator. Syntron, model #V-4, serial #0798, manufactured by Syntron Co., Homer, PA. Used to vibrate recirculating polymer deposition chamber.

Motor. 115, AC-DC series, Type N53, 5000 rpm, 0.6 amps, manufactured by Krebs Electrical and Mfg. Co., New York, NY. Used to drive polymer extruder.

Motor. 90 V, DC, catalogue #6P7406, serial #386B, 33:1 reducer, 104 rpm output, manufactured by Baldor Industrial Motor, Fort Smith, AR. Used to drive fiber wind-up.

Motor. 90 V, DC, catalogue #6P7406, serial #5/86B, 33:1 reducer, 104 rpm output, manufactured by Baldor Industrial Motor, Fort Smith, AR. Used to drive fiber wind-off.

Motor. 115 V AC-DC series, model #2M145, 10000 rpm, manufactured by Dayton Electric Manufacturing Co., Chicago, Ill. Used to drive fan of recirculating polymer deposition chamber.

Variable gear reducer. Zeromax, model #E1, 0-400 rpm, manufactured by Zeromax Co., Minneapolis, MN. Used to control traverse rate.

Gear reducer. 50:1,Model E, 1750 input rpm, manufactured by Browning, Maysville, KY. Used on wind-up drive.

Gear reducer. 100:1, catalog #TW109, serial #R007438, manufactured by Boston Gear Works, Quincy, MA. Used on polymer extruder drive.

Gear reducer. 4:1, model #10A45, manufactured by Metron Instrument Co., Denver, CO. Used on polymer extruder drive.

Gas rotameter. Tru-Taper, tube size 4-15-1, serial #C-4724, manufactured by Brooks Rotameter Co., Lansdale, PA. Used to control nitrogen flow rate to recirculating polymer deposition chamber.

Shop vacuum. Craftsman, model #113.17917, 2.5 hp, variable speed, serial #7202.V1215, manufactured by Sears, Roebuck and Co., Chicago, IL. Used to supply vacuum to fiber spreader.

Potentiometer. 75 k ohm, model #CU 7531, manufactured by Ohmite Inc., Dayton, OH. Used in dancer arm to control wind-off motor speed.

Tensiometer. Mini-Tens R-046, serial #8223, manufactured by Rothschild Inc., Zurich, Switzerland. Used to determine fiber tension.

LITERATURE CITED

1. Margolis, J. M., "Advanced Composites for Airframes and Car Bodies," Chemical Engineering Progress, (83)12, 30-43 (1987).

2. Gantt, B. W., M. S. Thesis, Clemson University, Clemson S. C. (1987).

3. Margolis, J. M. (ed.), Advanced Thermoset Composites, Van Nostrand Reinhold Co., New York, NY (1986).

4. Worthy, W., "Wide Variety of Applications Sparks Polymer Composites Growth," Chem. and Eng. News, March 16 (1987).

5. St. Clair, T. L., N. J. Johnston, R. M. Baucum, "High Performance Composites Research at NASA-Langley," NASA Technical Memorandum 100518, January (1988).

6. Vannucci, R. D., "PMR Polyimide Compositions for Improved Performance at 371°C," SAMPE Quart., (19)1, 31-36 (1987).

7 Serafini, T.T., "Polymer Matrix Composites Research at Lewis Research Center," Tough Composite Materials, Noyes Publications, Park Ridge, NJ, 350-373 (1985)

8. King, J., M. Chaudhari, G. Disalvo,"Thermoset Resins for High Performance Composites," 32nd Intl. SAMPE Symp., April 6-9 (1987).

9. Johnston, N. J., P M. Hergenrother, "High Performance Thermoplastics: A Review of Neat Resin Properties," 32nd Intl. SAMPE Symp., April 6-9 (1987).

10. Madan, S., M. Wallach, "Engineering Resins: High Technology Materials," SPI/SPE Plastics-West Conference Proceedings, Las Vegas, NV, Oct. 21-22 (1987).

11. Kumar, S, "Thermoplastic Matrix Composites," Intl. Fiber Jour., (3)5, 4 (1988).

12. Hartness, T., "Thermoplastic Powder Technology for Advanced Composite Systems," 33rd Intl. SAMPE Symposium, Mar. 7-10 (1988).

13. Carpenter, J. F., "Thermal Analysis and Crystallization Kinetics of High-Temperature Thermoplastics," SAMPE Jour., Jan./Feb. (1988).

14. Majidi, A. P., M. J. Rotermund, L. E. Taske, "Thermoplastic Preform Fabrication and Processing," SAMPE Jour., Jan./Feb. (1988).

15. Clemans, S. R., E. D. Western, and A.C. Handermann, "Hybrid Yarns for High Performance Thermoplastic Composites," Preprint for Proceedings SAMPE 8th Intl. Conf., Labaule, France, May 18-21 (1987).

16. Turner, R. M., F. N. Cogswell, "The Effect of Fiber Characteristics on the Morphology and Performance of Semi-Crystalline Thermoplastic Composites," 18th Intl. SAMPE Tech. Conf., Oct. 7-9 (1986).

17. Bigg, D. M., D. F. Hiscock, D. C. Schiltz, J. R. Preston, E. J. Bradbury, "High-Strength, Stampable Thermoplastic Composites," Plastics Eng., (44)3, 51-54 (1988).

18. Quinn, K. R., G. O'Brien, "Thermoplastic Composites for the Hot Jobs," Machine Design, Feb. 11 (1988).

19. "Chemical Resistance of High-Performance TP Composites," Machine Design, Mar. 10 (1988).

20. Chang, I. Y., "PEKK as a New Thermoplastic Matrix for High Performance Composites," SAMPE Quar., (19)4, 29-34 (1988).

21. Reilly, J. J., S. J. Thoman, and W. W. Lin, "Characterization of Hybridized Conductive Fiber Reinforced Thermoplastics," 18th Intl. SAMPE Tech. Conf., Oct. 7-9 (1986).

22. Beever, W. H., V. H. Rhodes, and J. R. Wareham, "Continuous Length Thermoplastic Composite Laminates," SAMPE Jour., Jan./Feb. (1988).

23. Lindenmeyer, P. H., N. T. Gerken, and C. H. Sheppard, "Relationship of Morphology to Mechanical Properties in Poly (p-Phenylene Sulfide) Composites," 18th Intl. SAMPE Tech. Conf., Oct. 7-9 (1986).

24. Burks, H. D., and T. L. St. Clair, "Processable Aromatic Polyimides," Jour. Appl. Poly. Sci., (30), 2401-2411 (1985).

25. Wedgewood, A. R., K. B. Su, and J. A. Narin, "Toughness Properties and Service Performance of High Temperature Thermoplastics and Their Composites," SAMPE Jour., Jan./Feb. (1988).

26. Driscoll, S. B., T. C. Walton, "Adhesion and Characterization of Prepreg Processable Polyimides," 32nd Intl. SAMPE Symp., April 6-9 (1987).

27. Peake, S. L., A. Maranci, and E. Sturm, "Thermoplastic Matrix Composites Based on Polyetherimides," 32nd Intl. SAMPE Symp., April 6-9 (1987).

28. Harris, F. W., M. W. Beltz, and P. M. Hergenrother, "A New Readily Processable Polyimide," 18th Intl. SAMPE Tech. Conf., Oct. 7-9 (1986).

29. Hergenrother, P. M., B. J. Jensen, and S. J. Havens, "Solvent Resistant Thermoplastic Composite Matrices," Tough Composite Materials, Noyes Publications, Park Ridge, NJ, 292-309 (1985).

30. St. Clair, A. K., and T. L. St. Clair, "The Developement of Aerospace Polyimide Adhesives," Polyimides, Vol. 2, K. L. Mittal ed., Plenum Publishing Corp., New York, NY, 977-1002 (1984).

31. A. K. St. Clair, and T. L. St. Clair, "A Multi-Purpose Thermoplastic Polyimide," SAMPE Quar., Oct. (1981).

32. Johnson, N. J., and T. L. St. Clair, "Thermoplastic Matrix Composites: LaRC-TPI, Polyimidesulfone and Their Blends," 18th Intl. SAMPE Tech. Conf., Oct. 7-9 (1986).

33. St. Clair, T. L., and H. D.Burks, "Thermoplastic/Melt-Processable Polyimides," Tough Composite Materials, Noyes Publications, Park Ridge, NJ, 310-327 (1985).

34. Yamaguchi, A., M. Ohta, "LaRC-TPI and New Thermoplastic Polyimides," 18th Intl. SAMPE Tech. Conf., Oct. 7-9 (1986).

35. Burks, H. D., T. L. St. Clair, and T.-H. Hou, "Characterization of Crystalline LaRC-TPI Powder, SAMPE Quar., (18)1, 1-8 (1986).

36. Hartness, T. J., "An Evaluation of a High Temperature Thermoplastic Polyimide Composite," 32nd Intl. SAMPE Symp., April 6-9 (1987).

37. Hou, T.-H., and J.-M. Bai, "Thermal Properties of Crystalline LaRC-TPI Powder," Proceedings SPE ANTEC '87, Los Angeles, CA (1987).

38. Hou, T.-H., J. M. Bai, and T. L. St. Clair, "Polymerization and Crystalline Behavior of a LaRC-TPI Powder," Jour. of Appl. Pol. Sci., (36), 321-333 (1988).

39. Hou, T.-H., N. T. Wakelyn, and T. L. St. Clair, "Investigation of Crystalline Changes in LaRC-TPI Powders," Jour. of Appl. Pol. Sci., (36), 1731-1739 (1988).

40. Hou, T.-H., J.-M. Bai, and T. L. St. Clair, "A DSC Study on Crystalline LaRC-TPI Powder - A New Version with Higher Initial Molecular Weight," SAMPE Quar., (18)4, 20-24 (1987).

41. Burks, H. D., and T. L. St. Clair, "High Temperature Polyimide Blends," SAMPE Quar., (19)1, 1-6 (1987).

42. Pratt, J. R., T. L. St. Clair, H. D. Burks, and D. M. Stoakley, "Polyimide Processing Additives," 32nd Intl. SAMPE Symp., April 6-9 (1987).

43. Egli, A. H., L. L. King, and T. L. St. Clair, "Semi-Interpenetrating Networks of LaRC-TPI," 18th Intl. SAMPE Tech. Conf., Oct. 7-9 (1986).

44. Hurwitz, F. I., "Ethynylated Aromatics as High Temperature Matrix Resins," SAMPE Jour., March / April (1987).

45. Kim, C., and R. A. Gray, "Development of Fiber Spreading Technique for Metal Matrix Composites," NRL Memorandum Report 5831, Naval Research Laboratory, Washington, DC 20375-5000, Dec. 30 (1986).

46. Kraus, J. D., Electromagnetics, 3rd ed., McGraw-Hill Book Co., New York, NY (1984).

47. Cable, J. W., Induction and Dielectric Heating, Reinhold Publishing Co., New York, NY (1954).

48. Davies, J., and P. Simpson, Induction Heating Handbook, McGraw-Hill Book Co., London, UK (1979).

49. Product Literature, "Strain Guage Installation with M-Bond 43-B, 600, and 610 Adhesive Systems," Instruction Bulletin B-130-9, Measurements Group Inc. (1979).

50. Product Literature,"Thornel Carbon Fibers," Amoco Performance Products, Inc. (1987).